UNIVERSITY OF MILANO - BICOCCA

DISAT

DISAT
DEPARTMENT OF EARTH AND ENVIRONMENTAL SCIENCES

HOLOCENE VEGETATION AND CLIMATE VARIABILITY AS RECORDED IN HIGH-ALTITUDE MIRES (WESTERN ITALIAN ALPS)

PH.D. SCHOOL IN ENVIRONMENTAL SCIENCES
XXVII Cycle
COORDINATOR: **PROF. VALTER MAGGI**

PH.D. CANDIDATE
FEDERICA BADINO
MAT. 760888

TUTOR: **PROF. VALTER MAGGI**
CO-TUTORS: **DR. ROBERTA PINI**
PROF. MATTIA DE AMICIS
EXTERNAL ADVISOR: **PROF. GIUSEPPE OROMBELLI**

Università degli Studi di Milano – Bicocca

Dipartimento di Scienze dell'Ambiente e del Territorio e di Scienze della Terra

Scuola di Dottorato di Scienze

Corso di Dottorato di Ricerca in Scienze Ambientali

Ciclo XXVII
Coordinatore: Prof. Valter Maggi

Tesi sottoposta per il conseguimento del titolo di Dottore di Ricerca in Scienze Ambientali

Presentata da **Federica Badino**

HOLOCENE VEGETATION AND CLIMATE VARIABILITY AS RECORDED IN HIGH-ALTITUDE MIRES (WESTERN ITALIAN ALPS)

Tutore: Prof. Valter Maggi
Co-tutori: Dr. Roberta Pini
Prof. Mattia De Amicis
Revisore esterno: Prof. Giuseppe Orombelli

Discussa il 26 Settembre 2016 davanti alla Commissione composta da:

Dr. Fabien Arnaud (membro)
Prof. Donatella Magri (membro)
Prof. Klaus Oeggl (membro)
Dr. Cesare Ravazzi (esperto)

Alla mia famiglia.

A Manuela Zanni, Luca Nassi*, Silvio Borrè*, Caterina Casadio**

**vinciamo noi ☺*

ACKNOWLEDGEMENTS

I would like to thank the support of many people: Cesare Ravazzi and Roberta Pini for fruitful discussions and for their help during field work and in the laboratory (Research Group on Vegetation, Climate and Human Stratigraphy, http://geomatic.disat.unimib.it/home/palinologia); Valter Maggi, Mattia De Amicis and Giuseppe Orombelli for their support and comments; I am grateful to Michele Brunetti, Francesco Maspero and Renata Perego; Elena Champvillair for her assistance and collaboration, Francesca Vallè and Giulia Furlanetto for their help with climate reconstructions; I acknowledge the many people helping during field and laboratory work: Andrea Tramelli, Marco Zanon, Davide Margaritora, Giovanni Baccolo, Michela Mariani and Sergio Pestarino for the logistic support.

INDEX

Manuscript 2 (prepared to be submitted to Quaternary Science Reviews)

ABSTRACT

Climate variability during the Holocene (the last 11700 calendar yr b2k) is relatively subtle whether compared with the higher amplitude characterizing the last glacial period. Nonetheless, several proxy data (e.g. pollen, plant macrofossils, glacier length variations), indicate detectable changes in temperature and/or moisture during this period. Retreating glaciers may uncover peat sequences that were once ice-buried. Palynological analysis of those organic deposits provides information on plant communities colonization in proglacial areas as well as long-distance vegetations signal.

The aim of this study is to investigate the potential of high-altitude pollen records for vegetation history and climate reconstruction during the Holocene in the south-western Italian Alps. The study sites are located in the Rutor Glacier area (La Thuile Valley). Within this thesis, modern (***a***) and past (***b***) vegetation and climate conditions have been analyzed using different methodologies;

a) Modern pollen rain, vegetation, climate and terrain parameters have been collected at 27 sampling sites placed along an altitudinal gradient from the village of Morgex (983 m asl) to the Rutor Glacier forefield (2668 m asl). This altitudinal transect has been designed **(i)** to provide a robust modern reference for reliable palaeoenvironmental and quantitative interpretations of past changes in vegetation composition; **(ii)** to integrate the newly-obtained pollen spectra into a large, continental dataset of modern pollen samples (EMPD - European Modern Pollen Database) for quantitative climate reconstructions.

b) New paleoecological, stratigraphical and geochronological data have been obtained from peat deposits (Valter mire, 2594 m asl) and integrated with the well-known buried peat sequences exposed at 2510 m asl by the '80es Rutor Glacier retreat. The result is a composite paleoecological record covering most of the Holocene.

At the base of the composite sequence, meltwater glacier sediments testify to the early Holocene development of a proglacial lake, before *Abies alba* expansion in the western Italian Alps. These sediments bear the palynological evidence of a

plant succession testifying to an ecological mechanism of colonization on deglaciated terrains. Moreover, macrofossil analysis highlighted the local presence of alpine dwarf - shrubland species (e.g. Ericaceae cf. *Vaccinium* and *Salix* cfr. *foetida*).

A large open forest belt formed by *Pinus cembra* developed in the glacier forefield over 2500 m a.s.l. since 8000 yrs cal BP, suggesting summer temperatures higher than the modelled climate normals for the reference period 1961-1990.

Between 8000 - 4000 yrs cal. BP timberline was higher than today. A radiocarbon age obtained from a *Pinus cembra* wood fragment suggests the occurrence of pines as high as ca. 2600 m asl at around 5650 yrs cal BP. The dated wood fragment cannot have been long-distance transported, thus it indicates the presence of this species *in situ*. Moreover, paleobotanical proxies and comparison with the July modeled climate normal at the modern treeline altitude (i.e. ca. 9.3° C at 2450 m asl), suggest a positive timberline shift of almost 300 m. For this interval, preliminary pollen-inferred TJul reconstructions show higher values (up to 3°C) than today (1981-2010).

At around 4000 yrs cal. BP *Picea abies* and *Alnus viridis* started to expand. A progressive climate-driven decline of *Pinus cembra* took place. Pollen-inferred TJul shows a cooling of ca. 3 ˚C, compared to the previous period. Locally, a possibly short-lived cold event occurred around 1140 yrs cal BP and a glacier-friendly phase may be related to the Late Middle Age (ca. 850 yrs cal. BP). Finally, the LIA Rutor Glacier advance (max occurred between 1751 – 1864 AD) is documented in the upper part of the sequence by fluvioglacial deposits.

KEYWORDS

Holocene, Paleoecology, Paleoclimate, Rutor, Alps

RIASSUNTO

La variabilità climatica durante l'Olocene (ultimi 11750 anni) ha avuto un'ampiezza moderata, se confrontata con l'ultimo ciclo Glaciale - Interglaciale. Tuttavia, alcuni *proxy data* come il polline fossile, i macroresti vegetali e i ghiacciai, possono registrare anche modeste variazioni di temperatura e/o umidità. Durante l'ultimo trentennio, il ritiro dei ghiacciai ha esposto sequenze di torba prima sepolte sotto il ghiaccio. L'analisi palinologica di questi depositi può fornire indicazioni relative a meccanismi di colonizzazione nelle aree proglaciali e alle trasformazioni della vegetazione a lunga distanza.

Lo scopo di questo lavoro è stato quello di produrre ed elaborare dati stratigrafici (pollinici, geochimici, radiocarbonici), in contesti di alta quota, per ricostruire la storia della vegetazione e della variabilità climatica olocenica nelle Alpi occidentali italiane. I siti di studio si trovano nell'area del Ghiacciaio del Rutor (Valle di La Thuile). Dati pollinici e vegetazionali attuali (***a***) e fossili (***b***) sono stati analizzati e confrontati utilizzando diverse metodologie;

a) Parametri ambientali attuali (pioggia pollinica, vegetazione, dati climatici e geomorfologici) provengono da 27 siti disposti lungo un gradiente altitudinale fra Morgex (983 m slm) e l'area antistante il Ghiacciaio del Rutor (2668 m slm). Il transetto altitudinale è stato realizzato **i**) per fornire un riferimento moderno alle ricostruzioni paleoambientali; **ii**) per integrare gli spettri pollinici qui ottenuti entro un dataset continentale (EMPD - European Modern Pollen Database) che raccoglie analoghi pollinici moderni.

b) Nuovi dati paleoecologici, stratigrafici e geocronologici sono stati ottenuti dallo studio di una torbiera ("Valter mire", 2594 m slm) ed integrati con le ben note sequenze di torbe (2510 m slm) rinvenute negli anni '80. Il risultato è un record paleoecologico composito che copre gran parte dell'Olocene.

Alla base della sequenza, depositi limosi testimoniano lo sviluppo di un lago proglaciale durante l'Olocene antico, precedente all'espansione di *Abies alba* nel settore occidentale delle Alpi. Contestualmente, si sviluppa una successione ecologica primaria di piante erbacee pioniere che colonizzano i terreni deglaciati.

Inoltre, l'analisi di macrofossili vegetali ha evidenziato la presenza *in situ* di arbusti striscianti (es. Ericaceae cf. *Vaccinium* e *Salix* cf. *foetida*).

Pinete con *Pinus cembra* si addensano progressivamente nella fascia alpina a partire da ca. 8000 anni cal BP, suggerendo una temperatura media estiva più elevata rispetto al trentennio di riferimento 1961-1990.

Fra 8000 - 4000 anni fa, il limite degli alberi si stabilizza a quote mediamente più elevate rispetto all'attuale. La datazione radiocarbonica di un frammento di legno di *Pinus cembra* suggerisce la presenza di questa specie ad una quota di ca. 2600 m slm intorno a 5650 anni cal BP. Inoltre, il confronto fra i dati paleobotanici e la temperatura attuale modellata per il limite degli alberi (T luglio: 9,3 ° C a 2450 m slm), ne suggerisce un innalzamento di circa 300 m durante la fase di Optimum climatico. Inoltre, ricostruzioni della temperatura del mese più caldo (T luglio) su base pollinica, mostrano valori più elevati (ca. 3 ° C) rispetto all'attuale (1981-2010).

A partire da circa 4000 anni fa, *Picea abies* e *Alnus viridis* si espandono, mentre un progressivo declino di *Pinus cembra* sembra essere influenzato dall'inizio di una fase di deterioramento climatico. Le ricostruzioni climatiche (T luglio) per questo intervallo evidenziano una diminuzione di ca. 3 ˚C, rispetto al periodo precedente. Localmente, un possibile evento freddo di breve durata è stato datato ca. 1140 anni cal BP. Una successiva fase di raffreddamento e possibile espansione del Ghiacciaio del Rutor è stata datata ca. 850 anni cal BP. Infine, durante la Piccola Età Glaciale, il Ghiacciaio del Rutor raggiunge la sua massima estensione (1751 - 1864 DC) BP, documentata nel record "Valter mire" da una sequenza di depositi fluvioglaciali.

PAROLE CHIAVE

Olocene, Paleoecologia, Variazioni climatiche, Ghiacciaio del Rutor, Alpi

1. INTRODUCTION

1.1. Climate variability: general concepts and identification of sensitive archives for its analysis and reconstruction

Since 1990, global mean temperatures have probably been higher than at any previous time during the last 1000 years (Osborn and Briffa, 2006). In the current discussion about past climatic variability and climatic change, an often-asked question is whether (and if so, why) comparably warm periods occurred earlier, in particular during the present interglacial: the Holocene (the last 11700 calendar yr b2k). Climate variability during the Holocene is relatively subtle if compared with the larger amplitude that characterized the last glacial period. Nonetheless, several proxy data (pollen and macrofossils, glacier length variations, lake level oscillations, tree rings width, lacustrine carbonates, stalagmites and ice cores) indicate detectable changes in temperature and/or moisture during this period.

Glaciers are especially sensitive to climatic variations on inter-annual to multi-millennial timescales (Six and Vincent, 2014), as indicated by the modern widespread glacier retreat coincident with warming over the last century. Detailed morphological mapping of the moraines, soil stratigraphy in lateral and terminal moraines, lithostratigraphy of mires close to glacier tongues, pollen analysis, dendrochronology and lichenometry were combined with archaeological and historical methods to track changes in glacier size during the Holocene (Ivy-Ochs et al., 2009).

Climatic warming since the mid-1980s led to rapid shrinkage of glacier tongues. Since then, peat sequences and plant debris have been exposed, allowing to recognize periods when the glaciers were close to or smaller than their present sizes (e.g. Joerin et al., 2006). Mires are known to be very sensitive archives of past climatic and environmental changes. In addition, remote mountain sites probably offer the only organic archives where continuous high-resolution records with little or no human impact throughout the Holocene are available. The palaeobotanical analysis of those organic deposits provide information on plant communities colonization in proglacial areas as well as long-distance vegetation signal.

High-elevation environments are particularly sensitive to rapid climate changes (e.g. Gottfried et al., 2012). In mountainous regions, steep climatic gradients offering over a short geographical distance many different climate-related ecosystems. Therefore, sites located at or near an ecotone are well suited for studies of long-term vegetation history and climate dynamics. In the following the timberline is understood to be the transition zone between closed forest (density depends on the tree species and the site conditions) and the most advanced individuals of the forest-forming tree species (Holtmeyer, 2009, Smith et al., 2003). It is the most conspicuous vegetation limit in high-mountain areas, a more or less wide ecotone that has to be understood as a space- and time related phenomenon. In many cases the existence of a timberline ecotone is the result of oscillations of the climate, persistence of tall (mature) trees and regeneration under changing conditions (Holtmeyer, 2009). Since the elevation of the upper treeline (i.e. the uppermost limit of trees reaching at least a 3 m-height) in mountain areas is strongly controlled by climate, especially by temperature range during the growing season (Körner, 1998), past changes in treeline position have been widely used to infer climate variations. Treeline changes during the Holocene have been reconstructed in various ways, mainly using pollen analyses, sometimes supplemented by plant macrofossil data (Tinner & Theurillat 2003).

While the suitability of **pollen data for palaeoenvironmental reconstructions** has long been tested and proved, its **potential for quantitative paleoclimate estimations** has not yet been fully explored and understood. The application of calibration and regression techniques on paleoecological records offers the opportunity to obtain pollen-based quantitative estimations of past climate variables (temperature and precipitation). A continental dataset of modern pollen samples (**EMPD - European Modern Pollen Database**; Davis et al., 2013) has been designed for this purpose. Such approach enlarges the potential of pollen data, that can be used not only for qualitative descriptions of past vegetation, but also as climate proxies. With nearly 4800 modern pollen samples, the EMPD covers a wide variety of ecosystems, from lowland coastal areas to high-altitude mountain sites. Preliminary tests suggest the potential of pollen data as proxies for quantitative climate reconstructions (Birks et a., 2010), but also highlight a

main current limitation of the EMPD database, lacking a sufficient number of taxonomically-accurately identified pollen spectra from high-altitude alpine sites (Ortu, 2006). Thus, modern samples along **altitudinal gradients in mountain areas** are needed.

Moreover, studies of modern pollen assemblages and their relationship with vegetation and key environmental factors (e.g. local slopes, exposure to dominant winds and aspect) are one of the best tools for qualitative and quantitative reconstruction of paleoenvironments in the light to facilitate the interpretation of past vertical shifts and changes in vegetation composition (Cañellas-Boltà et al., 2009). Since very few studies of modern pollen rain have been attempted in mountain environments of southern European countries (e.g. Court-Picon et al., 2005, 2006), this procedure remains to be tested against other sites, plant community and fossil records.

1.2. Aims of the present work

This PhD research aims at **investigating the potential of high-altitude pollen records for vegetation history and climate reconstruction during the Holocene** in the western Italian Alps. The sites selected for multiproxy paleoecological analysis are located in the Rutor Glacier area (La Thuile Valley). Within this thesis, modern (*a*) and past (*b*) vegetation and climate conditions have been analyzed using different methodologies;

a) Modern pollen rain, vegetation, climate and terrain parameters have been collected at 27 sampling sites placed along an altitudinal gradient from the village of Morgex (983 m asl) to the Rutor Glacier forefield (2668 m asl). This altitudinal transect has been designed **(i)** to provide a robust modern reference for reliable palaeoenvironmental and quantitative interpretations of past changes in vegetation composition; **(ii)** to integrate the newly-obtained pollen spectra into a large, continental dataset of modern pollen samples (EMPD - European Modern Pollen Database) for quantitative climate reconstructions.

This part of the research is presented in chapter 1 (***Modern pollen-vegetation-environmental relationships along an altitudinal transect in the western Italian Alps close to the Rutor Glacier***)

b) New paleoecological, stratigraphical and geochronological data have been obtained from peat deposits (Valter mire, 2594 m asl) and integrated with the well-known buried peat sequences exposed at 2510 m asl by the '80es Rutor Glacier retreat. The result is a composite paleoecological record covering most of the Holocene.

This part of the research is presented in chapter 2 (***Glacier contraction, primary plant succession and the early-middle Holocene optimum in the Italian Alps. New evidence from a classical site at the Rutor Glacier***) and chapter 3 (***Climate-driven vegetation dynamics during the Mid-to-Late Holocene as recorded in an elevational peat bog close to the Rutor Glacier***).

REFERENCES

Birks, H. J. B., Heiri, O., Seppä, H., & Bjune, A. E. (2010). Strengths and Weaknesses of Quantitative Climate Reconstructions Based on Late-Quaternary. The Open Ecology Journal, 3(1).

Cañellas-Boltà, N., Rull, V., Vigo, J., & Mercadé, A. (2009). Modern pollen-vegetation relationships along an altitudinal transect in the central Pyrenees (southwestern Europe). The Holocene, 19(8), 1185-1200.

Court-Picon, M., Buttler, A., & de Beaulieu, J. L. (2005). Modern pollen–vegetation relationships in the Champsaur valley (French Alps) and their potential in the interpretation of fossil pollen records of past cultural landscapes. Review of Palaeobotany and Palynology, 135(1), 13-39.

Court-Picon, M., Buttler, A., & De Beaulieu, J. L. (2006). Modern pollen/vegetation/land-use relationships in mountain environments: an example from the Champsaur valley (French Alps). Vegetation History and Archaeobotany, 15(3), 151-168.

Davis, B. A., Zanon, M., Collins, P., Mauri, A., Bakker, J., Barboni, D., ... & Bradshaw, R. H. (2013). The European modern pollen database (EMPD) project. Vegetation History and Archaeobotany, 22(6), 521-530.

Gottfried, M., Pauli, H., Futschik, A., Akhalkatsi, M., Barancok, P., Benito Alonso, J.L., Coldea, G., Dick, J., Erschbamer, B., Fernandez Calzado, M.R., Kazakis, G., Krajci, J., Larsson, P., Mallaun, M., Michelsen, O., Moiseev, D., Moiseev, P., Molau, U., Merzouki, A., Nagy, L., Nakhutsrishvili, G., Pedersen, B., Pelino, G., Puscas, M., Rossi, G., Stanisci, A., Theurillat, J.-P., Tomaselli, M., Villar, L., Vittoz, P., Vogiatzakis, I., Grabherr, G. (2012). Continent-wide response of mountain vegetation to climate change. Nat. Clim. Change 2, 111-115.

Holtmeier, F. K. (2009). Mountain timberlines: ecology, patchiness, and dynamics (Vol. 36). Springer Science & Business Media.

Ivy-Ochs, S., Kerschner, H., Maisch, M., Christl, M., Kubik, P. W., & Schlüchter, C. (2009). Latest Pleistocene and Holocene glacier variations in the European Alps. Quaternary Science Reviews, 28(21), 2137-2149.

Joerin, U. E., Stocker, T. F., & Schlüchter, C. (2006). Multicentury glacier fluctuations in the Swiss Alps during the Holocene. The Holocene, 16(5), 697-704.

Körner, C. (1998). A re-assessment of high elevation treeline positions and their explanation. Oecologia, 115(4), 445-459.

Ortu, E., Brewer, S., & Peyron, O. (2006). Pollen-inferred palaeoclimate reconstructions in mountain areas: problems and perspectives. Journal of Quaternary Science, 21(6), 615-627.

Osborn, T.J., Raper, S.C.B., Briffa, K.R. (2006). Simulated climate change during the last 1,000 years: comparing the ECHO-G general circulation model with the MAGICC simple climate model. Climate Dynamics 27, 185–197.

Six, D., & Vincent, C. (2014). Sensitivity of mass balance and equilibrium-line altitude to climate change in the French Alps. Journal of Glaciology, 60(223), 867-878.

Smith, W. K., Germino, M. J., Hancock, T. E., & Johnson, D. M. (2003). Another perspective on altitudinal limits of alpine timberlines. Tree physiology, 23(16), 1101-1112.

Tinner, W., & Theurillat, J. P. (2003). Uppermost limit, extent, and fluctuations of the timberline and treeline ecocline in the Swiss Central Alps during the past 11,500 years. Arctic, Antarctic, and Alpine Research, 35(2), 158-169.

Manuscript 1

(In preparation)

Modern pollen-vegetation-environmental relationships along an altitudinal transect in the western Italian Alps close to the Rutor Glacier

1. INTRODUCTION

In mountain areas, climate parameters vary strongly with altitude, largely determining the zonation of vegetation, reflected in turn by the pollen rain record at different elevations. However, if relationships between plant composition in different vegetation belts and relative pollen percentages recorded in spectra from high-elevation sites are affected by local vegetation cover, they also depend on local slopes, exposure to dominant winds, and aspect. Very few studies of modern pollen rain have been attempted in mountain environments of southern European countries (Court-Picon et al., 2005, 2006; Cañellas-Boltà et al., 2009; Ortu et al., 2010). Analyses of modern pollen rain are essential for a better understanding of fossil pollen sequences in a particular region, and thus for pollen-based palaeoenvironment and palaeoclimate reconstructions. In this aim, moss samples are commonly used as surface samples for local modern pollen deposition. They are assumed to record an average of several years of pollen deposition (Räsänen et al., 2004; Pardoe et al., 2010; Lisitsyna & Hicks, 2014) and can be profitably used as analogues for fossil pollen assemblages.

This paper presents a new altitudinal transect developed in the western Italian Alps (Aosta Valley). Here modern pollen rain, vegetation, climate and terrain parameters have been collected at 27 sampling sites placed along an altitudinal gradient stretching from the village of Morgex (983 m asl) to the Rutor Glacier forefield (2668 m a.s.l). The transect has been designed (I) to estimate the effect of local (morphometric) parameters on the relationships linking pollen percentages variations, elevation and climate; (II) to provide a robust modern reference for reliable palaeoenvironmental and quantitative interpretations of past vertical shifts and changes in vegetation composition, as recognized in the pollen

records from the high-altitude mires; (III) to integrate the newly-obtained pollen spectra into a large, continental dataset of modern pollen samples (EMPD - European Modern Pollen Database; Davis et al., 2013) for quantitative climate reconstructions (Birks et al., 2010).

2. STUDY AREA

The study area lies in the La Thuile Valley (Western Alps, Italy; N 45˚64' E 78˚01') (**Fig. 1**). The area, displaying mostly a north-west aspect, is characterized by steep slopes alternating with more flat areas perpendicular to the ice flow direction. A rocky spur located between 2100 – 2200 m asl hosts a flat area named Plan de la Lière with the Lac du Glacier; a second one (2400-2500 m asl) dams up the Lac du Ruitor and Lac des Seracs basins. Finally, a third ridge culminating at about 2500-2600 m asl hosts two small lakes, named lac Vert and Lac Gris. These latter lakes occupy the depressions left by the glacier after the LIA advance (Little Ice Age) and are mainly filled by glacial sediments and meltwater. Meltwaters also feed the Rutor Stream, which forms the three cascades that can be admired along the path leading to the Deffeyes mountain hut.

Vegetation is arranged in a typical altitudinal succession defining three main belts (montane, subalpine and alpine). These boundaries vary with local topographic and climatic conditions. Human activities in this area, possibly cattle raising and forest exploitation, have always played a marginal role, being restricted to the lower altitudes. This zone is still relatively undisturbed in comparison with other areas within the same geographical region (Aosta Valley).

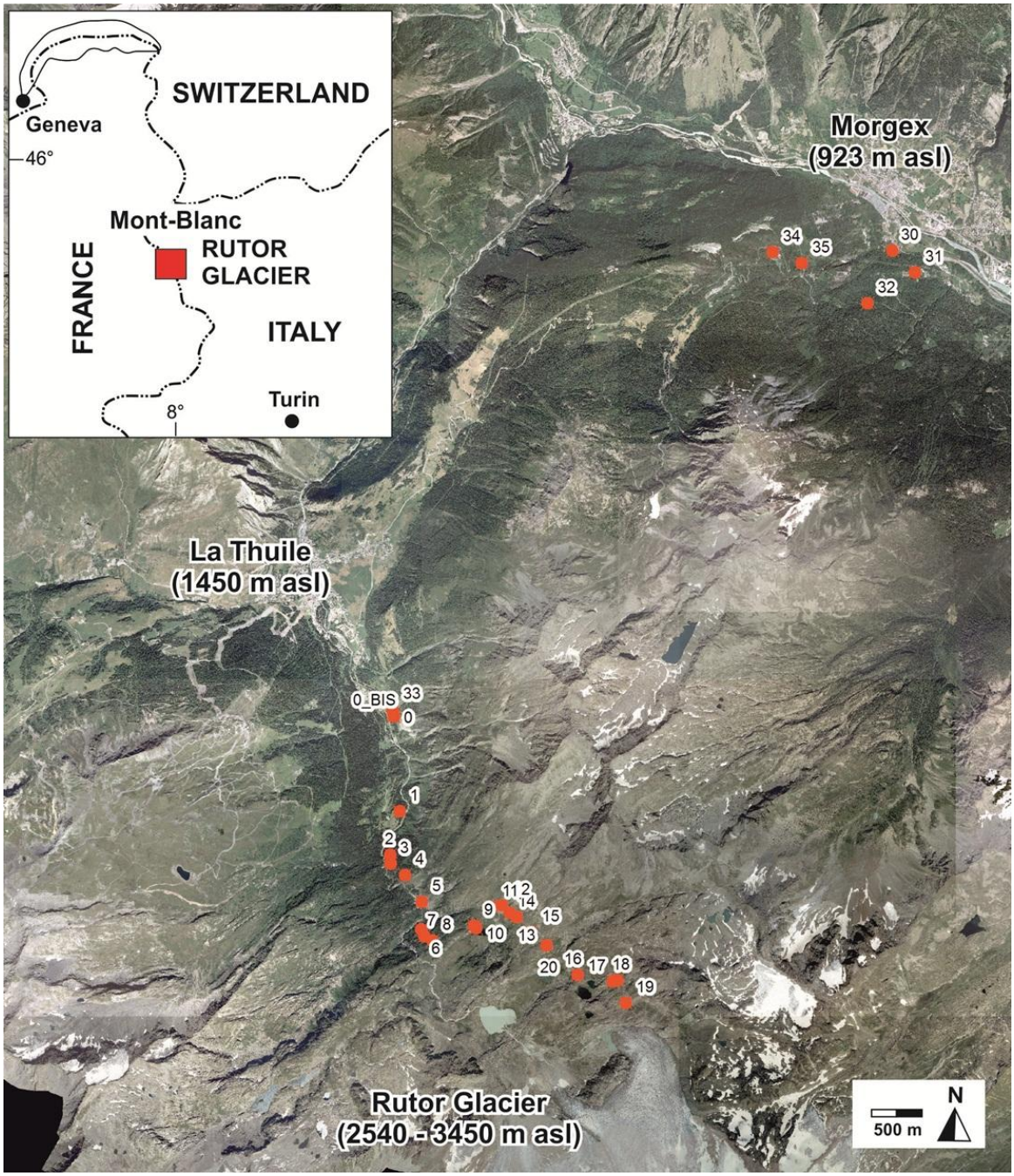

Fig. 1- Location of the studied area is indicated by the red square. Sampling sites are highlighted by red dots on the ortho-image**.**

3. MATERIALS AND METHODS

3.1. Development of an altitudinal transect and sampling strategy

A transet composed by 27 sampling sites (acronyms from Rutor TRS 0 to TRS 35) was developed (**Fig. 1**) during September-October 2014. The precise location and descriptive information of the sampling sites are listed in **Table 1**. Sampling sites correspond to areas where mosses grow and are mainly located in the openings of the forest, at least 10 - 15 m far from the nearest tree. To record their geographical coordinates and altitudes, a hand - held GPS was used. At each site, digital photos of the sampled moss and four photographs of the landscape, looking N, S, E and W from the sample point, were taken. Concentric circles of 1.8 and 10 m-radius around each sampling site were considered for vegetation surveys following the Braun-Blanquet method (**Fig. 2**). Furthermore, main arboreal species were listed and a cover estimation was carried out within a 100 m radius circle.

3.2. Pollen analysis – modern pollen rain data

At each site, three moss samples were collected for pollen analysis within a circular area of 1,8 m radius (ca 10 m^2) to account for small-scale differences in pollen circulation (**Fig. 2**). Moss samples may preserve and integrate several years of pollen rain (Räsänen et al., 2004; Pardoe et al., 2010; Lisitsyna & Hicks, 2014). The thickness of the samples (depth of the moss) varies between ca. 4 and 8 cm. Mosses were sampled down to, but not including, the mineral soil. All moss samples were processed following standard methods at the Lab. of Palynology and Palaeoecology of CNR-IDPA in Milano, after adding *Lycopodium* tablets for pollen and micro-charcoal concentration estimations (Stockmarr, 1971). A minimum count of 600 pollen grains (e.g. a minimum of 200 grains per moss) was obtained at each sampling site, aquatics, spores and non-pollen palynomorphs excluded. Identification was carried out at x400, x630 and x1000 magnifications under a Leica DM-LB light microscope. Pollen identification followed Moore et al. (1991), Punt and Blackmore (1976-2009), Reille (1992-1998), Beug (2004) and the CNR pollen reference collection. Non-pollen

palynomorphs were named after van Geel (1978) and van Geel et al. (1981). Pollen diagrams were drawn using Tilia ver. 1.7.16 (Grimm, 1991-2011) and Corel Draw X6 for further graphic elaborations. Pollen zonation was obtained by a constrained incremental sum of squares cluster analysis, using the Cavalli Sforza's chord distance as dissimilarity coefficient (CONISS, Grimm, 1987). Clustering was restricted to taxa whose pollen reached over 2%.

Rutor-TRS sites	Site description	Altitude (m asl)	Latitude	Longitude
TRS 19	Lightly LIA (Little Ice Age) morain colonized by dry grasslands (e.g. *Achillea moschata, Trifolium badium* and isolated patches of *Carex curvula*)	2668	45°40'12.44560"N	6°59'53.19031"E
TRS 18	Rocky slopes with dwarf shrubs (e.g. *Salix herbacea*)	2606	45°40'21.02228"N	6°59'48.15957"E
TRS 17	Telmatic meadows (*Nardus stricta* and *Leontodon* cf. *helveticus*) surrounded by dwarf shrubs (e.g. *Salix herbacea*)	2599	45°40'20.59097"N	6°59'45.67814"E
TRS 16	Mire surrounded by dry grasslands on steep slopes with scattered shrubs (e.g. *Juniperus nana, Rhododendron ferrugineum, Vaccinium gaultherioides* and *Vaccinium uliginosum*)	2518	45°40'22.72214"N	6°59'26.31072"E
TRS 20	Small fountainhead with telmatic plants (e.g. *Carex foetida, Carex fusca*) and briophytes. In the surrounding area: alpine meadows (e.g. *Nardus stricta*) on the east facing slopes	2483	45°40'33.73127"N	6°59'09.14109"E
TRS 15	Small mire surrounded by dry meadows on rocky slopes (*Nardus stricta* and *Leontodon helveticus*). *Pinus cembra* krummholz on rocky patches	2467	45°40'38.67876"N	6°59'00.56391"E
TRS 14	Cold moorland with Ericaceae (e.g. *Rhododendron ferrugineum, Vaccinium gaultherioides* and *Vaccinium myrtillus*) together with dwarf shrubs (e.g. *Salix herbacea* and *Salix foetida*). Scattered trees, the nearest at ca. 70 m far is a *Pinus cembra* specimen	2348	45°40'44.39524"N	6°58'52.41553"E
TRS 13	Wet grassland close to a waterfall surrounded by scattered *Larix decidua*, *Pinus cembra* and *Alnus viridis* specimes	2298	45°40'45.82689"N	6°58'48.56166"E

Rutor-TRS sites	Site description	Altitude (m asl)	Latitude	Longitude
TRS 12	Scree slope with scattered *Larix decidua*, *Pinus cembra* and *Alnus viridis*	2266	45°40'48.77154"N	6°58'44.08702"E
TRS 11	Fallow land with scattered *Larix decidua*, *Pinus cembra*, *Alnus viridis*. At ca. 50 m far, a lodge with ruderal species occurred	2219	45°40'48.05674"N	6°58'38.60473"E
TRS 9	Dry grassland (e.g. *Agrostis*) on the top of a rocky boulder. In the surrounding area: *Pinus cembra* and *Larix decidua* trees	2159	45°40'40.66425"N	6°58'28.93368"E
TRS 10	Mire surrounded by scattered *Larix decidua* and *Pinus cembra* specimens	2143	45°40'39.66540"N	6°58'30.28653"E
TRS 8	Open forest with *Pinus cembra*, *Larix decidua*	2090	45°40'34.55567"N	6°58'06.43781"E
TRS 7	Open forest with *Pinus cembra*, *Larix decidua* and shrubs (eg. Ericaceae)	2014	45°40'36.07078"N	6°58'01.84590"E
TRS 6	Megaforb community in woodland with Larix decidua and Pinus cembra	1922	45°40'38.66495"N	6°58'00.13285"E
TRS 5	Avalanche rill with scattered *Larix decidua* and *Pinus cembra* trees. Grazed dry meadows in the surroundings.	1846	45°40'49.23728"N	6°58'00.18381"E
TRS 4	Sunny opening in wooded area (*Picea abies, Larix decidua*, *Pinus cembra*, *Alnus glutinosa*) near (ca. 100 m far) a lodge surrounding by mown meadows and megaforbs (e.g. *Rumex* and *Epilobium*)	1781	45°40'59.35931"N	6°57'50.62548"E
TRS 3	Small opening area in *Picea abies* woodland with *Sorbus aria* specimens.	1722	45°41'03.64927"N	6°57'42.47135"E
TRS 2	Small hollow within dense *Picea abies* woodland. *Larix decidua*, *Acer pseudoplatanus* and *Salix* cf. *caprea* are also present	1663	45°41'07.04184"N	6°57'42.10082"E

Rutor-TRS sites	Site description	Altitude (m asl)	Latitude	Longitude
TRS 1	Shaded small opening in wooded area with *Picea abies, Larix decidua* and sparse *Pinus cembra* specimens	1618	45°41'23.82291"N	6°57'46.88648"E
TRS 33	Grazed dry meadows (e.g. *Nardus stricta*) with scattered shrubs (*Juniperus communis, Juniperus nana, Berberis vulgaris*) surrounded by *Larix* and *Picea* forest	1520	45°42'02.87050"N	6°57'41.40393"E
TRS 0	Shaded small opening in wooded area with *Picea abies* and *Larix decidua*	1510	45°42'00.36854"N	6°57'42.23790"E
TRS 34	Mown meadows near a track surrounded by open deciduous thicket (*Corylus, Betula, Fraxinus excelsior*) and coniferous trees (*Larix decidua, Picea abies* and *Pinus sylvestris*)	1563	45°45'02.03072"N	7°01'03.29547"E
TRS 35	Slope mire with *Molinia coreulea* in open woodland (e.g. *Betula alba, Alnus incana, Acer pseudoplatanus, Larix decidua*)	1446	45°44'58.08240"N	7°01'19.50509"E
TRS 32	Opening in *Abies alba* forest with subordinated *Larix decidua, Picea abies, Sorbus aucuparia, Populus tremula, Betula alba*	1298	45°44'43.19404"N	7°01'56.00547"E
TRS 31	Mown meadows surrounded by deciduous trees (e.g. *Fraxinus excelsior, Betula alba, Corylus avellana, Larix decidua, Picea abies*)	1050	45°44'55.58848"N	7°02'21.61815"E
TRS 30	Heavily grazed meadows in a rural context. Open thicket with *Acer pseudoplatanus, Fraxinus excelsior, Tilia cordata, Juglans, Picea abies, Larix decidua*	983	45°45'03.71943"N	7°02'08.88244"E

Table 1 - Descriptive information of the 27 sampling sites. Vegetation type and main plant genera/species are given in the site description.

3.3. Vegetation data: surveying strategy (Braun-Blanquet system)

At each sampling site, vegetation surveys were carried out using the Braun–Blanquet abundance/dominance scale (Braun–Blanquet, 1979) within circular areas of 1,8 m radius (ca 10 m^2) and 10 m radius (ca 314 m^2) (**Fig. 2**). In this system, a semi-quantitative abundance-dominance index is used to estimate the plant cover for each species, according to the following scale: 5 (80-100%), 4 (60-80%), 3 (40-60%), 2 (20-40%), 1 (1-20%), + (scarce), r (rare). Finally, within the circular areas of 100 m radius was estimated the abundance of the major arboreal taxa. This methodology was focused on producing good estimates of the abundance of the major taxa (the producers of the pollen types which are the major components of current and past pollen rain in the study area) rather than recording every species present.

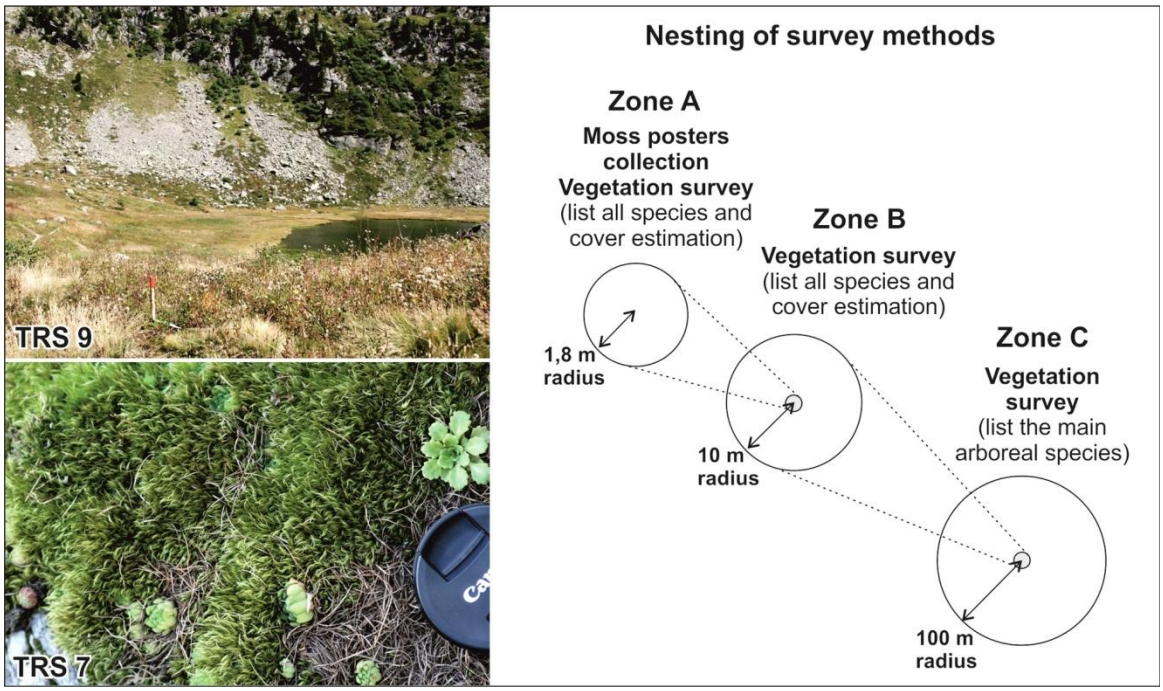

Fig. 2 – Vegetation sampling method and moss samples collection scheme used for each sampling site.

3.4. Estimation of climate normals along the altitudinal transect

Monthly temperature and precipitation series from 1981 to 2010, for each Rutor-TRS site of the altitudinal transect were obtained by means of the procedure described in Brunetti et al. (2012), which takes also into account locally important drivers such as aspect and slope using a digital elevation model with a resolution of 30 arc-seconds (often referred to as 1-km spatial resolution). Climate data obtained at this very high resolution may be essential for studies in mountain environments with strong climate gradients and low density of climate stations (Brunetti et al., 2014). From these monthly series, spring temperature (T spring), summer temperature (T summer), temperature of the coldest month (Tjan) and the mean annual rainfall (P annual) were calculated for the interval 1981-2010, which is considered here as reference period for the pollen rain represented in the collected moss samples.

3.5. Calculation of morphometrical parameters in GIS environment

Morphometrical parameters (Aspect, Slope, Insolation, Curvature) were derived from different raster surfaces:

- DTM (grid cell size of 2 m x 2 m) from LIDAR data acquired by the Valle d'Aosta Italian Region (2005-2008)
- DTM (grid cell size of 20 m x 20 m) provided by the Earth and Environmental Sciences Department (DISAT) of the University of Milano-Bicocca

GIS applications (ESRI, ArcMap) have been used as a tool for morphometric analysis within the 100 m radius buffers. Mean values obtained for each parameter are listed in **Table 2**.

3.5.1. Aspect

Aspect identifies the downslope direction of the maximum rate of change in value from each cell to its neighbors. It can be thought of as the slope direction. The values of each cell in the output raster indicate the compass direction that the surface faces at that location. It has been measured clockwise in degrees from 0˚

(due North) to 360˚ (again due North), coming full circle. Flat area having no downslope direction was given a value of -1.

3.5.2. Slope

Slope (gradient, or rate of maximum change in z-value) represents the rate of change of elevation for each DTM cell. Basically, the maximum change in elevation over the distance between the cell and its eight neighbors identifies the steepest downhill descent from the cell. The output slope raster has been calculated in degrees (0 to 90˚). The lower the slope value, the flatter the terrain; the higher the slope value, the steeper the terrain.

3.5.3. Curvature

The Curvature function displays the shape or curvature of the slope. The curvature has been calculated by computing the second derivative of the surface.

There are three parameters in the Curvature function:

- Input Raster - A DEM raster where each pixel stores the elevation.
- Curvature Type - The curvature type accentuates different aspects of the slope. There are three options for Curvature Type: Profile, Planform, and Standard.
- Z Factor—The z-factor adjusts the units of measure for the z units when they are different from the x,y units of the input surface. If the x,y units and z units are in the same units of measure, the z-factor should be set to 1. The z-values of the input surface are multiplied by the z-factor when calculating the final output surface.

The units of the curvature has been expressed as one hundredth (1/100) of a z-unit. The primary output is the curvature of the surface on a cell-by-cell basis, as fitted through that cell and its eight surrounding neighbors. A positive curvature indicates the surface is upwardly convex at that cell. A negative curvature indicates the surface is upwardly concave at that cell. A value of 0 indicates the surface is flat.

3.5.4. Insolation

The solar radiation analysis tools calculate insolation across a landscape or for specific locations, based on methods from the hemispherical viewshed algorithm developed by Rich et al. (1994) and further developed by Fu and Rich (2000, 2002).

The output radiation rasters is a floating-point type and have units of watt hours per square meter (Wh/m^2).

3.6. Data analyses

Fidelity and dispersibility indices were calculated for individual taxa based on pollen and plant presence/absence data (Davis, 1984; McGlone and Meurk, 2000). Fidelity was calculated as the percentage of sites where a given taxon coincides both in pollen and vegetation, as a function of those sites in which the taxon is present in the vegetation. Dispersibility was calculated as the percentage of sites where a given taxon is only recorded in the pollen rain, as a function of those sites in which the taxon is absent from the vegetation. Taxa with less than 2% in pollen percentages and 1% in plant cover within circular areas of 10 m radius at any sample were excluded from these calculations. After plotting fidelity versus dispersibility indices, pollen types were grouped into five main groups based on similarity of values (Deng et al., 2006; Fletcher and Thomas, 2007; Fall, 2012).

Ordination techniques are considered appropriate for assessing and displaying the relationship between pollen percentages recorded in modern pollen rain, vegetation data, climatic and terrain variables. These statistical analyses have been frequently used to detect structures or patterns within pollen and vegetation data. They provide an efficient low-dimensional representation of complex multivariate data and serve to indicate their major gradients and the relative contribution of each taxon to each of these gradients. All the plants present an ecological optimum and tolerance to most environmental gradients, justifying the use of a biological unimodal response model (ter Braak, 1987, 1988). In this work, Canonical Correspondence Analysis (CCA), the constrained form of CA (ter Braak 1986) was used as direct gradient analysis to highlight the relationships

between pollen, vegetation and the environmental parameters. Several CCA ordinations have been performed using altitude, insolation, aspect, slope, curvature, Tspring, Tsummer, Tjan and P annual as the sole constraining variable to assess their importance on the variance of pollen and vegetation (1.8 m and 10 m radius) assemblages. Moreover, CCA with all environmental parameters together were also carried out.

Prior to the CCA analysis, pollen percentages were square-root transformed, for variance stabilization (Prentice, 1980) and pollen taxa with percentages below 2%, were removed. A reviewed pollen dataset was used, removing outliers namely TRS 17, *Polygonum aviculare* type and *Ulmus.* In the vegetation analysis, rare elements (those designed with '+' and 'r') were not considered. The significance of all CCA were tested with ANOVA (p <0.05, after 999 unrestricted permutations).

4. RESULTS

4.1. Plant abundance data

Based on the altitudinal arrangement of vegetation (**Fig. 3**), the montane zone between 983 and 1500 m asl is characterized by deciduous forests dominated by *Tilia cordata*, *Fraxinus excelsior*, *Betula alba*, *Acer pseudoplatanus*, *Prunus avium* and *Juglans regia*. Broad-leaved forests are mixed with *Abies alba* and other conifers e.g.: *Picea abies* and *Larix decidua*. A slope mire at 1446 m asl (TRS 35) represents a local environment with flowing water and acid anmoor soil dominated by *Molinia coerulea*, *Cirsium palustris, Juncus* sp. and *Potentilla erecta*. Human disturbance is frequent at this altitude, as evidenced by villages, pasture and cultivation, often abandoned and replaced by secondary forests.

Between 1500 and 1780 m asl, forests are dominated by *Picea abies* with shrubs understory made by *Juniperus communis* and *Vaccinium vitis–ideae.* Moving towards higher altitudes, from 1780 to 2100 m asl, the landscape is characterized by forests with *Pinus cembra* and *Larix decidua. Pinus cembra* grows mainly on north-facing rocky slopes. At around 1800 m asl sporadic *Pinus sylvestris* and *Pinus uncinata* formations were recognized. *Alnus glutinosa* occurs only in

moister sites. Along valley slopes, running water and higher soil moisture promote megaforbs communities colonization (*Peucedanum ostruthium*, *Epilobium angustifolium*, *Adenostyles alliariae, Rumex alpestris*). Here, the woody component is characterized by *Sambucus racemosa* and *Sorbus aucuparia.* From about 2100 m asl, open forest with scattered pines (*Pinus cembra*) and *Larix decidua* take the place of the lower close coniferous forest. This transitional belt is mostly characterized by shrub formations (*Rhododendron ferrugineum*, *Vaccinium myrtillus*, *Vaccinium vitis-ideae* and *Juniperus nana*). A wide mire is located at 2140 m asl (Plan de la Lière). This habitat includes musci (mainly *Sphagnum* sp.) and aquatic plants (*Carex* sp., *Eriophorum angustifolium, Menyanthes trifoliata*).

In the alpine belt between 2400 and 2600 m asl, a more open vegetation with scattered *Larix* up to ca. 2400 m asl and *Pinus cembra* specimens (defined by the 3 m tree growth forms) occurred up to ca. 2455 m asl marked the modern treeline position. Progressively younger pines occurred in the upper altitudinal belts up to 2520 m asl, where stunted and deformed *Pinus cembra* krummholz are sparsely present. Among the herbs and shrubs, *Nardus stricta* and *Leontodon helveticus* arid meadows alternating with moorland of *Vaccinium myrtillus*, *Vaccinium gaultherioides* and *Juniperus nana* characterize this open areas. Several swamps and small mires are dominated by sedges (mainly *Carex fusca*, *Carex foetida*). Arctic-alpine species *(Salix herbacea, Alchemilla pentaphyllea* and *Homogyne alpina)* represents locally hydromorphic conditions (abundantly filled with water by the melting snow). Up to 2500 m asl, pioneer vegetation (e.g. *Trifolium badium*, *Oxyria digyna*, *Carex curvula*) dominate the Rutor Glacier foreland.

The high species–environment correlation obtained in the CCA ($r = 0.945$, $p < 0.001$) shows that altitude satisfactorily explains the species distribution gradient in statistical terms. In a biplot of the site scores using the first two axes, four groups can be recognized (**Fig. 4**). Group 1 includes the sites of the lower part of the transect, up to 1520 m asl, characterized by mixed deciduous forest with coniferous trees (e.g. *Abies alba, Picea abies* and *Larix decidua*). Site TRS 35 from group 1 is from a slope mire (e.g. *Molinia coreulea, Parnassia* and *Eriophorum*) and occupies the lower right part of the diagram. Group 2 includes

sites that support coniferous forests (eg. *Picea abies* and *Larix decidua*), located at middle elevations (1618 to 2090 m asl). Group 3 is formed by open forest with *Pinus cembra*, *Larix decidua* and shrubs (eg. Ericaceae) between 2143 and 2450 m asl, above (up to 2518 m asl) alpine meadows occurred. Site TRS 10 is from a small mire above the timberline bearing some particular features (*Carex, Juncus, Eriophorum angustifolium, Potentilla*). Finally, group 4 corresponds to the highest altitudinal belt, above 2599 m asl, characterized by dry grasslands (e.g. *Achillea moschata, Trifolium badium* and isolated patches of *Carex curvula*). The general arrangement of sampling sites suggests that axis 1 reflects the main altitudinal gradient of samples and vegetation, confirming the importance of altitude for explaining the vegetation array. According to the position of these four groups, the treeline, located at ca. 2450 m asl, may be situated around the score -0.5 of this axis. Axis 2 is more difficult to interpret, as most samples are situated around middle values. However, the detached position of the two sites: TRS 10 and TRS 35 from the other sites, suggests some gradient related to open/humid environments to denser canopy.

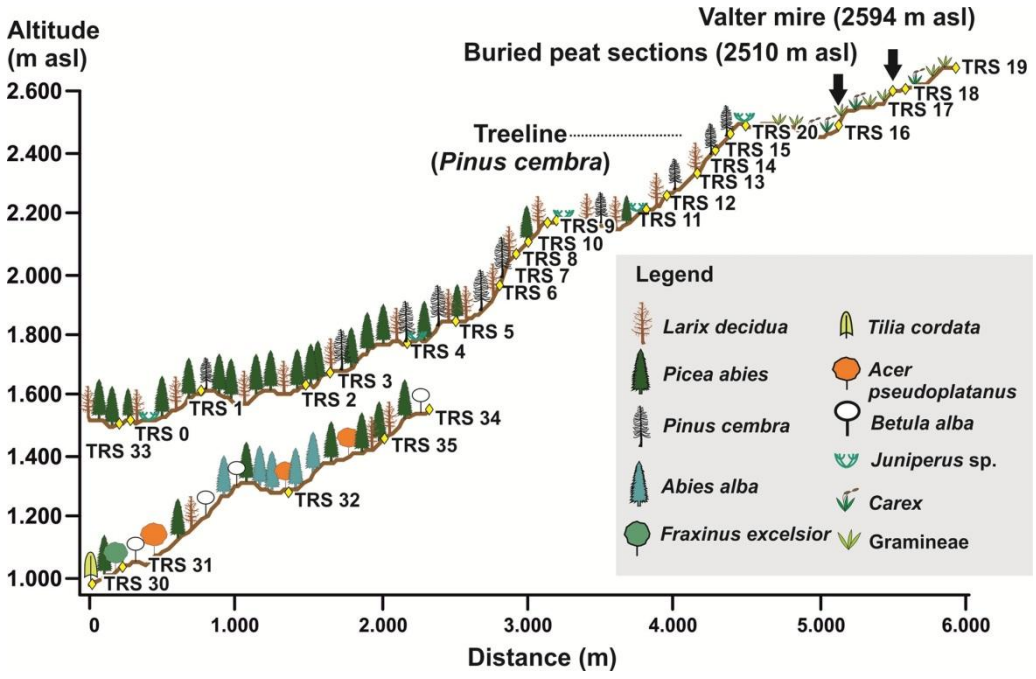

Fig. 3 - Sketch of the altitudinal arrangement of vegetation. Acronyms (TRS) correspond to sampling sites. Treeline position is indicated. Black arrows highlighted the location of the fossil sites.

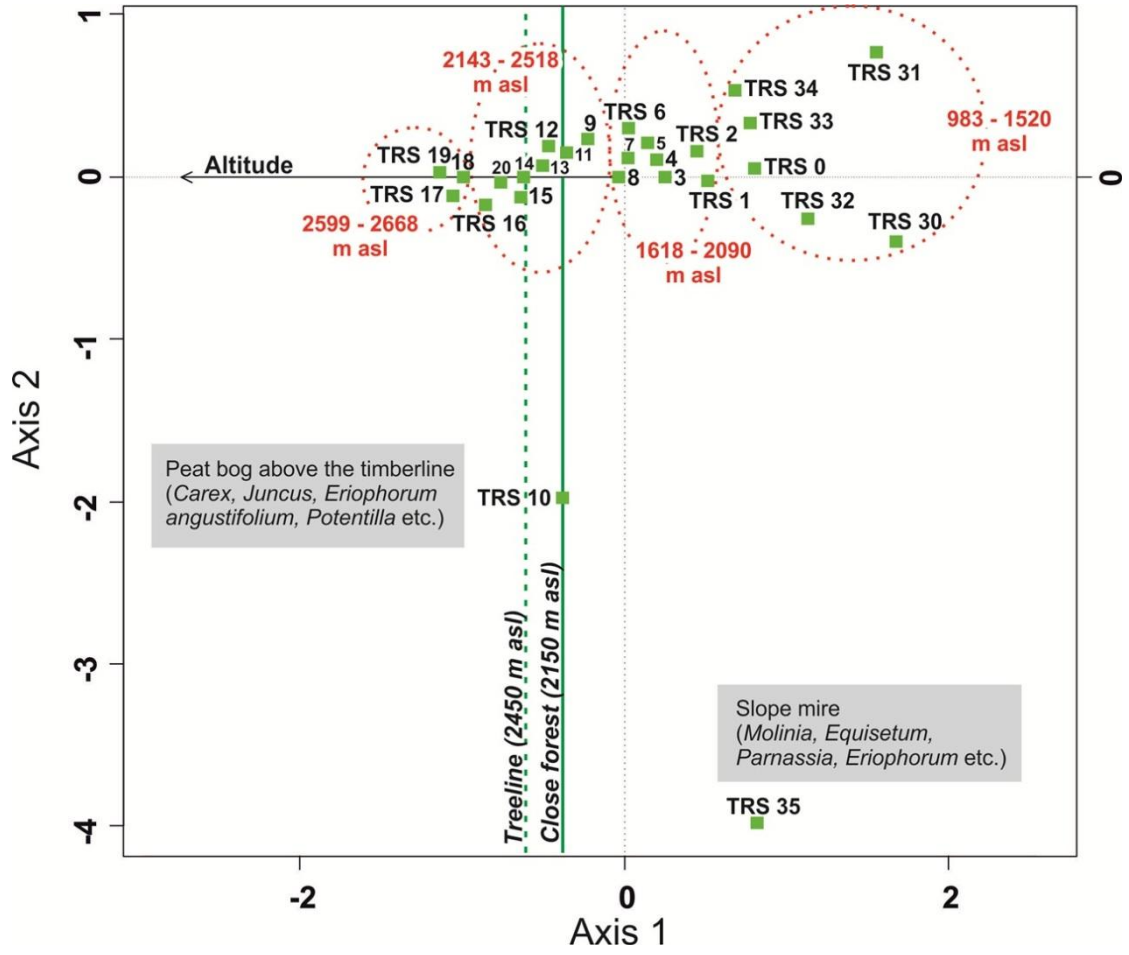

Fig. 4 – Biplot of the first two CCA axes for the vegetation data-set, representing the dispersion and grouping of sampling sites.

4.2. Modern pollen assemblages

The pollen spectra of 27 surface samples are presented in a synthetic percentage diagram, which includes selected pollen types and total microcharcoal concentrations (**Fig. 5 A-B**). The lower part of the diagram is clearly dominated by tree pollen types, while herbaceous species and shrubs are more poorly represented. At higher altitudes, herbaceous pollen becomes more abundant (especially above 2100 m), while trees and shrubs experience a small decrease. Five zones were found to be statistically significant. **Zone I** (from the base to 1563 m asl) shows a low taxonomic richness, and is dominated by *Picea, Pinus sylvestris/mugo, Betula* and *Corylus*. Notably, *Pinus cembra* percentages are low, while the higher values of *Abies alba* beside all pollen record is documented in this pollen zone (ca. 8%). Cultivated trees are also present (e.g.

Juglans regia, *Castanea* and *Olea*). Among herbs, Gramineae are abundant, whereas most of the other herb types have low percentages (e.g. Cichorioideae, Umbelliferae, Cruciferae and Ranunculaceae). Likewise, anthropogenic indicators (*Rumex acetosa* and *Plantago lanceolata*) show low values, under 1%. The dung spore *Sporormiella* reach its maximum value at the site TRS 34 (1,7%). Microcharcoal concentration (especially the large size class: 50<D>250 μm), shows the highest values in this pollen zone, up to 1000 part./cm^3.

Zone II ranges from 1510 m to 1722 m asl and is characterized by the dominance of *Picea* and the relatively high abundance of *Pinus cembra* and *Pinus sylvestris/mugo*. *Abies* and *Larix* are important in some sites of this zone. Among deciduous trees, *Alnus glutinosa, Betula and Corylus* are the most common ones. Herbs are scarce. This pollen zone shows high AP (arboreal pollen) values up to 80-90%, which is indicative of close coniferous woodlands. However, the TRS 33 site has lower AP value: the open structure (dry meadows surrounded by coniferous woodland) and the presence of possibly grazed areas (*Plantago lanceolata* reach 8%) may explain the under-representation of AP taxa. **Zone III** embraces all samples between 1781 m and 2090 m asl. It is characterized by relatively high abundance of coniferous taxa (*Pinus cembra*, *Picea* and *Pinus sylvestris*) and low deciduous trees and shrub pollen, except for *Alnus glutinosa*. Besides grasses, other herb pollen types are present e.g. Umbelliferae, Caryophyllaceae, Ranunculaceae and *Aster* type. The amount of AP is high, ca. 80%.

The following **Zone IV** (2143 – 2518 m asl) is above the close forest and encompasses the treeline ecotone. Compared with the lower belts, *Picea* shows lower pollen % values while *Pinus cembra* maintains steady percentages, while higher % values are recorded by *Pinus sylvestis/mugo*. Furthermore, an increase in both abundance and diversity of herbs and shrubs pollen is evident. Among shrubs, *Alnus viridis* records its higher values (up to 8%), together with relatively high abundance of *Vaccinium* and *Juniperus*. A general increase in % values of Gramineae, Caryophillaceae, Umbelliferae, *Plantago alpina*, Saxifragaceae are also evident. As for anthropogenic indicators, *Rumex acetosa* type and *Plantago lanceolata* type reach the maximum value respectively at the site TRS 13 (9,9%) and TRS 15 (5,2%). In both sites the dung spore *Sporormiella* is missing (TRS

15) or present with very low abundances (0,2% at the site TRS 13). Mires and wetland situated within this altitudinal range (TRS 16, 15, 10) show higher values of herbs pollen, notably Gramineae and Cyperaceae. Low percentages of cultivated trees pollen (eg. *Juglans, Castanea* and *Olea*) occurs also in this zone.

Zone V embraces all samples above 2599 m asl and is characterized by relatively high abundance of Gramineae, and low tree pollen, except for *Pinus sylvestris/mugo*. Among shrubs, only *Salix* reaches high values in TRS 17. Besides grasses, other herb pollen types are represented by Cruciferae, *Anthemis* type, *Aster* type, *Campanula*, *Galium* and Saxifragaceae. The only pollen grain of *Cerealia* identified in the whole transect is documented at the site TRS 17. In general, zone V shows increasing abundance and diversity of herb pollen. As in the case of vegetation, there is a well-defined altitudinal gradient that explains the distribution of pollen content of the different samples (species–environment correlation: $r = 0.98$, $p < 0.001$), which is represented by axis 1 (**Fig. 6**). Treeline, which occurred between the sites TRS 14 (2348 m asl) and TRS 15 (2467 m asl), may be situated around the score -0.3 of the axis 1. Axis 2 has a higher separation power, indeed it clearly divides the middle-altitude sites (between TRS 1 and TRS 7) from the lower/higher-altitude sites, suggesting some gradient related to forested sites towards more open areas characterized by higher NAP.

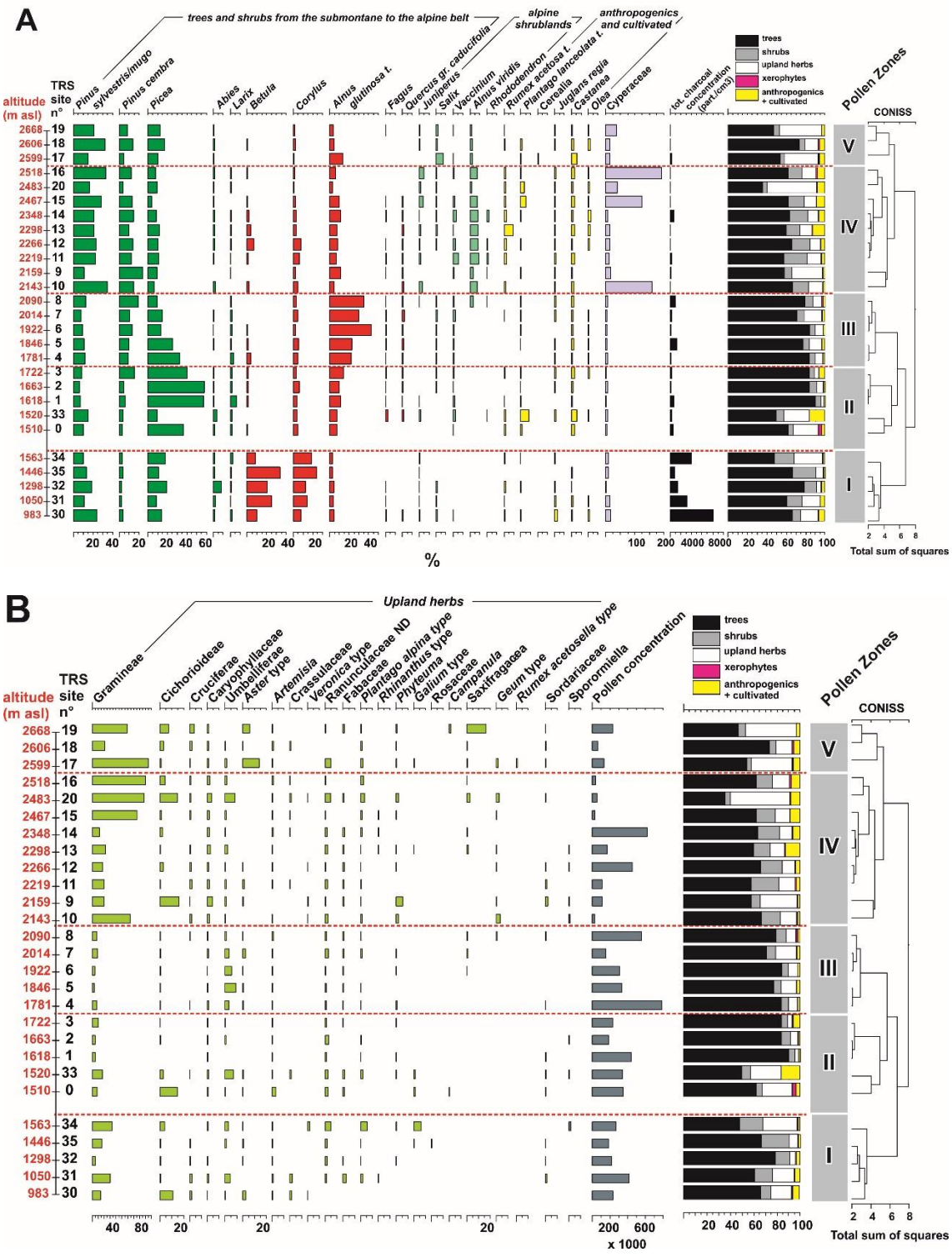

Fig. 5 - Percentage palynological record of selected taxa plotted on altitude scale and zoned by constrained clustering. (A) Green: Conifers; Red: deciduous taxa; Light green: shrubs; Yellow: anthropogenic and cultivated taxa; Light grey: Cyperaceae; Black: microcharcoal concentration. (B) Olive green: upland herbs; Dark grey: pollen concentration.

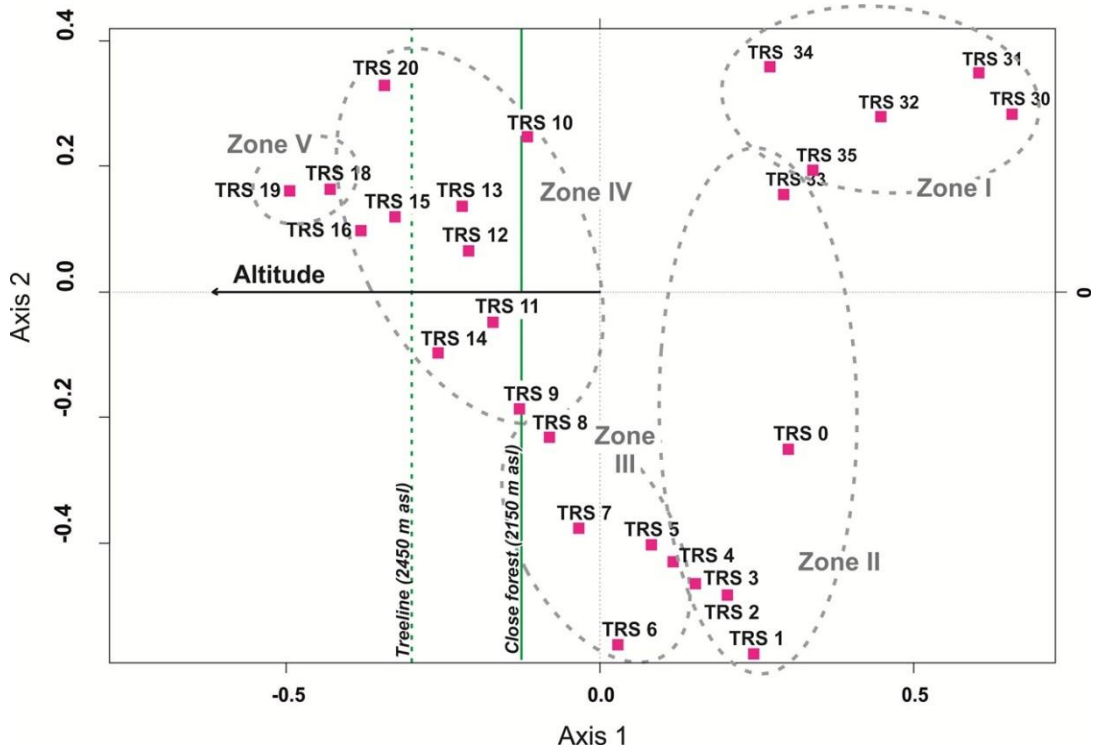

Fig. 6 - Biplot of the first two CCA axes for the pollen data set, with sampling sites grouped according to the pollen zones obtained.

4.3. Estimated climate and terrain parameters

The mean values of the calculated seasonal temperature Tspring (March, April, May), Tsummer (June, July, August), the temperature of the coldest month (Tjan), and the total annual precipitation (Pannual) are listed in **Table 2.** Those variables have been used in the statistical analysis and have been associated to each moss sample site collected. In **Table 2** are also presented the mean values obtained for the morphological parameters: aspect, slope, insolation and curvature.

Rutor TRS sites	Morphometric parameters					Climate parameters			
	Altitude (m asl)	Aspect (degrees)	Slope (degrees)	Insolation (Wh/m^2)	Curvature (m^{-1})	Pann (mm)	Tspring (°C)	Tsummer (°C)	Tjan (°C)
TRS 19	2668	190.24	21.06	1469594.83	0.29	1194	-2.66	6.58	-7.45
TRS 18	2606	217.93	27.09	1302222.21	-0.32	1177	-2.25	7.00	-7.19
TRS 17	2599	233.54	20.52	1216576.6	-0.05	1172	-2.19	7.05	-7.16
TRS 16	2518	254.26	29.03	1253724.40	-0.11	1129	-1.67	7.60	-6.85
TRS 20	2483	126.10	21.11	1332474.97	0.12	1173	-1.34	7.83	-6.72
TRS 15	2467	259.32	27.54	1248347.28	-0.09	1170	-1.24	7.94	-6.68
TRS 14	2348	275.48	37.41	1116379.17	-0.35	1095	-0.55	8.75	-6.12
TRS 13	2298	249.70	39.76	1209792.03	-0.31	1082	-0.11	9.10	-5.90
TRS 12	2266	236.31	39.65	1285117.84	-1.39	1068	0.10	9.32	-5.77
TRS 11	2219	205.16	27.56	1457917.53	-0.33	1041	0.32	9.63	-5.56
TRS 9	2159	195.43	16.83	1173581.80	-0.13	975	0.75	10.04	-5.23
TRS 10	2143	169.01	2.56	1261076.72	-0.05	992	0.92	10.14	-5.22
TRS 8	2090	305.50	37.06	830322.70	0.04	939	1.21	10.51	-4.94
TRS 7	2014	314.51	41.80	748392.16	-0.09	907	1.72	11.03	-4.60
TRS 6	1922	303.99	40.99	678646.78	-0.11	866	2.36	11.64	-4.18
TRS 5	1846	257.39	29.60	1037674.18	-0.48	849	2.88	12.15	-3.84
TRS 4	1781	234.92	22.56	1189620.72	0.08	824	3.37	12.57	-3.62
TRS 3	1722	253.43	32.99	858631.10	-0.34	798	3.73	12.96	-2.97
TRS 2	1663	287.58	30.47	876864.11	-0.02	786	4.14	13.33	-2.70
TRS 1	1618	204.45	19.83	977089.70	0.03	774	4.43	13.62	-2.49
TRS 33	1520	261.04	20.16	1161193.92	0.20	749	7.91	16.98	0.10
TRS 0	1510	252.32	19.05	1179965.55	-0.23	750	5.00	14.21	-2.08
TRS 34	1563	119.04	15.22	1303580.55	-0.10	814	6.33	15.66	-1.09
TRS 35	1446	92.64	19.54	1175918.26	-0.46	752	5.01	14.23	-2.05
TRS 32	1298	34.71	30.44	763496.50	-0.23	684	5.47	14.67	-1.82
TRS 31	1050	44.69	20.89	957623.93	0.14	592	4.72	13.89	-2.63
TRS 30	983	63.14	20.41	882342.19	-0.38	549	8.31	17.39	-0.14

Table 2 – Mean values of morphometric and climate parameters for each sampling site.

4.4. Fidelity and dispersibility

When considering co-occurrence of pollen and plant taxa regardless of the vegetation type, indices of fidelity and dispersibility help to decide whether a taxon can be a good indicator of its nearby presence or whether its pollen is effectively dispersed from its source. The representation of major taxa in the pollen rain based on the data for all sites was defined according to values of fidelity and dispersibility indices (**Fig. 7**). The following patterns were distinguished: 1) taxa having very high values of fidelity and dispersibility (over 80%), include only Cyperaceae, *Alnus glutinosa* type, *Picea*, Gramineae and *Pinus cembra*; 2) taxa presenting high values of fidelity (~100%) and low dispersibility (0–25%), include tree taxa: *Tilia*, *Abies*, *Fraxinus excelsior* and *Betula*; 3) taxa characterized by fidelity values between 30% and 60%, but low dispersibility (less than 20%), comprising only a tree taxa (*Larix*), shrubs (*Vaccinium* and *Rhododendron*) and herbs (*Plantago alpina* type, Cichorioideae, *Aster* type) among others; 4) taxa defined by low fidelity (25–10%) and low dispersibility (less than 20%), including *Anthemis* type, *Geum* type, *Veronica* type and *Galium* type while among dwarf shrubs: *Salix*. *Alnus viridis* is represented reasonably well in the pollen record with moderate dispersibility, generally reflecting the local presence of the taxa. Of particular note, some outliers characterized by very low values of fidelity and variable dispersibility values (10-40%) are *Phyteuma*, Cruciferae, Ranunculaceae and *Juniperus*. The latter is a relatively common pollen taxon, but its pollen was not recovered from the location where the plant grew.

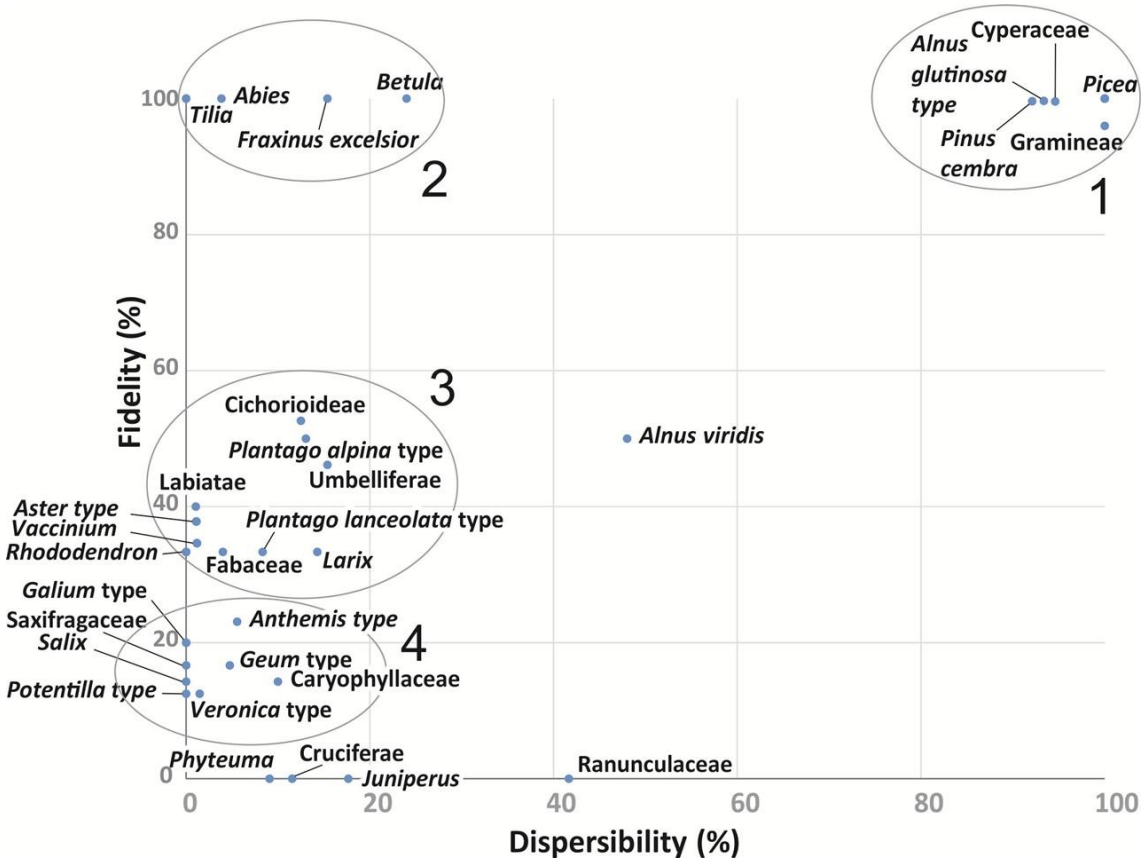

Fig. 7 – Dispersibility index (percentage of sites where a taxon is only recorded in the pollen rain) versus fidelity index (percentage of sites where a taxon coincides both in pollen and vegetation) scores for individual taxa over 2% of abundance in at least one sample. Four patterns were recognised: 1) very high fidelity and dispersibility, 2) high fidelity and moderate dispersibility, 3) high fidelity and low dispersibility and 4) very low fidelity and dispersibility.

4.5. Canonical Correspondence Analysis (CCA)

This study aims at emphasizing pollen/vegetation/environmental relationships at a local scale. Indeed, although extra-local and regional non-arboreal pollen is present in the modern pollen spectra, herbaceous pollen assemblages appear to reflect predominantly local vegetation rather than wider landscape units, as also demonstrated by Hjelle (1999), Caseldine and Pardoe (1994) and Pardoe (2001). The canonical correspondence analysis (CCA) of the vegetation and pollen data-sets, suggests that the variation in the vegetation and pollen assemblages is strongly correlated to the altitudinal gradient, to such a degree that possible relationships between pollen/vegetation and climate or morphometric variables

are largely obscured. The variances explained by each environmental parameter, calculated with CCA ordinations with unique constrained, are presented in **Table 3**. For the vegetation 1.8 m, the six more significant explanatory variables (after 999 unrestricted permutations) are: altitude (8,19%), aspect (7,25%), Tspring (7,52%), Tsummer (7,55%), Tjan (7,42%) and Pannual (8,08%). Other explanatory variables seem to be less relevant, namely insolation, slope and curvature ($p > 0.05$, after 999 unrestricted permutations). For the vegetation 10 m, the variance explained are altitude (9,64%), insolation (6,16%), aspect (7,96%), slope (5,73%), Tspring (8,63%), Tsummer (8,65%), Tjan (8,39%) and Pannual (9,43%). Curvature is not significant. For pollen assemblages, the seven significant variables are: altitude (17,10%), insolation (9,51%), aspect (11,87%), Tspring (16,06%), Tsummer (16,16%), Tjan (16,12%) and Pannual (16,57%). Curvature and slope are not significant ($p > 0.05$, after 999 unrestricted permutations).

CCA plots (axes 1 and 2) of the 27 sites and 37 selected vegetation species (radius=1,8 m and radius=10 m) in relation to nine explanatory variables, considered all together, are respectively shown in **Fig. 9** and **Fig. 10.** In **Fig. 9** the 9 variables explain 44,78% of the variation in the vegetation data on a very local scale: 1,8 m radius (ca. 10 m^2). Axis 1 contrasts lower altitude on the positive side of the plot with higher altitude sites, on the negative side. Furthermore it is well correlated and shows a strong gradient with altitude, Pannual and Tjan, Tspring, Tsummer. Axis 2 contrasts forested sites on the negative side of the plot with treeless/humid sites on the positive side. A weaker correlation with the second axis include slope, aspect and curvature. The relationship between the alpine belt sites (TRS 13, 14, 16, 18, 19, 17) with Pannual and insolation is noteworthy. Moreover the correspondence between individual species (e.g. *Nardus stricta*) and insolation is shown in **Fig. 9**. Aspect seems to be particularly important for intermediate altitude sites (between TRS 0 and TRS 12) characterized by the importance of *Pinus cembra, Picea* and *Larix decidua*. There is also a clear association between lower sites (TRS 30, 31, 32, 34, 35) and *Plantago lanceolata*. A similar pattern is shown in **Fig. 10**. Here, the nine climate and morphometric variables explain 43,74% of the variation in the vegetation data on a local scale: 10 m radius (ca. 314 m^2). Insolation is important

for higher altitudinal sites, especially for some species: *Geum montanum*, *Nardus stricta*, *Salix erbacea* and *Ligusticum mutellina*. Moreover, *Salix foetida* is related to the precipitation parameter. Aspect and slope are important variables for the middle altitude sites. It is noteworthy the correspondence between the variable slope and the species *Pinus cembra*. Temperature has a major relationship with lowermost sites and in particular with the species *Picea abies*. The montane belt is characterized mainly by *Betula alba, Abies alba, Salix capraea, Fraxinus excelsior, Plantago media* and *Plantago lanceolata*.

Fig. 11 shows the CCA plot (axes 1 and 2) of the 27 sites and 38 selected pollen taxa in relation to the nine explanatory variables. All variables explain 57,23% of the variance within pollen data. Axis 1 is well correlated with altitude, Pannual and Tjan, Tspring, Tsummer. Axis 2 shows a weak correlation with slope, aspect and insolation. The latter has an influence on higher sites and with some pollen types: *Juniperus, Rumex acetosa* type*, Anthemis* and *Plantago alpina* type*.* Precipitation is the most important parameter for *Alnus viridis*, while slope and aspect variables seems to be important for sites at the timberline (TRS 8, 7, 6). The sites at lower altitudes (TRS 30, 31, 32, 33, 34, 35), dominated by *Corylus, Larix, Tilia, Betula* and *Abies,* display major relation with temperature.

Pollen % Dataset

	terrain parameters					climate parameters			
	altitude	insolation	aspect	slope	curvature	Tspring	Tsummer	TJan	Pann
variance explained	17.10%	9.51%	11.87%	5.91%	3.70%	16.06%	16.16%	16.12%	16.57%
p	0.001***	0.003**	0.001***	0.105	0.528	0.001***	0.001***	0.001***	0.001***

Vegetation 1.8 m Radius Dataset

	terrain parameters					climate parameters			
	altitude	insolation	Aspect	slope	curvature	Tspring	Tsummer	TJan	Pann
variance explained	8.19%	5.22%	7.25%	5.12%	3.76%	7.52%	7.55%	7.42%	8.08%
p	0.001***	0.069	0.001***	0.128	0.627	0.001***	0.001***	0.001***	0.001***

Vegetation 10 m Radius Dataset

	terrain parameters					climate parameters			
	altitude	insolation	aspect	slope	curvature	Tspring	Tsummer	TJan	Pann
variance explained	9.64%	6.16%	7.96%	5.73%	3.34%	8.63%	8.65%	8.39%	9.43%
p	0.001***	0.001***	0.001***	0.013	0.666	0.001***	0.001***	0.001***	0.001***

Significance codes: *** 0.001; **0.01

Table 3 – Proportions of variance explained by each explanatory variable as the sole constrained and permutational-repeated measures analysis (ANOVA) obtained for pollen % data-set and vegetation data-set (surveys at 1,8 m and 10 m radius circles).

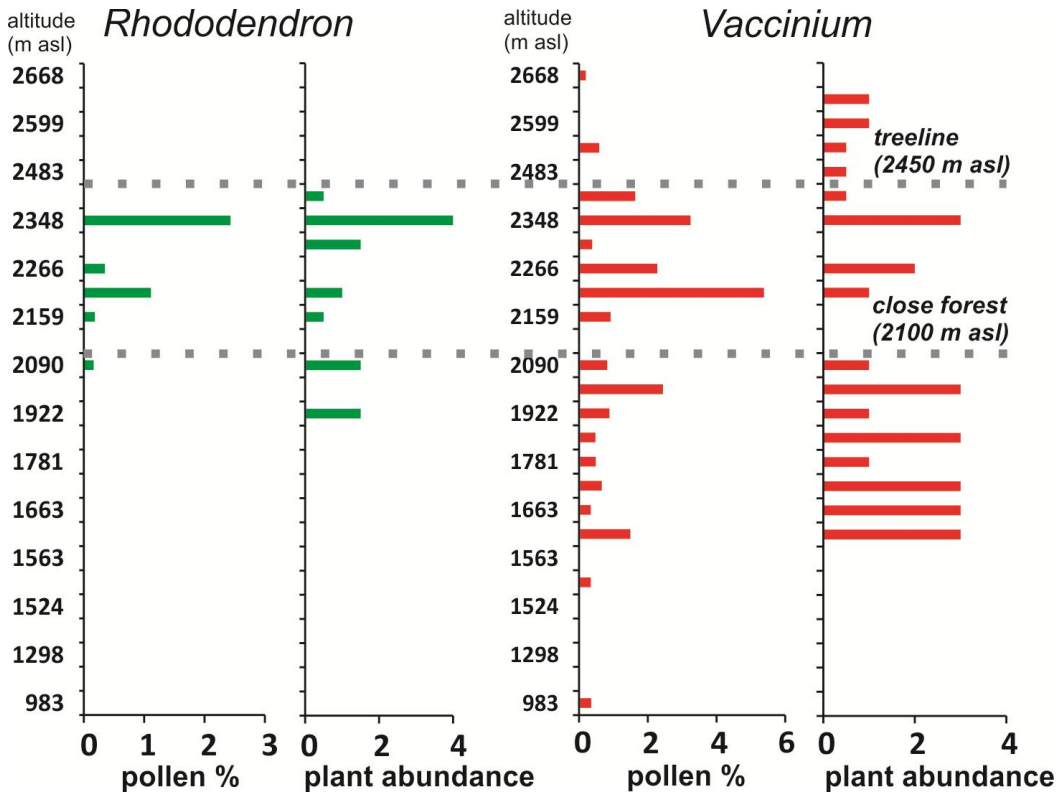

Fig. 8 – Comparison of pollen percentages and plant abundance of two good indicator taxa along the altitudinal transect: *Rhododendron* and *Vaccinium*

5. DISCUSSION

5.1. Pollen-Vegetation relationships

Arboreal pollen types dominate nearly in all the moss spectra, so that herb and dwarf-shrub pollen is only poorly represented, generally showing relatively low values, except for a few cases (e.g. Gramineae in the sites TRS 19, 17, 16, 20, 15, 10 and Cyperaceae in the sites TRS 16, 20, 15, 10). Pollen spectra from sites located in conifer forests are generally characterized by high amounts of AP, up to 90%; the same is true for spectra from open mixed deciduous forest (e.g. TRS 35), where AP reaches 60-70%. The AP/NAP ratio is never below 40%, not even in treeless sites, where AP can reach more than 70%. These results thus highlight the difficulty of making reliable reconstructions about forested versus open landscapes based on AP/NAP ratio, often believed to be a good index of local tree cover. Pollen belts tend to be wider and with less defined boundaries than vegetation; this is likely due to the homogenizing effect of wind dispersal,

especially from lower to upper altitudinal levels. This effect is clearly shown by *Pinus*; pine trees do not penetrate into the upper alpine belt, but pine pollen is abundant up to the highest part of the transect. The most striking feature is the strong pollen signal of *Pinus sylvestris/mugo* over the whole study area, especially for places where no other efficient wind-pollinated plants are locally common. This evidence is also documented in a transect in the French Alps (Court-Picon, 2006). Pollen of *Pinus cembra* appears in almost all plots, even where this tree doesn't occur or it is rare. Its fidelity and dispersibility indices > 80% (Group 1 in **Fig. 7**) highlight its strong dispersal ability. This over-representation of *Pinus* in the pollen assemblages is well documented by numerous authors (e.g. Broström et al. 1998; Brugiapaglia et al. 1998; Ortu et al. 2005, 2006; Court- Picon et al., 2005, 2006, Cañellas-Boltà et al., 2009). Deciduous trees (*Betula, Corylus, Quercus, Tilia* and *Alnus*) also show upward wind transport, but to a lesser extent and abundance.

The most abundant herb pollen belongs to the family Gramineae which is well represented in multiple ecological conditions, from mown meadows (TRS 31 and TRS 34) to grazed dry meadows (TRS 33), from semi-natural grasslands above the timberline (TRS 9, 11, 13) to telmatic meadows (*Nardus stricta* with *Leontodon* cf. *helveticus*) strongly adapted to the seasonal hydrological cyclicity (TRS 17). Except for mires and wetland sites (TRS 16, 15, 10), the proportions of Gramineae are globally higher in the alpine belt above the treeline rather than in forested sites; a large amount of this pollen type may therefore be considered as an indicator of open conditions. Some herbs are mainly present above the coniferous close forest (ca. 2100 m asl): e.g. *Hypericum* and *Veronica* type. Interestingly, *Geum* type is only present in the uppermost pollen spectra, within the timberline ecotone. However, the little contribution to pollen rain and poor transport ability (see Group 4 in **Fig. 6**) suggest that their lack from the pollen assemblages cannot be interpreted as absence in the local vegetation. Indeed, *Geum* type is characterize by reduced sexual reproduction and supported by clonal offspring to ensure population growth in less favourable years (Weppler et al., 2006).

The precise altitudinal treeline placement is not easily reconstructed with the aid of pollen spectra only. However, some taxa can help to broadly define thresholds

to distinguish different environments: e.g. the close forest, the timberline ecotone and the treeless alpine meadows. For example, pollen % of Cichorioideae, Saxifragaceae, Crassulaceae, *Aster* type and *Plantago alpina* type increase above the treeline (ca. 2450 m asl). Among these, only *Plantago alpina* type and Cichorioideae show relatively high fidelity and moderately low dispersibility values (Group 3 in **Fig. 6**) and would appear to be good indicators of local occurrence when the pollen is found. Likewise, the dwarf shrubs *Salix herbacea* and *Salix foetida* are present and locally more abundant above the treeline (**Fig. 5**) but they could be rare in a pollen record due to their fidelity and dispersibility low values (Group 4 in **Fig. 6**). Among shrubs, Ericaceae is considered an excellent indicator of the montane/subalpine belts (Cañellas-Boltà et al., 2009). In our study, the identification of pollen types within this family allows to highlight different altitudinal patterns of pollen and relative parent taxa. Interestingly, *Rhododendron ferrugineum* shows a consistent pollen–vegetation altitudinal pattern restricted to the timberline ecotone between 2100 and 2400 m asl (**Fig. 8**) and relatively high fidelity and moderate low dispersibility values (Group 3 in **Fig 6**). Furthermore, it could be useful as a key taxa for past vegetation boundaries reconstructions. Differently, *Vaccinium* pollen type shows a wider distribution from the montane to the alpine belts, due to its identification at genera level, thus it results less suited for this purpose. As for parent taxa, between 1600 and 2200 m asl occurred *Vaccinium vitis idaea*, accompanied by *Vaccinium myrtillus* up to 2400 m asl. At higher altitudes (2350 - 2600 m asl) *Vaccinium gaultherioides* is a common species, occurring on steep slopes with scattered shrubs (*Juniperus nana* and *Rhododendron ferrugineum*).

However, the use of other types of evidence, such as PARs (Pollen Accumulation Rates), macrofossils and conifer stomata remains are needed to trace past treeline displacements (Hansen, 1995; Tinner et al., 1996; Hicks, 2001; Tinner & Theurillat, 2003; Seppä and Hicks, 2006; Finsinger et al., 2007).

Other herbs do not show any potential as altitude indicators, indeed they have been recorded in all samples, both from open and forested sites. These are notably Caryophyllaceae, Umbelliferae, Labiatae and Ranunculaceae. In these cases, issues of detailed pollen identification (up to the genus/species level) may be involved; most of the genera and species of herbaceous plants from various

vegetation types are identified at the family or genera level, which leads to some homogenization of pollen assemblages. The record of *Artemisia* is a clear example of a well-dispersed taxa. It produces high amount of pollen and occurs systematically in all pollen spectra (**Fig. 5 B**) as already reported in other studies (Gaillard et al. 1992, 1994; Hjelle, 1997; Bunting, 2003). A single pollen grain of *Cerealia* is documented in the site TRS 17 at 2599 m asl. The lack of cultivated fields along the altitudinal transect suggests a long distance transport from the valley floor. Indeed, the long distance pollen transport of *Cerealia* is a well-known feature, especially in mountain environments (Brugiapaglia et al., 1998; Hicks et al., 2001). Note, however, that *Plantago lanceolata*, traditionally associated with grazing (Behre, 1981), is present along all transect with pollen values fluctuating around 0,5% (only two peaks occurred at 1520 m asl and 2467 m asl, slightly higher than 5% - **Fig. 5A**). Hjelle (1998) suggests that *Plantago lanceolata* pollen percentages lower than 5% indicate the absence or low frequencies of the plant within 10x10-m plots. Moreover, *Plantago lanceolata* shows a positive relationship between pollen and plant percentages only when the plant is present with frequencies up to 10%. Court-Picon (2005) highlighted the good pollen dispersal of this taxon and its no or little indicative value for human practice along an altitudinal transect in the French Alps. Furthermore, Brostrom et al. (2004) calculated relative pollen productivity estimates (PPEs) for several herbs including *Plantago lanceolata*, showing its higher PPEs than Poaceae. Indeed, this species is characterized by long-distance transport and may originate from a wide landscape, for these reasons it should be interpreted with caution in fossil pollen assemblages.

The case of *Olea* is especially noteworthy. In our transect, despite the absence of the parent plant which is confined in the valley floor, its pollen occurs regularly at any altitude with maximum values around the treeline (1-2%). *Olea* is a lowland mediterranean tree and the known dispersion power of this pollen type is of about 50 km from its source (Osborne et al., 2000). Likewise, the influence of upslope wind dispersal of other arboreal pollen taxa e.g. *Castanea* and *Juglans* have to be taken into account and interpreted with caution in the fossil records.

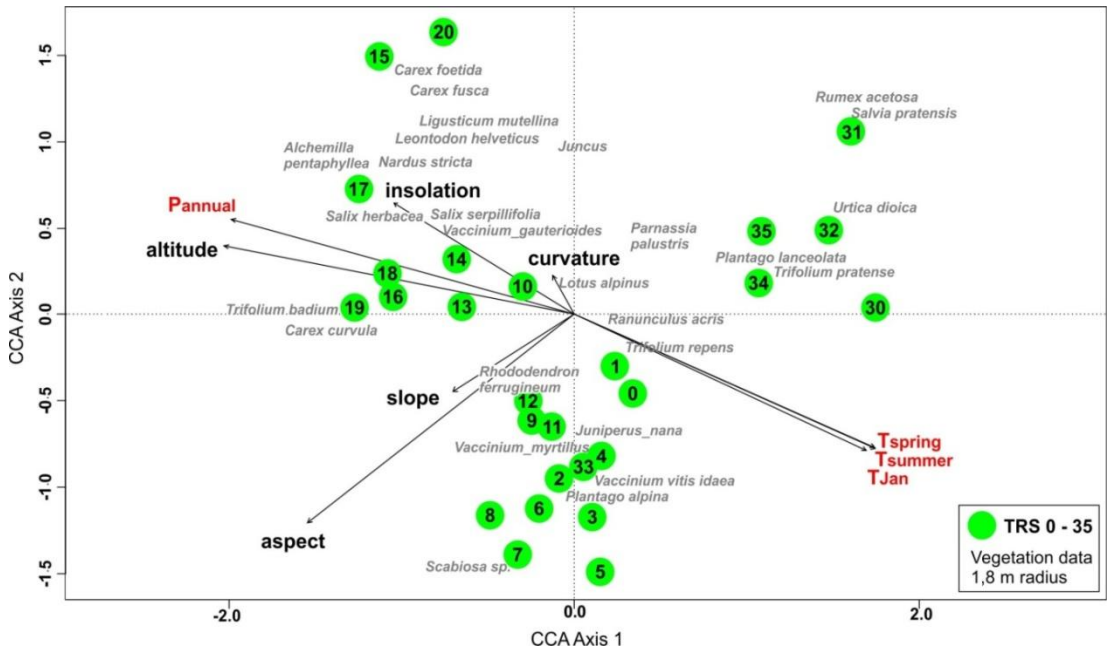

Fig. 9 – Canonical correspondence analysis (CCA) plot of the vegetation data (survey at 1,8 m radius circles) in relation to 4 climate variables (in red) and 5 morphometric variables (in black) on CCA axes 1 and 2 (CCA1: 19,2%, CCA2: 14,5%). The total variance explained by all parameters is 44.78%.

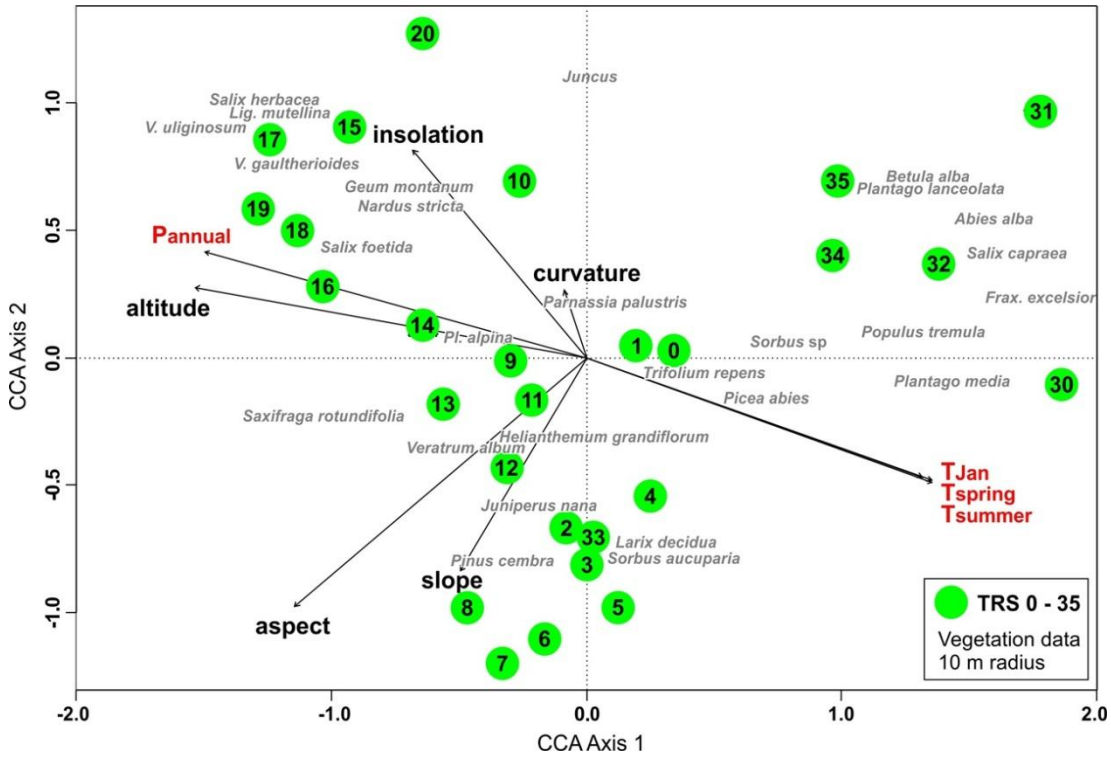

Fig. 10 - Canonical correspondence analysis (CCA) plot of the vegetation data (survey at 10 m radius circles) in relation to 4 climate variables (in red) and 5 morphometric variables (in black) on CCA axes 1 and 2 (CCA1: 23,3%, CCA2: 14,9%). The total variance explained by all parameters is 43.74%.

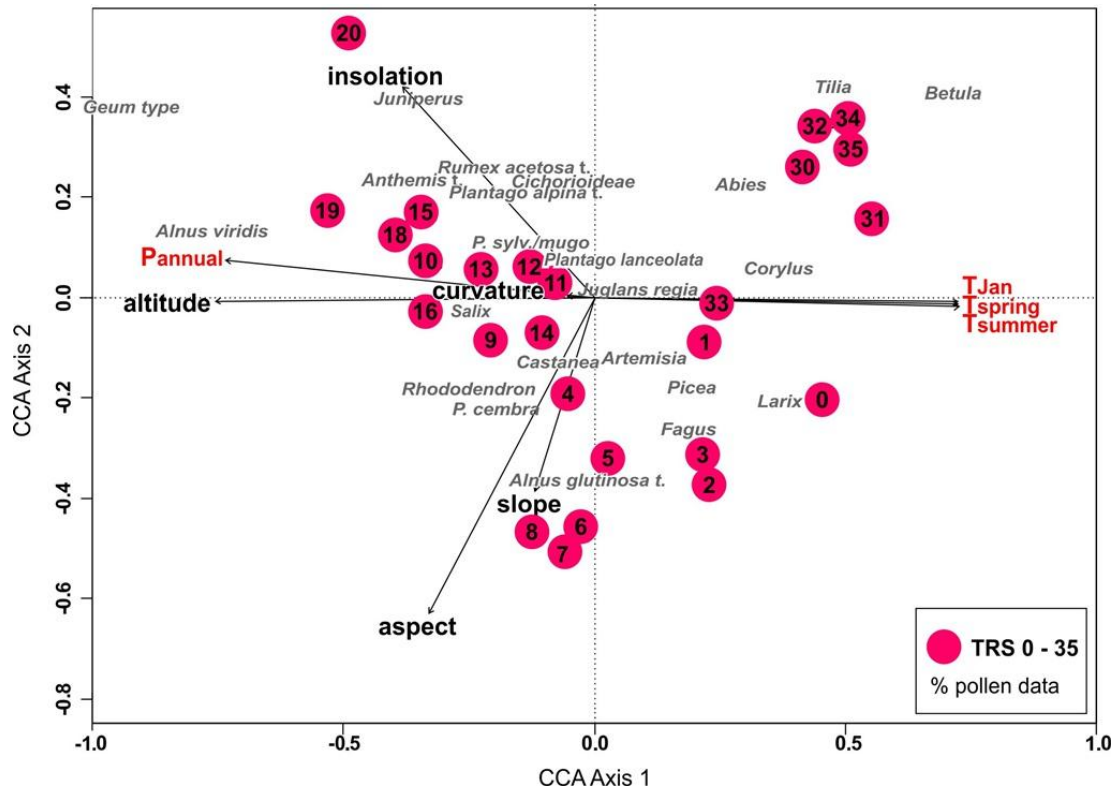

Fig. 11 - Canonical correspondence analysis (CCA) plot of the pollen % data in relation to 4 climate variables (in red) and 5 morphometric variables (in black) on CCA axes 1 and 2 (CCA1: 32,7%, CCA2: 21,4%). The total variance explained by all parameters is 57.23%.

5.2. Pollen/climate/environment relationships

Our data are in agreement with previous studies which identified altitude as the main gradient controlling modern pollen assemblages and vegetation distribution across mountain regions (Bonnefille et al., 1993; Vincens et al., 1997; Weng et al., 2004; Court-Picon 2005, 2006; Rull, 2006; Cañellas-Boltà et al., 2009). Axis 1 of the CCA plots (**Fig. 9-10-11**) represents an altitudinal gradient, from lower (positive values) to higher (negative values) altitudes, clearly separating sites of the lower eastern part of the valley (village of Morgex) from those collected in the N-W upper part (La Thuile). Together with altitude, climate variables: temperature (Tspring, Tsummer, TJan) and the rainfall (Pann), are highly positively correlated to CCA axis 1. Moreover, these variables are found to be stronger in the pollen data-set (**Fig. 11**). Here, e.g. *Alnus viridis* shows high association with the rainfall variable (**Fig. 11**). In mountain environments, factors associated with altitude

(decrease in temperatures and length of the growing season, increase in rainfall and snow cover) play a significant role in diminishing the tree cover (Tranquillini, 1979, Körner, 2007).

Deciduous mixed forest with *Abies alba* sites (TRS 30-35) have their best fit on the positive side of axis 1 of the CCA plots where they are grouped and well separated from the uppermost sites. Sites above 1500 m asl show a continuous gradient along axis 1, while they seem to be better separated in different groups along axis 2. Here a more complex gradient from dense canopy towards more open vegetation (inferred from pollen data) and water availability (visible from vegetation data) is documented. In the lower half of the CCA plot close coniferous woodlands sites are well segregated from open treeless sites above treeline, which are arranged in the upper left quadrant of the plot. Between these two groups, sites located in the transitional zone of the open forest/treeline ecotone are also influenced by aspect and slope variables. Slope, noteworthy, is highly positively correlated with *Pinus cembra* (**Fig. 10**).

At a local vegetation scale (1,8 m radius) as well as at a larger scale (10 m radius), the scores of the mires and wetlands sites are placed in the upper left quadrant of the plot according to their surrounding vegetation (TRS 20, 15, 17, 10).

Treeless sites above 2450 m asl are related to the insolation variable. Insolation increases with altitude because of reduced atmospheric turbidity (increased transmissivity). However, for solar radiation in general, and the dose per day in particular, there is no global altitudinal trend (Körner, 2007). In the study area insolation increases with altitude, spanning between ~882.342 Wh/m^2 (983 m asl) and ~1.469.594 Wh/m^2 (2668 m asl). The distribution of *Nardus stricta* grasses seems to be connected with this variable (**Fig. 9-10**), whereas *Juniperus* is strongly associated with insolation in the pollen dataset (**Fig. 11**). Thus, between 1500-2660 m asl, altitude effects on temperature interact with land surface characteristics (eg. inclination/direction of slopes and aspect) and concurrent solar radiation, producing evaporative forcing that differs strongly from standard meteorological data from lowlands.

Other species seem to be even related to rainfall (snow cover) variable: e.g. *Salix herbacea, Salix foetida* together with herbs such as *Alchemilla pentaphyllea* and *Geum montanum* (**Fig. 9-10**). The dwarf shrub willow displays a clear preference for wet ground and very exposed sites (Whittaker, 1985).

The curvature variable remains close to the origin in all the CCA plots, suggesting its slight and statistically insignificant effect on modern pollen and vegetation assemblages.

6. CONCLUSIONS

The development of an altitudinal transect in the western Italian Alps represents a first step in understanding the complex relationships between modern pollen, vegetation, elevation and key climate and environmental parameters: e.g. temperature, precipitation, aspect, insolation and slope, with implications for palaeoenvironmental and palaeoclimate reconstruction in this area.

High AP (arboreal pollen) values revealed that strong pollen producers and long-distance dispersed pollen taxa, especially *Pinus,* are dominant in almost all of the samples despite the large variation of landscape openness along the transect. This is mainly due to the increase in extra-local transport characterizing mountainous environments and lead to some homogenization of pollen assemblages. Thus, if it is possible to identify the major vegetation types by means of their modern pollen rain, it becomes more difficult to identify specific thresholds (e.g. treeline).

To overcome these limitations, several potential indicator pollen taxa of alpine/subalpine belts documented in this study could be useful for this purpose: *Rhododendron*, *Vaccinium*, *Salix* among shrubs and *Geum* type, *Hypericum* and *Veronica* type among herbs.

The results of CCA analysis demonstrated a general good agreement with previous studies, which identified altitude as the main gradient in the variation of modern pollen and vegetation assemblages in mountain areas. Together with altitude, climate variables: temperature (Tspring, Tsummer, TJan) and the rainfall (Pannual), are highly positively correlated to CCA axis 1. Notably, *Alnus viridis*

shows strong association with the rainfall variable. Moreover, at higher altitudes, CCA axis 2 becomes important showing a more complex gradient through dense canopy to more open vegetation (pollen data) and water availability (vegetation data). Our study highlights the increasing interplay of morphometric variables (e.g slope, aspect and insolation) along the altitudinal gradient and the combined effect with altitude-related trends. Slope, notable, is highly connected with *Pinus cembra.* Above the treeline, *Nardus stricta* and *Juniperus* are strongly associated with insolation.

Finally, the newly-obtained 27 pollen spectra and the climate data along the transect have been integrated into a continental dataset of modern pollen samples (EMPD - European Modern Pollen Database; Davis et al., 2013) and used for pollen-inferred climate reconstructions of fossil records in the Rutor area (**Chapter 2**).

REFERENCES

Behre, K. E. (1981). The interpretation of anthropogenic indicators in pollen diagrams. Pollen et spores, 23(2), 225-245.

Beug, H.J. (2004). Leitfaden der Pollenbestimmung für Mitteleuropa und angrenzende Gebiete. Verlag Dr. Friedrich Pfeil, München.

Birks, H. J. B., Heiri, O., Seppä, H., & Bjune, A. E. (2010). Strengths and Weaknesses of Quantitative Climate Reconstructions Based on Late-Quaternary. The Open Ecology Journal, 3(1).

Bonnefille, R., Buchet, G., Friis, I. B., Kelbessa, E., & Mohammed, M. U. (1993). Modern pollen rain on an altitudinal range of forests and woodlands in South West Ethiopia. Opera Botanica, 121, 71-84.

Braun-Blanquet J (1979). Fitosociologica. Blume, Madrid.

Broström, A., Gaillard, M. J., Ihse, M., & Odgaard, B. (1998). Pollen-landscape relationships in modern analogues of ancient cultural landscapes in southern Sweden—a first step towards quantification of vegetation openness in the past. Vegetation History and Archaeobotany, 7(4), 189-201.

Broström, A., Sugita, S., & Gaillard, M. J. (2004). Pollen productivity estimates for the reconstruction of past vegetation cover in the cultural landscape of southern Sweden. The Holocene, 14(3), 368-381.

Brugiapaglia, E., de Beaulieu, J. L., Guiot, J., & Reille, M. (1998). Transect de pluie pollinique et étagement de la végétation dans le massif du Taillefer (Isère, France). Géographie physique et Quaternaire, 52(2), 209-218.

Brunetti, M., Lentini, G., Maugeri, M., Nanni, T., Simolo, C., & Spinoni, J. (2012). Projecting North Eastern Italy temperature and precipitation secular records onto a high-resolution grid. Physics and Chemistry of the Earth. 40-41, 9-22.

Brunetti, M., Maugeri, M., Nanni, T., Simolo, C., & Spinoni, J. (2014). High-resolution temperature climatology for Italy: interpolation method intercomparison. International Journal of Climatology, 34(4), 1278-1296.

Bunting, M. J. (2003). Pollen-based reconstruction of cultural landscapes: an investigation of pollen source area for non-arboreal taxa. Rev Palaeobot Palynol, 125, 285-298.

Cañellas-Boltà, N., Rull, V., Vigo, J., & Mercadé, A. (2009). Modern pollen-vegetation relationships along an altitudinal transect in the central Pyrenees (southwestern Europe). The Holocene, 19(8), 1185-1200.

Caseldine, C., & Pardoe, H. (1994). Surface pollen studies from alpine/sub-alpine southern Norway: applications to Holocene data. Review of Palaeobotany and Palynology, 82(1), 1-15.

Court-Picon, M., Buttler, A., & de Beaulieu, J. L. (2005). Modern pollen–vegetation relationships in the Champsaur valley (French Alps) and their potential in the interpretation of fossil pollen records of past cultural landscapes. Review of Palaeobotany and Palynology, 135 (1), 13-39.

Court-Picon, M., Buttler, A., & De Beaulieu, J. L. (2006). Modern pollen/vegetation/land-use relationships in mountain environments: an example from the Champsaur valley (French Alps). Vegetation history and archaeobotany, 15(3), 151-168.

Davis, O.K. (1984). Pollen frequencies reflect vegetation patterns in a Great Basin (U.S.A.) mountain range. Rev. Palaeobot. Palynol. 40, 295–315.

Davis, B. A., Zanon, M., Collins, P., Mauri, A., Bakker, J., Barboni, D., ... & Bradshaw, R. H. (2013). The European modern pollen database (EMPD) project. Vegetation history and archaeobotany, 22(6), 521-530.

Deng, Y., Horrocks,M., Ogden, J., Anderson, S. (2006). Modern pollen–vegetation relationships along transects on the Whangapoua Estuary, Great Barrier Island, northern New Zealand. J. Biogeogr. 33, 592–608.

Fall, P. (2012). Modern vegetation, pollen and climate relationships on the Mediterranean island of Cyprus. Rev. Palaeobot. Palynol. 185, 79–92.

Finsinger, W., & Tinner, W. (2007). Pollen and plant macrofossils at Lac de Fully (2135 m asl): Holocene forest dynamics on a highland plateau in the Valais, Switzerland. The Holocene, 17(8), 1119-1127.

Fletcher, M.-S., Thomas, I. (2007). Modern pollen–vegetation relationships in western Tasmania, Australia. Rev. Palaeobot. Palynol. 146, 146–168.

Fu, P., Rich, P., & Wang, J. (2000). Integration of GIS with user models. In ESRI User Conference.

Fu, P., & Rich, P. M. (2002). A geometric solar radiation model with applications in agriculture and forestry. Computers and electronics in agriculture, 37(1), 25-35.

Gaillard, M. J., Birks, H. J. B., Emanuelsson, U., & Berglund, B. E. (1992). Modern pollen/land-use relationships as an aid in the reconstruction of past land-uses and cultural landscapes: an example from south Sweden. Vegetation history and archaeobotany, 1(1), 3-17.

Gaillard, M. J., Birks, H. J. B., Emanuelsson, U., Karlsson, S., Lagerås, P., & Olausson, D. (1994). Application of modern pollen/land-use relationships to the interpretation of pollen diagrams—reconstructions of land-use history in south Sweden, 3000-0 BP. Review of Palaeobotany and Palynology, 82(1-2), 47-73.

van Geel, B. (1978). A palaeoecological study of Holocene peat bog sections in Germany and The Netherlands, based on the analysis of pollen, spores and macro- and

microremains of fungi, algae, cormophytes and animals. Review of Palaeobotany and Palynology 25, 1-120.

van Geel, B., Bohncke, S.J.P., Dee, H. (1981). A palaeoecological study of an upper Late Glacial and Holocene sequence from 'De Borchert', The Netherlands. Review of Palaeobotany and Palinology 31, 367-449.

Grimm, E.C. (1987). CONISS: a FORTRAN 77 program for stratigraphically constrained cluster analysis by the method of incremental sum of squares. Comput. Geosci. 13 (1), 13-35.

Grimm, E.C. (1991-2011). Tilia 1.7.16. Illinois State Museum, Research and Collection Center, Springfield.

Hansen, B. C. (1995). Conifer stomate analysis as a paleoecological tool: an example from the Hudson Bay Lowlands. Canadian Journal of Botany, 73(2), 244-252.

Hicks, S. (2001). The use of annual arboreal pollen deposition values for delimiting tree-lines in the landscape and exploring models of pollen dispersal. Review of Palaeobotany and Palynology, 117(1), 1-29.

Hjelle, K. L. (1997). Relationships between pollen and plants in human-influenced vegetation types using presence-absence data in western Norway. Review of Palaeobotany and Palynology, 99(1), 1-16.

Hjelle, K. L. (1998). Herb pollen representation in surface moss samples from mown meadows and pastures in western Norway. Vegetation History and Archaeobotany, 7(2), 79-96.

Hjelle, K. L. (1999). Modern pollen assemblages from mown and grazed vegetation types in western Norway. Review of Palaeobotany and Palynology, 107(1), 55-81.

Körner, C. (2007). The use of ‘altitude’in ecological research. Trends in ecology & evolution, 22(11), 569-574.

Lisitsyna, O. V., Hicks, S., & Huusko, A. (2012). Do moss samples, pollen traps and modern lake sediments all collect pollen in the same way? A comparison from the forest limit area of northernmost Europe. Vegetation history and Archaeobotany, 21(3), 187-199.

Mazier, F., Galop, D., Brun, C., & Buttler, A. (2006). Modern pollen assemblages from grazedvegetation in the western Pyrenees, France: a numerical tool for more precise reconstruction of past cultural landscapes. The Holocene, 16(1), 91-103.

McGlone, M.S., Meurk, C.D. (2000). Modern pollen rain, subantarctic Campbell Island, New Zealand. N. Z. J. Ecol. 24, 181–194.

Moore, P.D., Webb, J.A., Collinson, M.E. (1991). Pollen Analysis. Blackwell Scientific Publications. Oxford University Press.

Ortu E, David F, Caramiello R. (2005). Effet des paramètres locaux sur le développement de la végétation dans le Vallon de St. Anna di Vinadio (Alpes Maritimes; Italie). E´ coscience 12: 122–135.

Ortu, E., Brewer, S., & Peyron, O. (2006). Pollen-inferred palaeoclimate reconstructions in mountain areas: problems and perspectives. Journal of Quaternary Science, 21(6), 615-627.

Ortu, E., Klotz, S., Brugiapaglia, E., Caramiello, R., & Siniscalco, C. (2010). Elevation-induced variations of pollen assemblages in the North-western Alps: An analysis of their value as temperature indicators. Comptes rendus biologies, 333(11), 825-835.

Osborne, C. P., Chuine, I., Viner, D., & Woodward, F. I. (2000). Olive phenology as a sensitive indicator of future climatic warming in the Mediterranean. Plant, Cell & Environment, 23(7), 701-710.

Pardoe, H. S. (2001). The representation of taxa in surface pollen spectra on alpine and sub-alpine glacier forelands in southern Norway. Review of Palaeobotany and Palynology, 117(1), 63-78.

Pardoe, H. S., Giesecke, T., van der Knaap, W. O., Svitavská-Svobodová, H., Kvavadze, E. V., Panajiotidis, S., ... & Latałowa, M. (2010). Comparing pollen spectra from modified Tauber traps and moss samples: examples from a selection of woodlands across Europe. Vegetation History and Archaeobotany, 19(4), 271-283.

Prentice, I. C. (1980). Multidimensional scaling as a research tool in Quaternary palynology: a review of theory and methods. Review of Palaeobotany and Palynology, 31, 71-104.

Punt, W., Blackmore, S. (Eds.) (1976-2009). The Northwest European Pollen Flora. vol. I-IX. Elsevier Publishing Company.

Räsänen, S., Hicks, S., & Odgaard, B. V. (2004). Pollen deposition in mosses and in a modified ‘Tauber trap’from Hailuoto, Finland: what exactly do the mosses record?. Review of Palaeobotany and Palynology, 129(1), 103-116.

Reille, M. (1992-1998). Pollen et spores d'Europe et d'Afrique du nord, vol. 1 (Suppl. IeII). Faculte S. Jerome, Universite de Marseille, Marseille.

Rich, P. M., Dubayah, R., Hetrick, W. A., & Saving, S. C. (1994). Using viewshed models to calculate intercepted solar radiation: applications in ecology. American Society for Photogrammetry and Remote Sensing Technical Papers. In American Society of Photogrammetry and Remote Sensing (pp. 524-529).

Rull, V. (2006). A high mountain pollen-altitude calibration set for palaeoclimatic use in the tropical Andes. The Holocene, 16(1), 105-117.

Seppä, H., & Hicks, S. (2006). Integration of modern and past pollen accumulation rate (PAR) records across the arctic tree-line: a method for more precise vegetation reconstructions. Quaternary Science Reviews, 25(13), 1501-1516.

Stockmarr, J. (1971). Tablets with spores used in absolute pollen analysis. Pollen Spores 13, 615-621.

Ter Braak, C. J. (1986). Canonical correspondence analysis: a new eigenvector technique for multivariate direct gradient analysis. Ecology, 67(5), 1167-1179.

ter Braak, C. J. (1987). The analysis of vegetation-environment relationships by canonical correspondence analysis. In Theory and models in vegetation science (pp. 69-77). Springer Netherlands.

ter Braak, C. J., & Prentice, I. C. (1988). A theory of gradient analysis. Advances in ecological research, 18, 271-317.

Tinner, W., Ammann, B., & Germann, P. (1996). Treeline fluctuations recorded for 12,500 years by soil profiles, pollen, and plant macrofossils in the Central Swiss Alps. Arctic and Alpine Research, 131-147.

Tinner, W., & Theurillat, J. P. (2003). Uppermost limit, extent, and fluctuations of the timberline and treeline ecocline in the Swiss Central Alps during the past 11,500 years. Arctic, Antarctic, and Alpine Research, 35(2), 158-169.

Tranquillini, W. (1979). General Features of the Upper Timberline. In Physiological ecology of the alpine timberline (pp. 1-4). Springer Berlin Heidelberg.

Vincens, A., Ssemmanda, I., Roux, M., & Jolly, D. (1997). Study of the modern pollen rain in Western Uganda with a numerical approach. Review of Palaeobotany and Palynology, 96(1), 145-168.

Weng, C., Bush, M. B., & Silman, M. R. (2004). An analysis of modern pollen rain on an elevational gradient in southern Peru. Journal of Tropical Ecology, 20(01), 113-124.

Weppler, T., Stoll, P., & Stöcklin, J. (2006). The relative importance of sexual and clonal reproduction for population growth in the long-lived alpine plant Geum reptans. Journal of Ecology, 94(4), 869-879.

Whittaker, R. J. (1985). Plant community and plant population studies of a successional sequence Storbreen glacier foreland, Jotunheimen, Norway -Unpubl PhD thesis, Univ. Wales.

Manuscript 2

(Prepared to be submitted to Quaternary Science Reviews)

Glacier contraction, primary plant succession and the early-middle Holocene optimum in the Italian Alps. New evidence from a classical site at the Rutor Glacier.

Federica Badino, Amelia Aceti, Roberta Pini, Cesare Ravazzi, Francesca Vallè, Francesco Maspero, Michele Brunetti, Renata Perego, Giuseppe Orombelli

1. INTRODUCTION

In summer 1957, during a visit at the retreating front of Rutor Glacier (Western Italian Alps), Peretti (Peretti e Charrier, 1967) found thick blocks of compressed peat uprooted from a mire which had been overridden and deformed by earlier glacier advances. The persisting retreat trend during the Eighties of the past century uncovered the site where mire deposits are still *in situ*, though only their lower portion is preserved in stratigraphic position (**Fig. 12** and **13**). First radiocarbon dating and moraine mapping allowed to recognize a long phase of glacier contraction during the early-middle Holocene, implying glacier sizes smaller than modern ones for at least three millennia between 8400 and 6000 BP (Porter and Orombelli, 1985). Burga (1991) provided a first pollen record and suggested a positive treeline shift of at least ~300 m during Atlantic times in Rutor area. Otherwise, in the French and Swiss Alps, treeline is proposed to have been 100 - 200 m higher than today in the Early-Middle Holocene between 9 and 6.5 ka cal BP (Tinner and Theurillat, 2003; Heiri et al, 2006).

Such spectacular evidence testifies for a prolonged middle Holocene hypsithermal phase, which has been long known in boreal mountain glaciers (Porter, 1981; Nicolussi and Paztelt, 2000, 2001; Hormes et al., 2001; Joerin et al., 2006, 2008), but until late years the evidence from the Alps has remained doubtful. More recently, a comparison between Holocene glacier minima

highlighted a period of generally glacier-hostile climatic conditions between 10.5 and 3.3 ka (Ivy-Ochs et al., 2009).

The paleobotanical record of alpine mires provide information for environmental change in the highlands, and paleoecological proxies related to treeline oscillations are especially sensitive to climate change (pollen, stomata, plant macrofossils). Recently, quantitative methods for reconstructing climate parameters from pollen data have been set up (Juggins and Birks, 2012), although not yet directly tested on high-altitude sites. This issue may be afforded by establishing modern altitudinal transects matching vegetation, pollen and modern climatologies. Limited number of meteorological stations and geomorphological effects on local climate may bias the reconstruction of local climates in mountain regions. Indeed, topographic complexity generates a high diversity of micro-environments where climatic values are very difficult to predict (Daly et al. 1994, 2002). Yet, robust models have been made available for the entire Alps (Brunetti et al., 2012, 2014).

In this paper we consider the paleoecology and chronology of previously studied and newly discovered successions at the Rutor buried peat record (**Fig. 12** and **13**), producing a high-resolution pollen record including charcoal and NPP's (non-pollen palynomorphs) proxies and additional information from plant macrofossils. Given that the uppermost Late Holocene segment is not preserved at the classical site, we used an additional nearby record to obtain an almost complete record for the last 8800 years. We submitted such a composite record to quantitative reconstruction of past climate parameters, providing climate solutions both from regression and calibration methods based on the analogues techniques. An evaluation of the ecological requirements of timberline descriptors provided independent insight on climate change. This multiple palaeobotanical approach is eventually matched with the paleoglaciological evidence, thus supporting the extent and amplitude of the Atlantic warming phase in the high Alps.

2. GEOGRAPHIC AND ECOLOGICAL SETTING

The study area lies in the foreland of the Rutor Glacier (La Thuile Valley, Italy; N 45˚64' E 78˚01', 3450 - 2540 m a.s.l; **Fig. 12**). The area hosts several small basins formed either as glacial though or by morainic damming. In this context, the occurrence of organic deposits, accumulated in small mires exceptionally high in altitude, provides valuable archives of past vegetation and climate dynamics in high-alpine areas. The geology of the area is relatively homogeneous; both bedrock and moraine deposits consist of metamorphic rocks such as arenaceous and conglomeratic schists, or mica and garnet schists (Dal Piaz, 1992). Nowadays the Rutor Glacier extends over an area of about 8.5 km^2, bearing an overall north-west aspect. The end moraine system was built after several Holocene advances (Peretti, 1937; Peretti and Charrier 1967; Porter and Orombelli 1985) but mainly in the Little Ice Age, overriding but evenly preserving older records, and also giving rise to a number of new ice-contact and moraine-dammed lakes (Sacco 1917, Peretti, 1935; Orombelli 2005). From the mid-19^{th} century to AD 2004 the glacier terminus retreated 2 km, and lost about 75% of its volume (Villa et al., 2007; Villa et al., 2008), thus the ancient mires came to light.

The Rutor valley represents an excellent example of elevational ecological gradient in a continental region of the Alps, extending from 900 to 3480 m a.s.l. An altitudinal transect composed by 27 plots of pollen-vegetation-climate parameters is currently being developed (Chapter 1). The gradient spans the from the montane *Abies* forest uphill to a lower subalpine *Picea* formation which in turn is overlaid by an upper subalpine belt of open stone pine forest (*Pinus cembra*) currently forming the timberline. The open forest stops at 2360 m a.s.l., while uppermost isolated trees occur at 2455 m a.s.l. A dwarf heath formation composed by blueberries and juniper further rises to 2520 m a.s.l. The peat archives examined in this paper lie definitively over the uppermost heaths limit, woody plants being represented by snow-bed dwarf willows only, while cold-climate grasses (*Nardus stricta*) and sedges (*Carex curvula*) dominate a meadow community. The origin of such an Alpine meadow is currently under discussion (see Pini et al., submitted).

In the surroundings of the Rutor massif, the southern slope of the Mt. Fallère hosts a high-resolution, reference record for the vegetation and human history of the highlands of Valle d'Aosta, covering the last 13 ka (Pini et al., submitted; see **Fig. 12**).

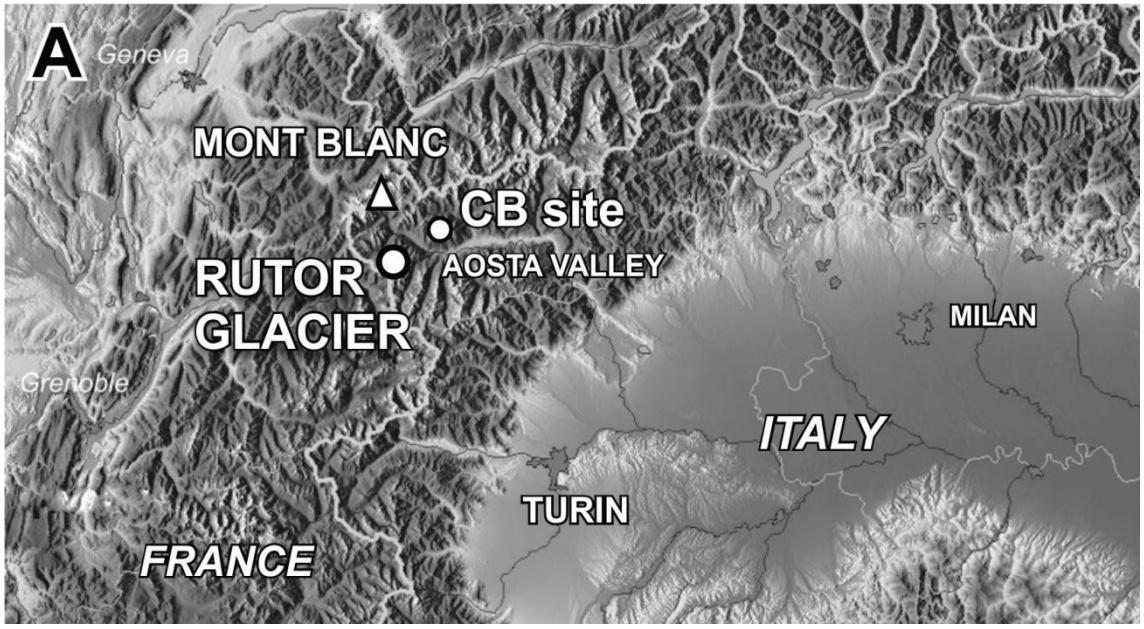

Fig. 12 - (A) Shaded-relief map of the study area in the western Italian Alps showing the location of the Mont Blanc Massif and the Rutor Glacier. Crotte Basse (CB) site cited in the text is also indicated.

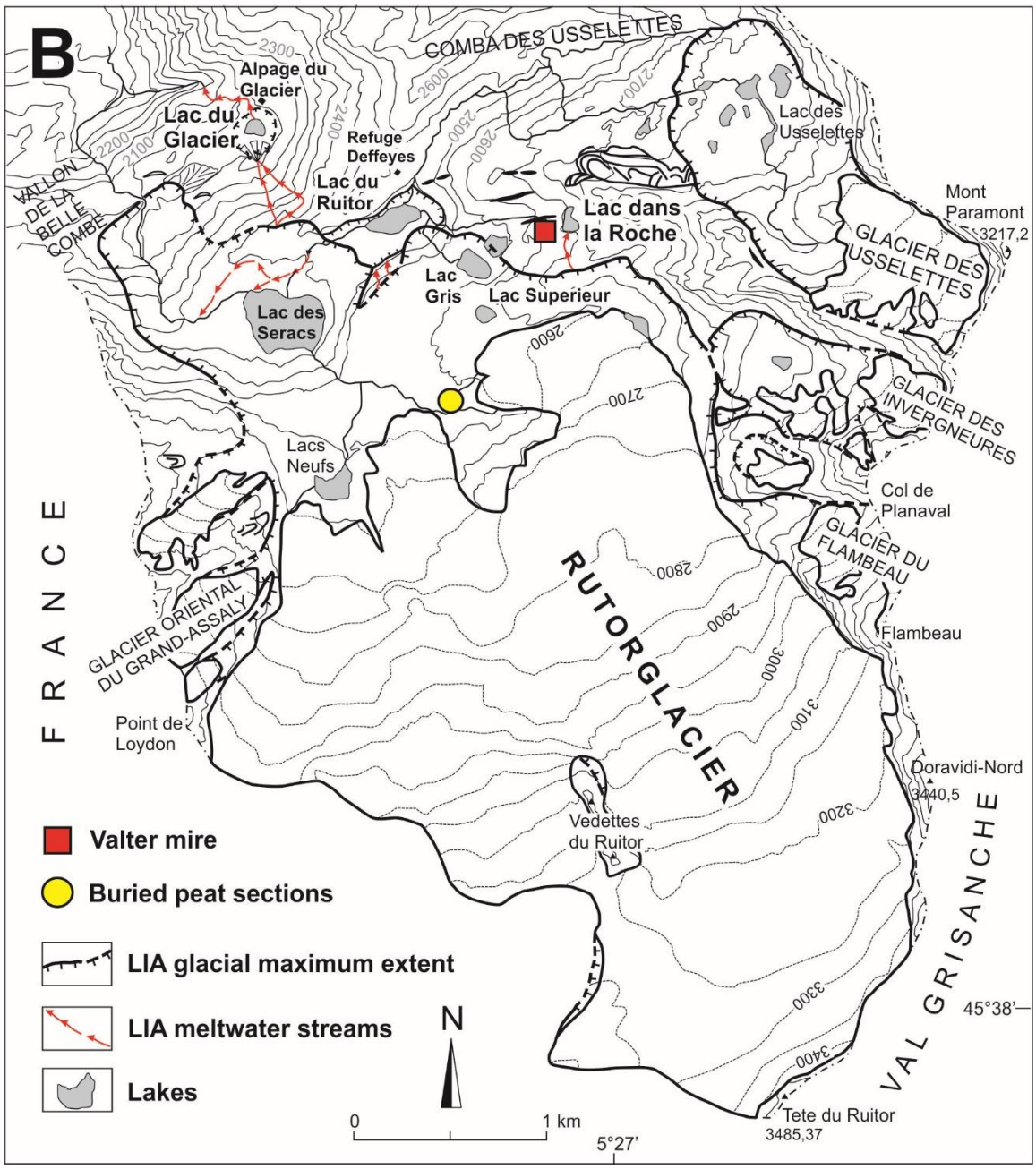

Fig 12 (B) - Sketch map of the Rutor glacier area: the maximum glacier extent during the LIA. Sites location are shown: Buried peat sections and the Valter mire; Modified from Orombelli, 2005

3. MATERIALS AND METHODS

The “Buried peat” succession (2510 m asl) was uncovered after glacier retreat during the Eighties of the past century. Thick seams of compressed and deformed moss and sedge peat are visible along the right bank of a braided meltwater stream in the outwash plain, buried under recent glacial and

fluvioglacial deposits. The outcrop is nearly continuous and exposed for about 15 m along the bank of a proglacial meltwater stream at 2510 m asl. At their basal contact, buried peats cover organic mud (gyttja), in turn underlined by fine silts and by ancient glacial deposits (**Fig. 13 – A, B, C**). Organic seams (~ 1 m thick) does not show any internal unconformity but they are imbedded with several thin silty-sandy layers, which proved to be useful for visual correlation (**Fig. 14**). Two sections of the buried peat, named henceforth section A and section C, were dug by hand and fresh exposures were sampled by metal boxes. In 2010 a further section, named section B, was open and correlated (**Fig. 13**). Recently, another mire was discovered higher up and outside the Rutor LIA maximum extent. This additional mire, namely Valter mire (2594 m asl, **Fig. 13**). Hopefully, organic deposits accumulated in a bedrock-shaped basin produced by ancient glacial erosion, but outside the eastern lobe of the LIA moraine system. The infilling mire was manually drilled down to 1,8 m depth.

We matched the pollen records from section A and Valter mire sequences to get a composite archive covering the last 8800 yrs.

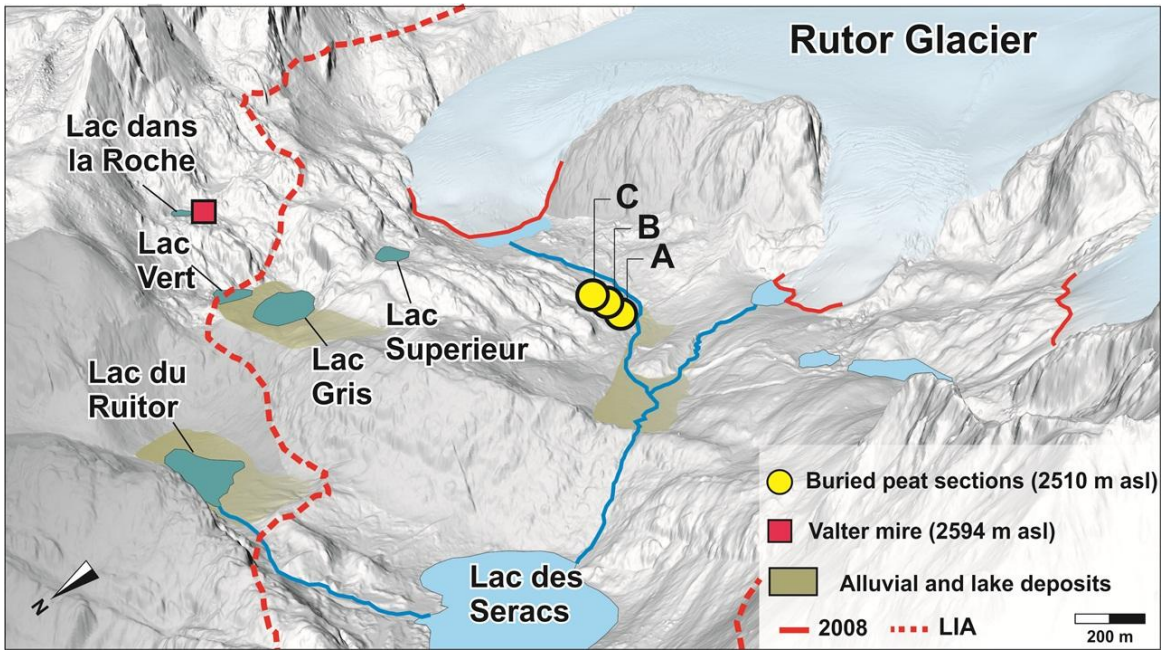

Fig. 13 - Digital Terrain Model of the the Rutor Glacier foreland, view from NW. Continuous red line: 2008 glacier extent;, red dotted line: LIA extent. Studied sites are shown: Buried peat sections (A, B,C; 2510 m asl) and the Valter mire (2594 m asl).

3.1. Radiocarbon dating and age depth model

Table 4 includes both AMS ^{14}C ages obtained from section A (this study; Aceti, 2006) and conventional ^{14}C dates from previous section C (Orombelli, 1998). Radiocarbon dates were calibrated using Calib 7.0.2 (Stuiver et al. 2013) based on the IntCal 13 calibration curve (Reimer et al., 2013). After stratigraphic correlation of all these deposits (**Fig. 14**), deposition rates were modeled using radiocarbon ages as parameters with wide tails student-t distributions (Christen and Pérez, 2009) through the software Bacon v 2.2 (R interface) (Blaauw and Christen, 2011). Two age-depth models were developed: Rutor_model 1 used all the available ages, while Rutor_model 2 retained only ages obtained on terrestrial plant material (**Fig. 15**).

3.2. Loss-On-Ignition

46 volumetric samples were taken between 142-234 cm depth of the section A, weighted and progressively heated at 105 ˚C, 550 ˚C, and 980 ˚C to estimate water, total organic matter + sulphides (TOM+s), inorganic carbon (IC) and the silicoclastic + oxides contents (RES) (**Fig. 15;** Gustafsson et al., 2001). Total organic carbon (TOC) and Carbonates + sulphides and sulphates fractions (CaCO3+ss) were determined stoichiometrically (Dean 1974).

3.3. Pollen, non pollen palynomorph, and stomata analysis

49 palynological samples were studied from the buried peat succession (section A), with a mean time resolution between samples of 28 years. Treatment followed standard methods (including HF and acetolysis) after adding *Lycopodium* tablets for pollen and micro-charcoal concentration estimations (Stockmarr, 1971) at the Lab. of Palynology and Palaeoecology of CNR-IDPA in Milano. Pollen identification was carried out at x400, x630 and x1000 magnifications under a Leica DM-LB light microscope, referring to Moore et al. (1991), Punt and Blackmore (1976-2009), Reille (1992-1998), Beug (2004) and to the CNR palynological collection. Identification of indicators herbs: e.g. *Oxyria, Rumex acetosa, Rumex acetosella* and *Trifolium badium* referring to Beug 2004 and Leeuwen et al. (1988), see also Supplementary Material A.

Non-pollen palynomorphs were named after van Geel (1978) and van Geel et al. (1981), fossil conifer stomata after Trautmann (1953). Pollen diagrams were drawn using Tilia ver. 1.7.16 (Grimm, 1991-2011) and Corel Draw X6 for further graphic elaborations. The pollen sum used for % calculations includes trees, shrubs, chamaephytes and all upland herbs except Gramineae, with a mean pollen count of 496 ± 80 pollen grains. Pollen zonation was obtained by a constrained incremental sum of squares cluster analysis, using the Cavalli Sforza's chord distance as dissimilarity coefficient (CONISS, Grimm, 1987). Clustering was restricted to taxa whose pollen reached over 2%.

3.4. Plant macrofossil and wood identification

Macrofossil analyses was carried out on samples from 2-cm thick slices of peat (volume 100 ml) cut from metal boxes. Samples were boiled in KOH 5% for 30–45 minutes to dissolve humic and fulvic acids, and then disaggregated on 1000 and 500 µm sieves. Samples were then poured into a petri-dish and scanned using a low-power (×4,6 - ×40 magnifications) stereo-zoom microscope with a square grid reticule. Plant macrofossil types were estimated as percentages of the whole sample (**Table 5**). Nomenclature follows Smith (1978) for bryophytes and Pignatti (1982). Thin sections were cut from wood fragments found during the analysis and mounted on microscope slides for identification at ×100 – ×400 (**Table 6**). Identification was performed using a combination of qualitative and quantitative features, referring to Schweingrüber (1990).

3.5. Estimation of climate normals along an altitudinal transect (27 new sites) integrating the EMPD dataset

The EMPD-European Modern Pollen Database (Davis et al., 2013) was used as modern pollen-climate transect for quantitative climate reconstructions based on pollen-spectra from the buried-peat successions. The EMPD dataset was integrated adding 27 sites (Rutor-TRS) collected during September – October 2014 along a 1700-m altitudinal gradient newly developed in the La Thuile Valley, close to the Ruitor Glacier (**Chapter 1**). A distance-weighted average of the anomaly temperature records of the neighbouring stations procedure, described in Brunetti et al. (2012), allowed the calculation of monthly temperature time

series for each of the new 27 sample sites from 1981 to 2010. The same method was applied to the selected EMPD samples in order to extract monthly temperature time series for each samples from 1951 to 2010. At last, from the obtained temperature time series, monthly temperature 30-years climatologies (see paragraph 3.6) could be calculated.

3.6. Pollen-based quantitative climate reconstructions

Reconstruction of past climate parameters was carried out with a pollen-climate calibration model, based on transfer functions and the modern analogue technique (MAT) (see paragraphs 3.6.1 and 3.6.2). A 217 modern pollen samples from the Alpine region were extracted from the EMPD and integrated with an original altitudinal transect designed for this study (see **Chapter 1**). In total, a dataset of 244 modern pollen samples were used for the construction of the transfer functions. The mean temperature values associated to each modern pollen sample, have been calculated over different 30-years intervals, based on the date of collection of the pollen sample. For the new 27 La Thuile Valley samples (see paragrafh 3.5) the 1981-2010 interval was chosen. For the EMPD samples the intervals were 1951-1980 or 1981-2010.

The model performance was evaluated as root mean square error (RMSE). The prediction error (RMSEP) resulted by comparing the observed and inferred environmental (T) values in a leave-one-out cross-validation (Wallach and Goffinet, 1989; Power, 1993). The scatter plots in **Fig. 18** show the relationship between the modern and predicted annual mean temperature values.

3.6.1. Modern Analogue Technique (MAT)

The standard MAT (Guiot, 1990) was applied to the fossil pollen spectra from the *"*Rutor composite record*"* using the program R 3.0.3 version (R Development Core Team, 2008; Juggins, 2015). For each fossil pollen assemblage a *k* number of modern pollen spectra is selected out of database as best analogues. The search for analogues is based on the squared-chord distance (Overpeck et al., 1985) using an equation to find a set of *k* (here *k* = 5) modern analogues for the fossil spectra (chord distance < 1,35). The reconstructed climate value for each fossil spectrum is the weighted-mean distance of the climate values associated

with the *k* best analogues (Jackson et al, 2004; Simpson, 2007). The MAT technique was used to reconstruct the mean temperature of the coldest month (TJan) and the mean temperature of the warmest month (TJuly).

3.6.2. Regression and calibration method (LWWA)

Locally-weighted weighted-averaging (LWWA) regression (Juggins and Birks, 2012) was applied to the fossil pollen spectra from the "Rutor composite record" using the program R 3.0.3 version (R Development Core Team, 2008) and the "rioja" package (Juggins, 2015). LWWA method was tested on different biological proxies (Hubener et al., 2008) using a WA over a so-called ''local'' or dynamic transect (Juggins and Birks, 2012), which is a subset (here k= 20) out of the complete transect, different for each fossil sample, defined on the distance criteria of MAT (see **paragraph 3.6.1**). The size of k, as with MAT, can be determined by cross-validation. This method was used to reconstruct the mean temperature of the coldest month (TJan) and the mean temperature of the warmest month (TJuly).

4. RESULTS

4.1. The buried peat study site - stratigraphy and deposits

The buried peat record in the foreland of the Rutor glacier provides evidence of different phases of sedimentation (**Fig. 14**).

At the base of the sequence, a blocky diamicton deposit testifies to an advance all over the outwash plain by the Rutor Glacier during the early Holocene. Glacial deposits are overlaid by silty, inorganic sediments (235 – 226 cm in **Fig. 14**). The detrital component, roughly estimated by the LOI silicoclastic component (RES), reaches about 90% of dry sediment weight (**Fig. 15**). The sharp transition between silicoclastic silt and organic mud (gyttja) at 225 cm represents the final event of meltwater glacial supply in the basin. Darker limnic deposits (gyttja, 225 - 210 cm) with higher TOM content ranging between 50 - 70% of the dry sediment weight point to the development of a shallow-water lake particularly sensitive to any rapid change in water level. During this interval it happens vascular plants of shallow water and pools to spread into the basin (*Sparganium*, *Thalictrum*, *Carex*

sp.), as shown by their consistent palynological and macrofossil record. A fiber-rich peat accumulated between 210 - 142 cm depth, mainly composed of moss stems and leaves, whereas less abundant are *Carex* rhizomes and epidermis (**Table 5**). Low and stable CaCO3+ss content, about ca. 3 - 4% of dry sediment weight, characterizes these deposits. However, TOM undertakes large fluctuations, due to imbedding of minerogenic layers. Slightly higher CaCO3+ss contents (ca. 5%) occur in these minerogenic layers representing an occasional meltwater input in the mire related to short-lived flood events and followed by prompt peat deposition resumption. Hiatuses or erosional events at the interface between detrital layers and the overlying peat deposits can be excluded given the lateral correlability of these layers at a visual inspection of the outcrop. The consistency of radiocarbon dates (**Fig. 15**) and the general stable pattern of pollen curves also supports this figure.

The upper part of the peat sequence was eroded by subsequent glacial advances, as shown by subsequent diamicton which contains uneven drifted peat fragments.

Sample acronym	Section	depth (cm)	Lab code	^{14}C Age BP	Material dated	Tecnique	95% calibration range (cal BP)	Median probability (yrs cal BP)	δ^{13}C VPDB	Reference
910901/13	Section C	**170**	UZ-2785	**6850 ± 70**	peat	Conventional	7840-7570	7689	-25.8	Orombelli, 1998
910901/12	Section C	**175**	UZ-2784	**6665 ± 75**	peat	Conventional	7660-7430	7538	-36.4	Orombelli, 1998
910901/11	Section C	**176**	UZ-2783	**6740 ± 75**	peat	Conventional	7720-7460	7602	-29.6	Orombelli, 1998
910901/10	Section C	**179**	UZ-2782	**7000 ± 70**	peat	Conventional	7960-7680	7833	-33.4	Orombelli, 1998
910901/9	Section C	**184**	UZ-2781	**6955 ± 75**	peat	Conventional	7950-7660	7790	-33.2	Orombelli, 1998
910901/8	Section C	**186**	UZ-2780	**7575 ± 75**	peat	Conventional	8270-8200	8383	-31	Orombelli, 1998
910901/7	Section C	**187**	UZ-2779	**6990 ± 70**	peat	Conventional	7950-7680	7823	-27.7	Orombelli, 1998
910901/6	Section C	**188**	UZ-2778	**6980 ± 75**	peat	Conventional	7950-7670	7813	-39.9	Orombelli, 1998
910901/5	Section C	**193**	UZ-2777	**7040 ± 75**	peat	Conventional	8000-7700	7868	-45.6	Orombelli, 1998
910901/4	Section C	**198**	UZ-2776	**7180 ± 70**	peat	Conventional	8170-7920	8002	-37	Orombelli, 1998
910901/3	Section C	**210**	UZ-2775	**7800 ± 75**	gyttja	Conventional	9000-8400	8586	-22	Orombelli, 1998
910901/2	Section C	**211**	UZ-2774	**8200 ± 80**	gyttja	Conventional	9410-9000	9174	-37.5	Orombelli, 1998
RTR2/box2	Section A	**142**	Ua-24626	**6760 ± 45**	peat	AMS	7690-7560	7617	-25.6	Aceti, 2005
RTR2/box2	Section A	**162-164**	Ua-24627	**6670 ± 45**	peat	AMS	7620-7460	7539	-23.1	Aceti, 2005
RTR2/box2	Section A	**179-180**	Ua-24628	**7035 ± 45**	peat	AMS	7960-7750	7875	-31.9	Aceti, 2005
RTR2/box1	Section A	**189-190**	Ua-23270	**7105 ± 65**	peat	AMS	8030-7760	7932	-29	Aceti, 2005
RTR2/box1	Section A	**212-214**	Ua-23271	**7915 ± 65**	gyttja	AMS	9000-8590	8763	-27.5	Aceti, 2005
RTR2/box1	Section A	**216-218**	UBA-32217	**7825 ± 50**	wood	AMS	8505-8771	8607	-26.3	Badino, 2016
RTR2/box1	Section A	**220-222**	UBA-32218	**7980 ± 47**	wood	AMS	8695-9000	8853	-26.2	Badino, 2016
RTR2/box1	Section A	**224**	Ua-23272	**8145 ± 70**	gyttja	AMS	9400-8750	9102	-27	Aceti, 2005

Table 4 - Radiocarbon chronology of the studied buried peat records (section A and section C).

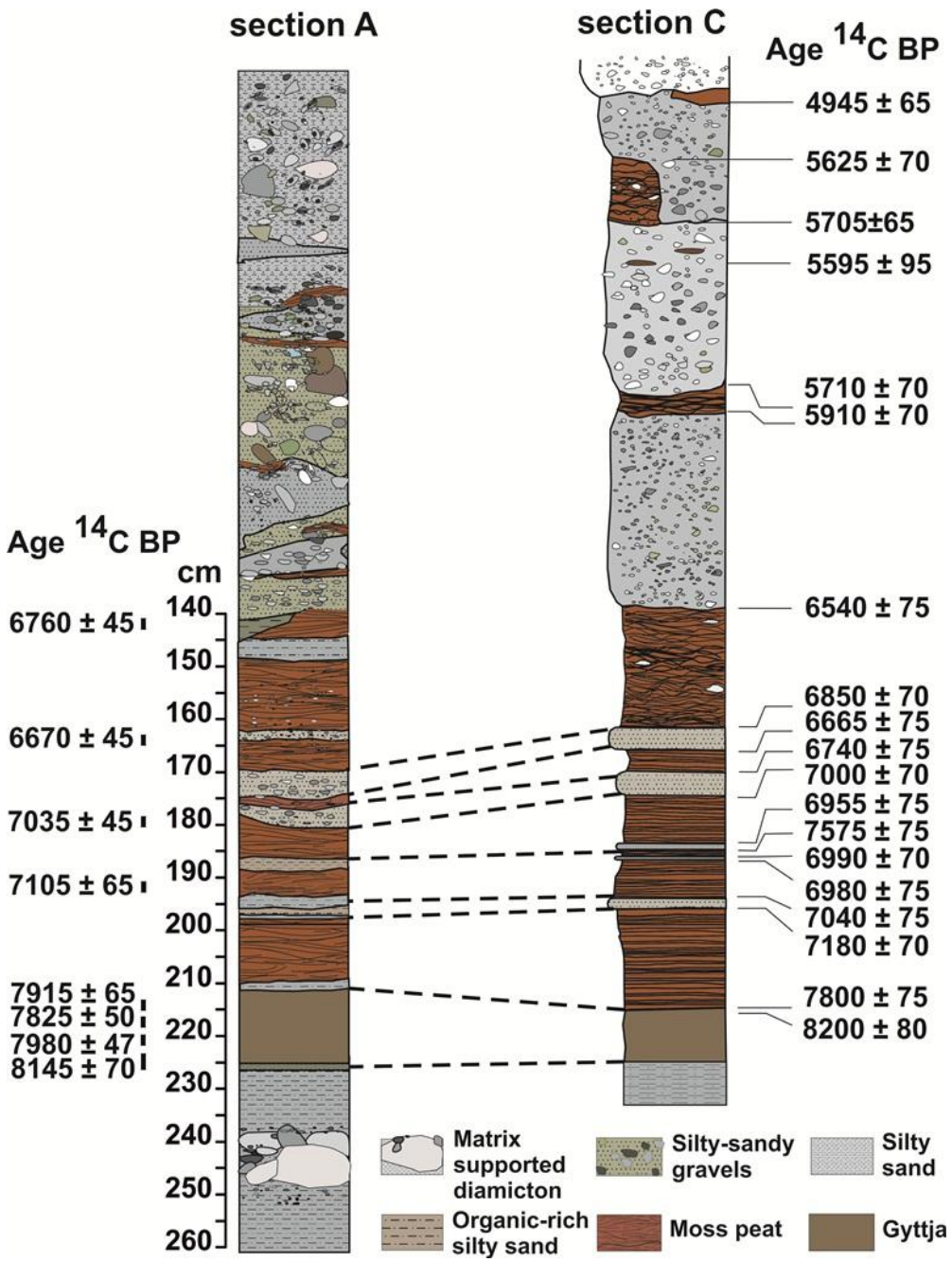

Fig. 14 - Lithostratigraphical correlation of section A and C (modified from Orombelli, 1998), including position of dated samples and uncalibrated radiocarbon ages.

4.2. Plant macrofossil record

Selected intervals in the buried peat sequence, either from the section A and the section B, were considered for macrofossil analysis (**Tab. 5**), to figure out the composition of organic deposits and the relative representation of aquatic and terrestrial local plants. The basal organic mud (*RUT-2* pollen zone) is mainly composed of *Carex* sp. and Poaceae remains; almost no mosses were found. Compressed small twigs of dwarf shrubs were identified as Ericaceae cf. *Vaccinium* (**Tab. 6** and **Fig. 17**). These findings suggest the presence of dwarf heaths around the pond.

The peat mire developed between 210 and 142 cm. A remarkable increase of mosses marks these deposits (**Tab. 5**). *Carex* sp. (biconvex achene, epidermis) and Poaceae (caryopsis) have been identified along with mosses.

The mire was colonized by *Salix* cf. *foetida*, as shown by identification of branches and buds (**Fig. 17**). This shrub is still abundant in the Rutor glacier foreland (Caccianiga et al., 2002). Willows are characterized by an "outlying" distribution, indicating a role poorly correlated with temporal controls (Matthews, 1978). They are capable of establishing on any terrain age provided with a suitable supply of moisture (Whittaker, 1993).

Moreover, some wood fragments have been identified in the Valter mire deposits (**Tab. 6**). A *Pinus cembra* wood fragment (**Fig. 17**) yielded a radiocarbon age of 4895 ± 35 yrs BP, suggesting the occurrence of Swiss stone pines around this site (ca. 2590 m asl) at 5600 - 5700 yrs cal BP. According to PAR values (see later), the Valter mire was lying in the timberline ecotone 5600 yrs ago, probably characterized by a mosaic of open *Pinus cembra* stands.

Section code		section A										section B	
Sample name		150-152 cm		162-164 cm		172-174 cm		186-188 cm		216-218 cm		Basal peat layer	
Mesh size (mm)		1	0,5	1	0,5	1	0,5	1	0,5	1	0,5	1	0,5
Taxa	**Type of remains**	**%**	**%**	**%**	**%**	**%**	**%**	**%**	**%**	**%**	**%**	**%**	**%**
Musci	stem	54	40	72	50	38,5	25	45	60	2		26	
Musci	leaf				30			5					40
Musci	**total**	**54**	**40**	**72**	**80**	**38,5**	**25**	**50**	**60**	**2**	**0**	**26**	**40**
ND	rhizome	40	57	20	10	50	60	30	30	10	20	25	30
Carex sp.	rhizome									15	20		
Carex sp.	biconvex achene	3	2	5	7	0,5		3			5	8	10
Carex sp.	epidermis											5	
Poaceae	caryopsis						0,5					+	
n.d.	stem base	+				3		2		9			
n.d.	stem			2		5		13		10		2	13
n.d.	epidermis						9,5		5	10	35	15	5
n.d.	black rootlets									5	15	5	
Herbaceous plant taxa	**total**	**4**	**2**	**7**	**7**	**8,5**	**10**	**18**	**5**	**49**	**75**	**36**	**28**
Ericaceae	twig									5			
Salix cf. *foetida*	twig/branch											6	
Salix cf. *foetida*	bud											4	
n.d.	twig			+						8			
Woody plant taxa	**total**			**+**						**13**		**10**	
Peat aggregates					2					**25**			
Insecta	different parts	**2**	**+**		**+**	**3**	**5**	**2**	**5**	**+**	**5**	**3**	2

Table 5 – Plant macroremains percentage record from selected peat levels; + = presence.

Section code	Section altitude (m asl)	Sample name	Type of remains	Taxa	N	^{14}C date BP (uncal.)	Calibration range (2 sigma, cal yrs BP)	Median probability (cal yrs BP)
Valter mire	2594	5 lap core 117 cm	branch fragment	*Pinus* cf. *cembra*	1			
Valter mire	2594	5bis core 116,5 cm	branch fragment	*Pinus cembra*	1	4895 ± 40	5586-5664	5627
Valter mire	2594	5 lap core 135 cm	wood fragment	n.d.	1	6200 ± 40	6994-7184	7093
Section B	2510	Basal peat layer	twig/branch	*Salix* cf. *foetida*	21			
			bud	*Salix* cf. *foetida*	6			
			bud connected to the twig	*Salix* cf. *foetida*	1			
Section A	2510	162 - 164 cm	twig	n.d.	1			
Section A	2510	216 - 218 cm	twig	n.d.	8			
			twig	Ericaceae	5			
			twig	Ericaceae	3	7825± 50	8505 -8771	8607
Section A	2510	220 - 222 cm	twig	n.d.	2	7980± 47	8695-9000	8853
			Twig	Ericaceae	1			

Table 6 - Wood record obtained from the studied peat sections.

4.3. Radiocarbon chronology and age-depth model

According to the composite sequence of radiocarbon ages, the Rutor buried peat continuous record extends for about two millennia between 8.7 and 7 ka cal BP and so far it is the most extensively radiocarbon-dated site in the Alpine chain recording the Early to Middle Holocene evolution in the high elevational belt of the Alps (**Fig. 15**). Despite the dating effort, a plot of the complete radiocarbon dataset shows an age shift between 8 and 8.5 ka cal BP at the basal gyttja / moss peat boundary (**Fig. 15 A**). However, there is a hiatus not supported by the pollen record which shows a stable increasing pine trend across (see **Fig. 16 A**). Once the ages obtained from bulk gyttja (organic mud, 225 – 210 cm) are removed, relying on terrestrial wood only, a continuous deposition in the basin is apparent since its deglaciation, somehow before the basal age of 8.7 ka cal BP, and lasting at least until 7.4 ka cal BP, thus excluding any glacial overriding at the 8.2 ka cal BP event.

The ages provided by bulk gyttja are about 200 years older than the imbedded wood. Here, a reservoir effect could be due to uptake of old carbon by aquatic plants forming the organic mud (mainly *Sparganium* cf. *angustifolium*). Submerged vegetation shows physiological adaptations to a low carbon availability in the water column including effective utilization of CO_2 contained in the sediment (Raven et al., 1988; Madsen, Olesen & Bagger, 2002). A recent experimental study documents that *Sparganium angustifolium* captures CO_2 directly from sediment pore water by root uptake to produce biomass. Additionally, *Sparganium angustifolium* produces floating leaves which enable supplementary uptake of atmospheric CO_2 (Lucassen et al., 2009). These ecophysiological mechanisms may explain a moderate reservoir effect and thus the observed bias in ages from *Sparganium* cf.*angustifolium* bulk sediment.

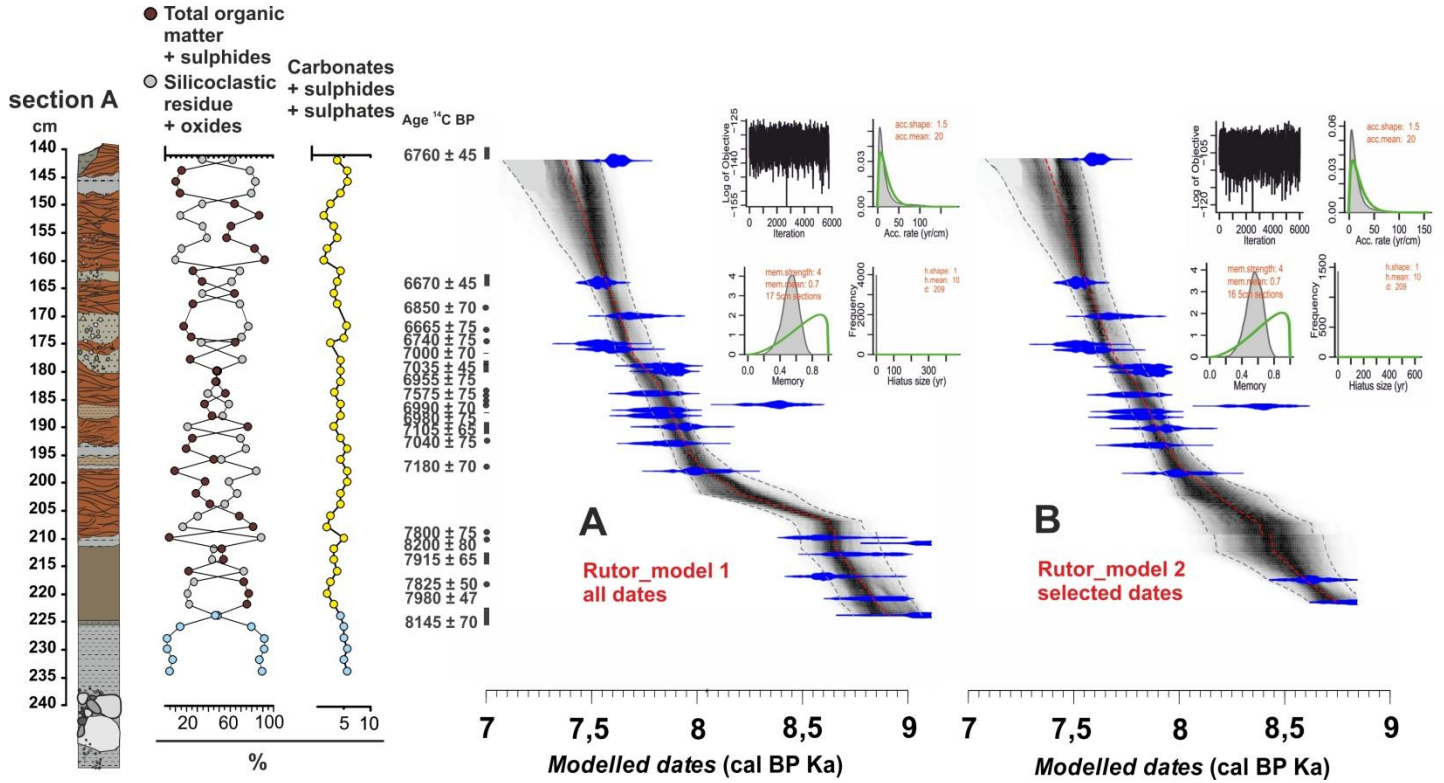

Fig. 15 - Section A including lithostratigraphic proxies: % TOM, % residue + oxides and % CaCO3 + ss (see materials and methods). Two age depth models was developed: (A) Model 1 was based on all available ^{14}C ages; (B) Model 2 discarded bulk gyttja and retained samples with bulk peat and terrestrial plants only. The latter was adopted for time plots.

4.4. Vegetation history and landscape reconstruction

The pollen record obtained from the buried peat sequence is shown in **Fig. 16 A - B**. The lowermost pollen zone (*RUT-1*) originates from detrital meltwater silts resting on glacial deposits. This interval is characterized by high percentages of *Pinus cembra* pollen (ca. 60 - 70%). The entire basal succession is polliniferous; but most pollen contained in the meltwater silt was likely released from melting ice and floated till the proglacial pond. Hence, relative pollen abundances and changes in meltwater silt do reflect taphonomical issues rather than vegetation dynamics (see light blue fill in pollen records, **Fig. 20**). In addition, enhanced flotation of saccate pollen (Ammann, 1994) might strongly affect the relative abundance of pine compared to other *taxa*. Hopefully, a thorough investigation of the whole palynological assemblages enabled the identification of several herbs testifying to early successional, despite their low pollen representation due to dilution in detrital sediments (e.g. *Eryngium alpinum*, *Oxyria*, *Trifolium badium*) (**Fig. 20**).

In *RUT-2* zone a gradual increase of *Pinus cembra* values from ca. 25% to ca. 40% points to expanding conifers in the glacier foreland. Locally, grasses and other herbs expanded (Gramineae e.g. *Nardus* and Cichorioideae cf. *Leontodon* spp.), together with mid-to-late successional dwarf shrubs (Ericaceae e.g. *Vaccinium*, *Calluna, Erica*). Among aquatic and telmatic plants, *Sparganium* and Cyperaceae display high percentage values. The wood analysis of small twigs from this interval documents the local presence of Ericaceae (cf. *Vaccinium* spp.) between 216-218 and 220-222 cm.

In *RUT-3* zone, an *Abies* sudden spread suggests development of a new forest formation in the mountain to lower subalpine belt. Swiss stone pine keeps expanding too. This tree became to dominate the upper subalpine forest belt. A marked increase in microcharcoal concentration at around 194 cm (ca. 7950 yrs cal BP) may be related to a biomass increase as a consequence of a shift towards denser forests. Low *Picea* values (ca. 1%) might be related to a long-distance pollen transport.

RUT-5 zone is framed by an established dominance of *Pinus cembra* in a large upper subalpine forest belt and the progressive rise of *Abies*. A similar scenario persists in the following zone (*RUT-6*); here, *Abies* reaches maximum values (ca. 15 - 20%), indicating a silver fir expansion in the mountain belt and in the subalpine environment as well. Sporadic *Larix* pollen grains occur. Local aquatic and telmatic plants expanded (Cyperaceae and *Sparganium*).

The uppermost *RUT-7* zone shows a moderate decrease of *Pinus cembra* and *Abies*, and increase of *Corylus* and *Pinus sylvestris/mugo*. The occurrence of *Juniperus* stomata suggests it had established close to the Rutor buried peat basin.

To better understand the local and regional dynamics of the main forest taxa, Rutor data have been compared with the Crotte Basse site pollen record (2365 m asl, **Fig. 12**), just a few km from the Rutor area. This site yields the first continuous record of vegetation and climate history for the western high-altitude Alps covering the last 13 ka (Pini et al., submitted). At both sites *Abies alba* reached values >2% at ca 8370 yrs cal BP (**Fig. 20**), while *Pinus cembra* curve shows different patterns. During the early Holocene, at the Crotte Basse site pine forests was already established in the mountain and subalpine belts as documented by the high pollen percentages (~60%) of *Pinus cembra* (**Fig. 20** - red dots). Moreover, since ca. 8800 yrs cal BP, a continuous *Pinus cembra* stomata curve suggests the presence of stone pine specimens around the site (2365 m asl). Differently, in the Rutor area *Pinus cembra* expansion was underway in the subalpine belt, starting from percentages of ca. 25% (**Fig. 20**).

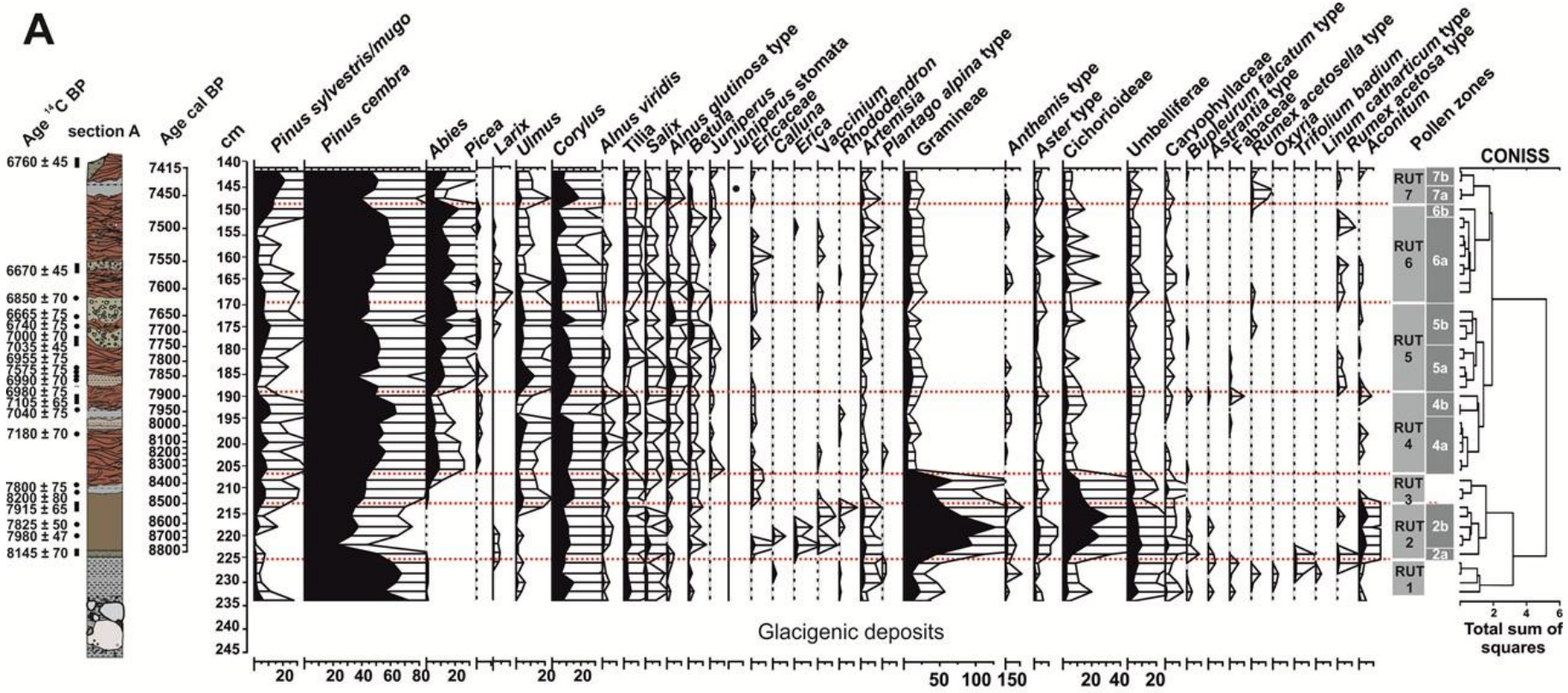
A
Age ¹⁴C BP
section A
Age cal BP
cm
Pinus sylvestris/mugo
Pinus cembra
Abies
Picea
Larix
Ulmus
Corylus
Alnus viridis
Tilia
Salix
Alnus glutinosa type
Betula
Juniperus
Juniperus stomata
Ericaceae
Calluna
Erica
Vaccinium
Rhododendron
Artemisia
Plantago alpina type
Gramineae
Anthemis type
Aster type
Cichorioideae
Umbelliferae
Caryophyllaceae
Bupleurum falcatum type
Astrantia type
Fabaceae
Rumex acetosella type
Oxyria
Trifolium badium
Linum catharticum type
Rumex acetosa type
Aconitum
Pollen zones
CONISS
6760 ± 45
6670 ± 45
6850 ± 70
6665 ± 75
6740 ± 75
7000 ± 70
7035 ± 45
6955 ± 75
7575 ± 75
6990 ± 70
6980 ± 75
7105 ± 65
7040 ± 75
7180 ± 70
7800 ± 75
8200 ± 80
7915 ± 65
7825 ± 50
7980 ± 47
8145 ± 70
7415
7450
7500
7550
7600
7650
7700
7750
7800
7850
7900
7950
8000
8100
8200
8300
8400
8500
8600
8700
8800
140
145
150
155
160
165
170
175
180
185
190
195
200
205
210
215
220
225
230
235
240
245
RUT 7
7b
7a
RUT 6
6b
6a
RUT 5
5b
5a
RUT 4
4b
4a
RUT 3
RUT 2
2b
2a
RUT 1
Glacigenic deposits
20
20 40 60 80
20
20
20
50 100 150
20 40
20
2 4 6
Total sum of squares

Fig. 16 A

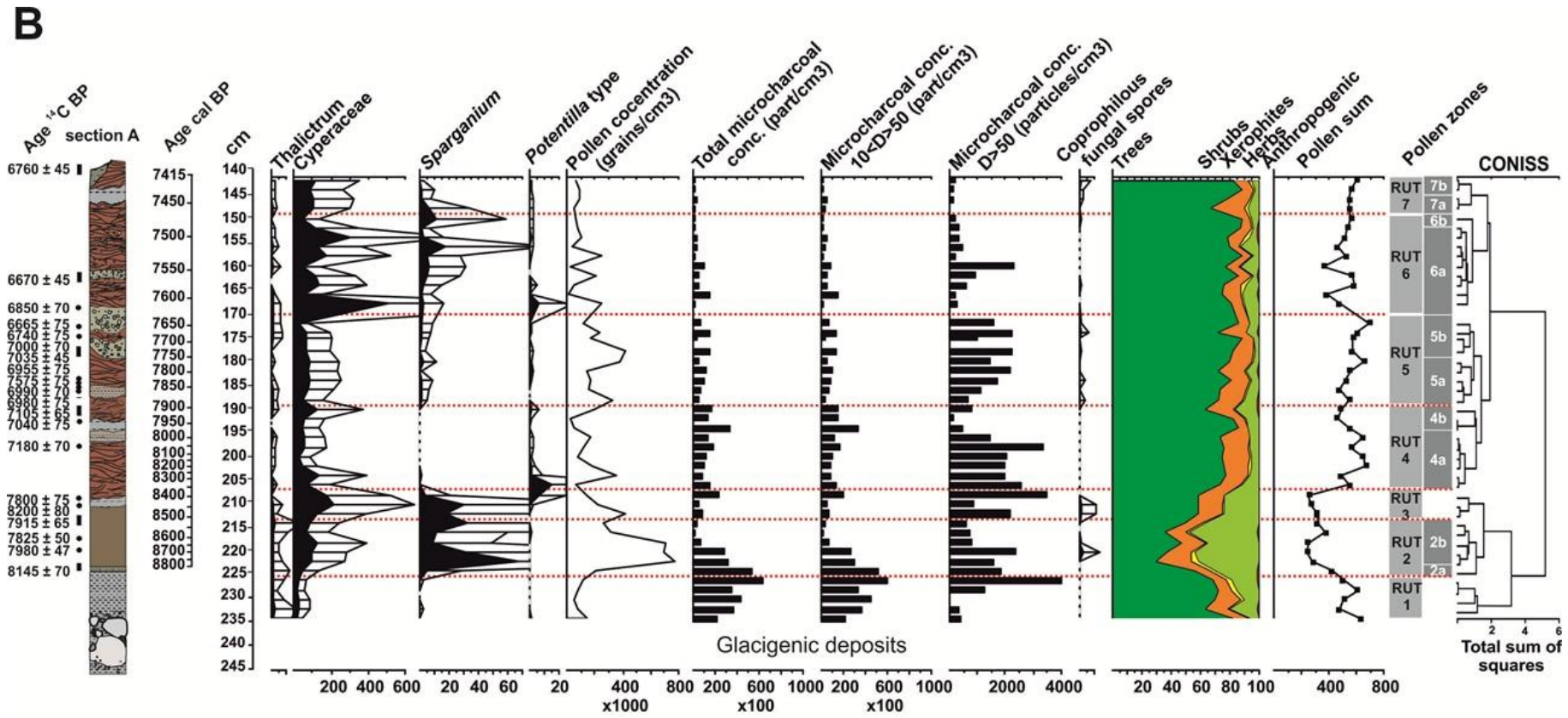

Fig. 16 (A-B) - Percentage palynological record of selected taxa plotted on stratigraphic scale and zoned by constrained clustering. Magnification of percentage curves x5. (A) Terrestrial plants; (B) Aquatic plants, concentration of pollen and microcharcoal fractions.

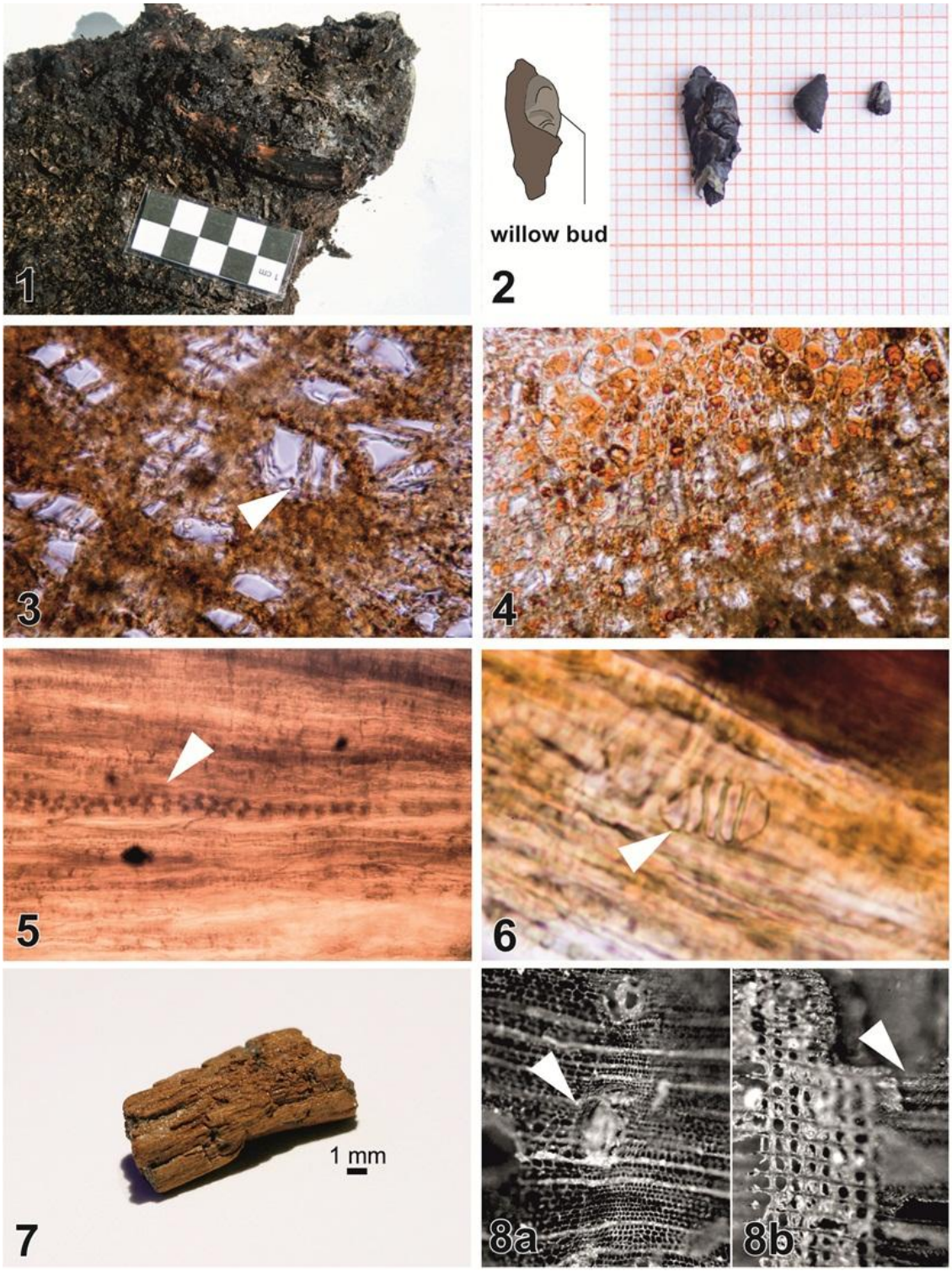

Fig. 17 - Selected wood macroremains from the studied peat sections: (1) Peat including compressed *Salix* cfr. *foetida* stems (Section B – basal peat layer); (2) A willow bud connected to the twig and some bud fragments (Section B – basal peat layer); (3) Transverse section of *Salix* cfr. *foetida* wood (x 630 magnifications, Section B – basal peat layer); (4) Filling cells structures (permineralizations?) of

fossil wood (x 200, section A – 216-218 cm); (5) Tangential section of Ericaceae cf. *Vaccinium* spp.: 2 to 3 – seriate rays (x200, section A – 216-218 cm); (6) Scalariform perforations in Ericaceae cf. *Vaccinium* spp.. The openings at the axial end show several bars (x 400, section A – 216-218 cm); (7) Branch fragment of *Pinus cembra* (Valter mire, 5 bis core section - 116,5 cm); (8a) Transverse section of *Pinus cembra* wood with resin ducts and (8b) radial section of *Pinus cembra* xylem with compression wood formations (Valter mire, 5 bis core section - 116,5 cm).

4.5. Pollen-inferred Temperature Reconstructions

TJuly and TJan reconstructions inferred from the composite pollen record (**Paragraph 3.6**) show a warmer Holocene between 8000 and 4000 yrs cal BP, with TJuly ca. 3 °C higher than today (1981 – 2010) and a cooling of ca. 3 °C during the late Holocene (4000 – 850 yrs cal BP) (**Fig. 19)**. During the early-middle Holocene, temperature of the warmest month reached mean values of 12,1 °C (LWWA, RMSEP= 2,28˚C) or 12,2°C (MAT, RMSEP= 2,08 ˚C). For the same period pollen-inferred coldest month temperature was about -3,2°C (LWWA, RMSEP= 1,51˚C) and -3,3°C (MAT, RMSEP= 1,40˚C). A first cooling step occurred between about 4000 and 3400 yrs cal BP, a second one between ca. 2900 and 2000 yrs cal. BP and a third from 1150 till the end of the record (853 yrs cal BP). The plots of observed versus predicted January and July mean temperatures (**Fig. 18)** show generally good results, but, according to the residuals (predicted-observed values compared with observed values in **Fig. 18 B**, the model is found to over-estimate the warmest modern temperatures and under-estimate the coldest modern temperatures.

Modern climate normals of the warmest (TJuly) and coldest (TJan) months at the study site (ca. 2510 m asl), for the period 1981-2010, are 8,6 °C and -6,8 ˚C, respectively.

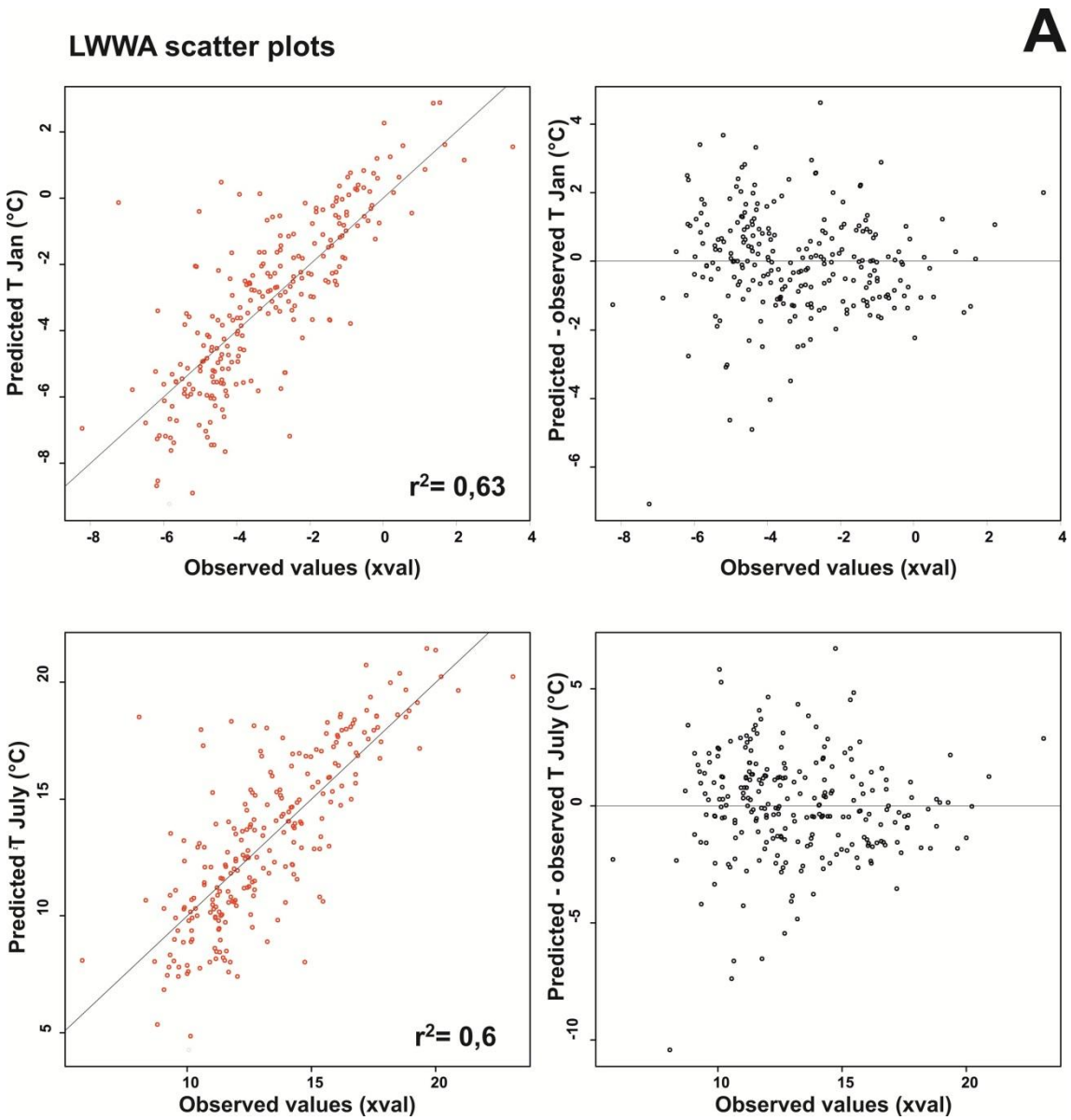

Fig. 18 A - January and July mean temperature predicted by LWWA (Modern Analogue technique) against observed January and July mean temperature;

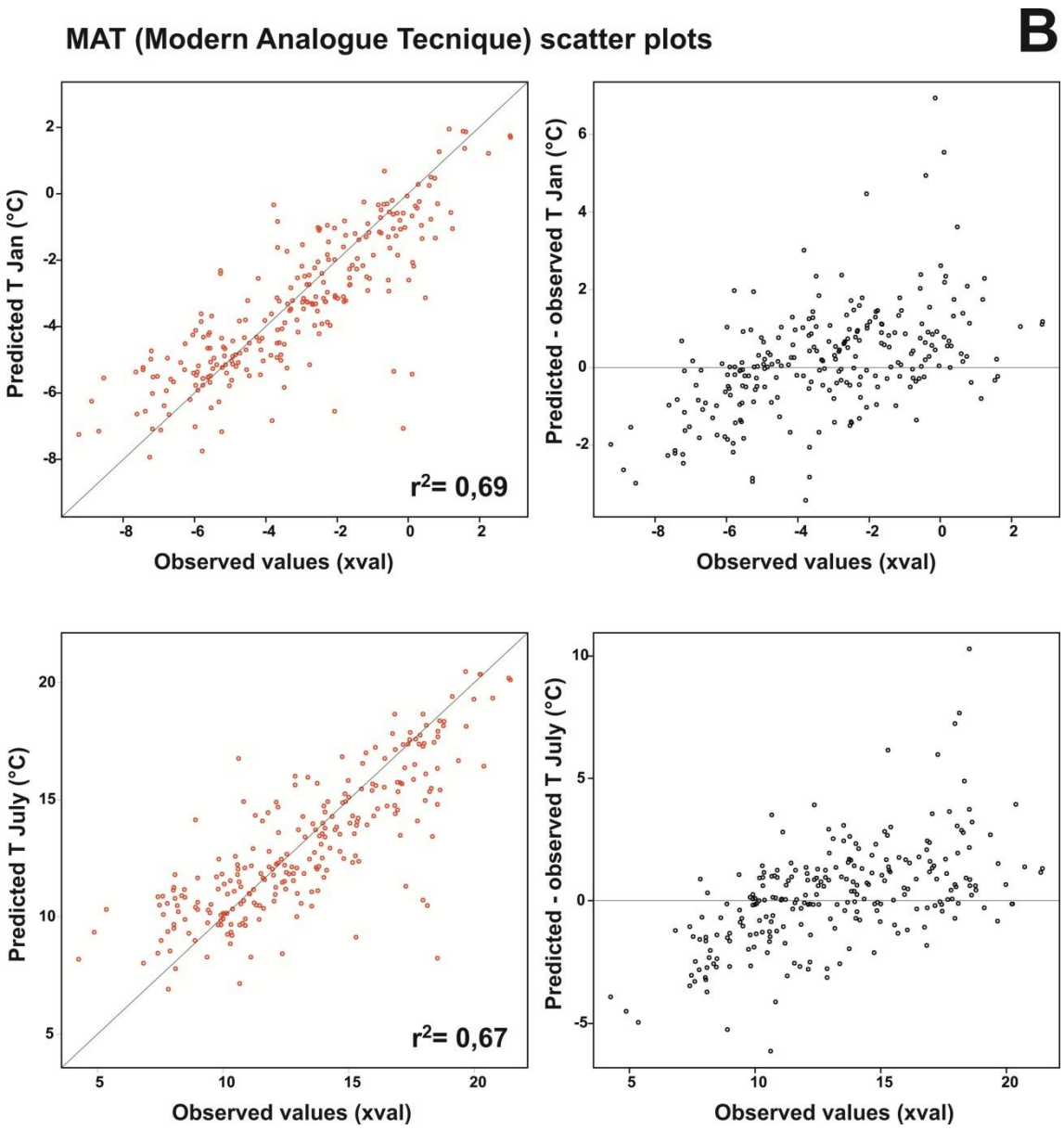

Fig 18 B - the same, predicted by MAT (Modern Analogue Technique). Plots on the right show relationship between residuals (e.g. predicted – observed temperature) and expected temperature.

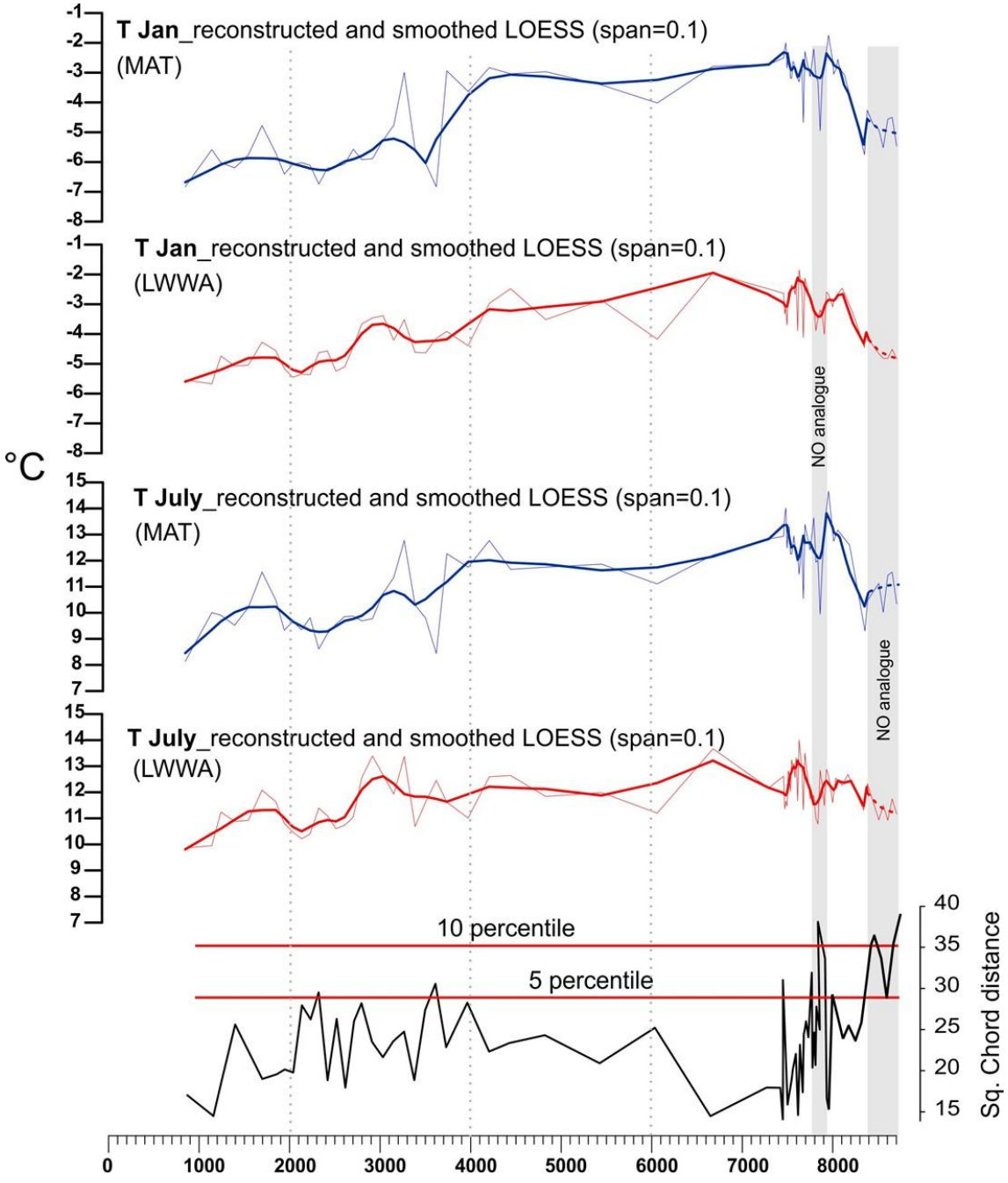

Fig. 19 - Pollen-inferred TJuly and TJan reconstructions from the "Rutor composite pollen record" (see paragraph 3). Reconstructed T values from the Valter mire (853-7300 years cal BP) were shifted of about 0,5 ˚C due to its ~80 m upward position from the buried peat site (8800-7400 yrs cal BP). A LOESS smoother (span 0.1) is fitted to the reconstructed values. Samples outside the 5th and 10th percentiles of the training set square-chord distances were identified as poor and no analogues, respectively. Square Chord distance values above the 10th percentile suggest the absence of good modern analogues.

5. DISCUSSION

5.1. Reproducibility of pollen data

In 1988, previous authors collected samples for pollen analysis and radiocarbon dating from a mire profile close to the study site presented here. Burga (1991) presented a radiocarbon-calibrated pollen record. Five radiocarbon dates on bulk sediments covered ca. 3000 yrs between 9255 yrs cal BP and 6066 yrs cal BP (median probability). The lithostratigraphical sequence described by Burga (1991) is coherent with the sequence presented in this study and pollen data are also comparable, although our time resolution is much higher. Indeed, Burga's *LPAZ 1* zone shows an early successional herb phase, rich in *Artemisia*, Cariophyllaceae, *Rumex/Oxyria* type, Asteraceae, Cichorioideae pollen grains. This pollen assemblage matches the composition of *RUT 1-2* pollen zones (**Fig. 16**). Burga's *LPAZ 2* pollen zone shows expansion of silver fir (*Abies*) as observed in *RUT 3-4* pollen zones. In *LPAZ 2-3*, high and stable *Pinus* percentages point to a phase of climate optimum at an average T rise of 2-3 ˚C (Burga, 1991). This scenario is comparable with our data: RUT 4-5-6-7 pollen zones (see **Fig. 16 A**) and the resuts of our climate reconstructions (**Fig. 19**).

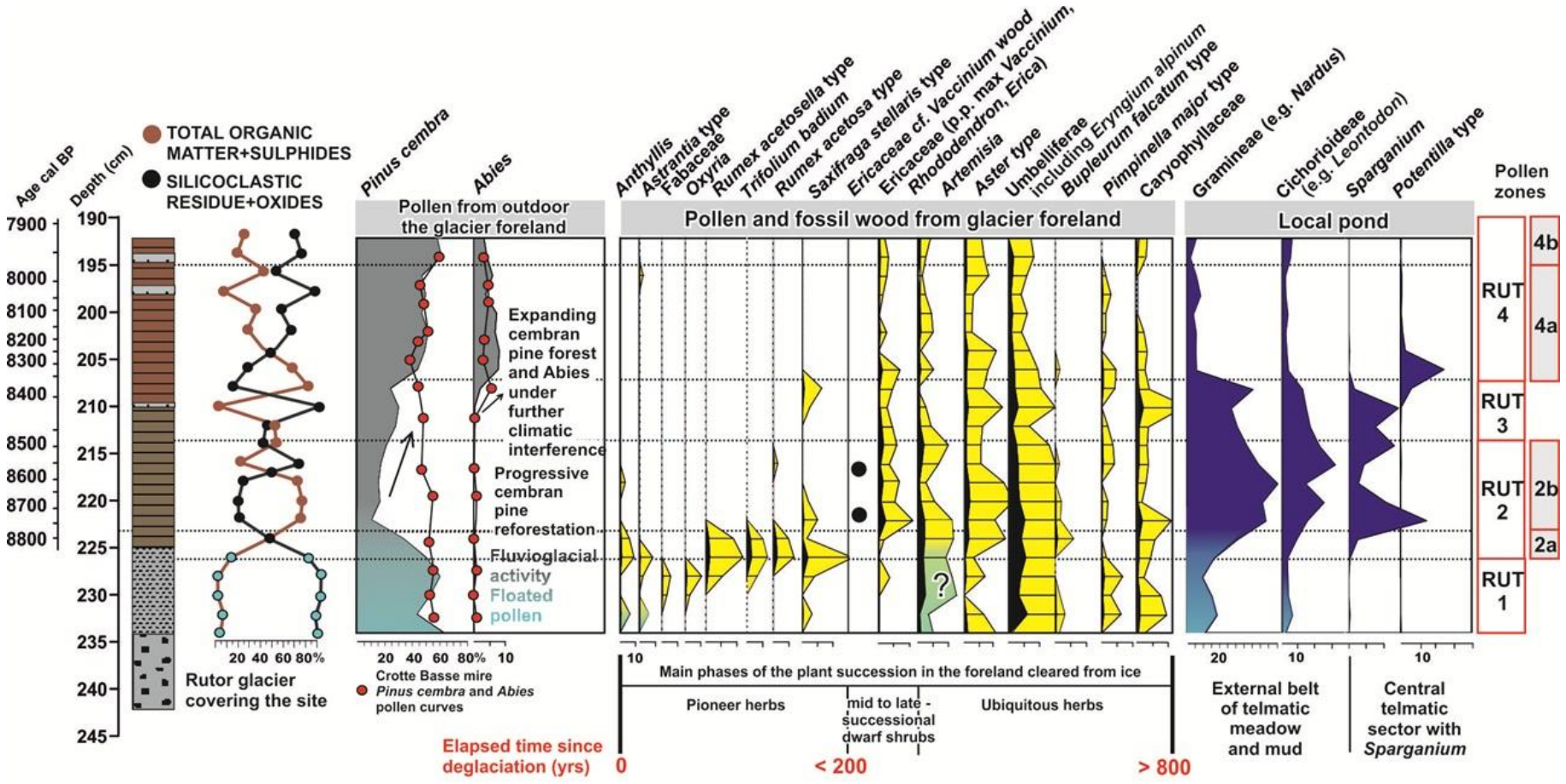

Fig. 20 - Pollen record of selected taxa (%) from section A, envisaging a primary succession. Light blue filling: floated pollen; Yellow filling: airborne pollen from the glacier foreland; Blue filling: pollen from plants growing in the sedimentary and peat basin. A light blue pattern filling marks high proportion of floated pollen, mostly concerning *Pinus*. Red dots show *Pinus cembra* and *Abies alba* pollen % from the Crotte Basse mire (Pini et al., submitted).

5.2. Pollen evidence of Early Holocene deglacial plant succession

The basin infilled by the buried peat sequence originated as a proglacial lake, most probably triggered by glacier retreat before 8800 years cal BP. Here, we discuss pollen stratigraphy during early phases of basin infill to infer stages of plant colonization on deglaciated terrains (**Fig. 20**).

First pioneer herbs (*Anthyllis, Astrantia*, Fabaceae, *Oxyria,*) established on bare terrain very quickly, but soon their pollen image disappeared (RUT 1 pollen zone: 225 to 235 cm depth). *Rumex acetosella, Rumex acetosa* and *Trifolium badium* established later in this stage (RUT 2a pollen zone: 226 - 223 cm depth). This is interpreted here as a succession of ruderal affinity (sensu Grime, 1977) which species are able to colonize deglaciated terrains via short-distance anemochory (Erschbamer et al. 2001). Brandani (1983) regards ruderalism as an adaptation to fluvioglacial disturbance whereas Körner (1999) advocates seasonal climatic disturbance. The role of ruderals in early stages of deglacial pioneering was highlighted by recent reports on current vegetation dynamics throughout the Rutor Glacier foreland (Caccianiga et al., 2004, 2006) with the ages of LIA moraine ridges used to construct a simple chronosequence for the landscape. Terrains exposed less than 68 years ago are occupied by pioneers (e.g. *Oxyria digyna*, *Trifolium badium* and *Cerastium uniflorum*), which are absent from terrains exposed more than 181 years ago (Caccianiga et al., 2006).

Pollen of dwarf shrubs is absent in the pioneer community, while expanding in the later successional stages. A peak of Ericaceae pollen curve (p.p. max *Vaccinium, Rhododendron* and *Erica*) at 222 cm along with blueberry wood fragments, support an *in situ* Ericaceae heath. Evidences of a mid-successional dwarf shrubs expansion (e.g. *Calluna vulgaris, Vaccinium vitis-idaea, Arctostaphylos uva-ursi*) were also recognized in the glacier foreland of Rotmoostal valley (Ötztal, Austria). These species occurred during the initial grasslands stage, which lead to the late-successional alpine grasslands establishment (e.g. *Carex sempervirens*, *Carex curvula*) (Raffl et al., 2004). Several authors suggest that this process needs more than 180 years (Matthews 1992, Caccianiga et al. 2001).

We also found pollen of other plants (Umbelliferae e.g. *Eryngium alpinum*, *Bupleurum falcatum* type and *Pimpinella major* type together with Cariophyllaceae cf. *Cerastium* and *Aster* type) that took part in the early successional colonization but persisted for at least the subsequent 300-500 yrs. These plants do not mark a specific successional stage.

Another group of herbs displays a different successional behavior. These herbs can be assigned, according to their modern ecology, to the colonization of wet habitats over fine sediments. Their sharp peaks in the pollen record are in agreement with their growing within the sedimentary basin (Gramineae pro maxima parte cf. *Nardus*, Asteraceae cf. *Leontodon, Sparganium, Potentilla* **Fig. 20,** group local pond). Gramineae cf. *Nardus* and Cichorioideae cf. *Leontodon* expanded between 8800 and 8400 yrs cal BP. Field vegetation surveys in the Rutor highlands show a *Nardus-Leontodon* expanding over high altitude, seasonally drained meadows ("*Hygronardetum*" according to Buia, 1963) Such wetland plants, e.g. *Nardus stricta* and *Potentilla palustris,* are adapted to survive in anoxic conditions by growing an entirely new root system each year from a perennating shoot base (Armstrong, 1979; Crawford, 1989). In pristine boreal biomes, without any sign of anthropic pasture, *Nardus* forms heath-meadows along creeks or along *Sparganium angustifolium*-pool banks (e.g. in the Fennoscandian timberline and Alpine biomes - Kalliola, 1972, Moen, 1990). It is proposed as one of the primary habitats of the *Nardus* in the Alps, before the onset of human impact. *Sparganium angustifolium* massive expansion (**Fig. 20**) could have been promoted by a great seasonal contrast combined with hot summers. Usually, this species grows in shallow waters with relatively high hydrodynamism and is able to survive under severe and prolonged drought stress (Ballesteros et al, 1989). All together, these plants bear a high pollen production and thus are expected to be well represented in high altitude palynological archives in the Alps.

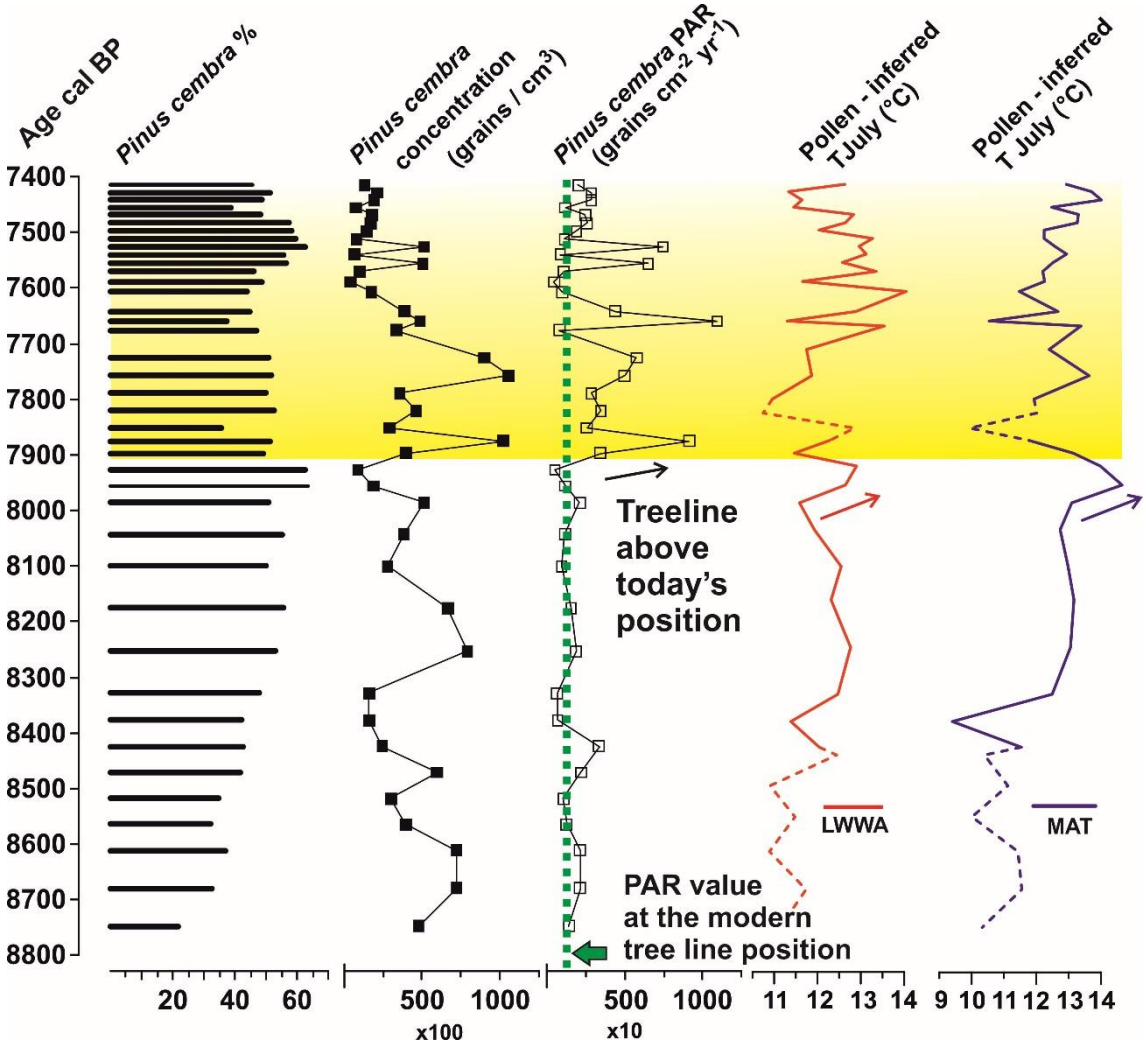

Fig. 21 - A comparison of *Pinus cembra* %, concentration and PAR (Pollen accumulation rate) beside pollen-inferred TJuly reconstructions (MAT and LWWA, dotted intervals= no statistical relevance). Green dotted line: PAR average value at the modern timberline ecotone.

5.3. Timberline response to Holocene climatic oscillations

Timberline limits are controlled by thermal variables (Jobbagy et al., 2000), and thus its variations have been used as a sensible indicator to past and present climate variability. The temperature of the growing season is widely considered the main factor affecting the position of both latitudinal and altitudinal forest and treelines (Tranquillini, 1979, D'Arrigo & Jacoby, 1993, Körner, 1998, Körner & Paulsen, 2004). In the following the timberline is understood to be the transition zone between closed forests (density depends on the tree species and the site

conditions) and the most advanced individuals of the forest-forming tree species (Holtmeyer, 2009, Smith et al., 2003). Timberline is the most conspicuous vegetation limit in high-mountain areas, a more or less wide ecotone that has to be understood as a space- and time related phenomenon. In many cases the existence of a timberline ecotone is the result of oscillations of the climate, persistence of tall (mature) trees and regeneration under changing conditions (Holtmeyer, 2009).

The current timberline limits and their inferred thermal controls in the Rutor area can be resumed as follows. The treeline (connecting elevational standing tree individuals, 3 m high) is formed by stone pine and culminates at 2450 - 2455 m asl, i.e. at a modern (1981-2010 period) TJuly normal of ca. 9,3 °C. Small, stunted and deformed stone pine individuals (krummholz) are scattered between 2460 – 2500 m asl. First stone pine tree grooves stand at 2290 - 2300 m asl, modern TJuly normal of ca. 10,2 ˚C. According to the macroscopic identification of their annual growth units has been evaluated empirically to assess the age (at least ~ 150 years old, see Caccianiga & Compostella, 2012). These pines mark the historic treeline position and possibly got through the cooling period of the latest phases of the Little Ice Age. The closed forest line marks an irregular boundary at about ca. 2100-2150 m asl at a modern TJuly normal of ca. 11,5 ˚C.

In the Alpine areas subjected to continental climate, stone pine is considered the best adapted tree to colonize the upper subalpine belt, and even the lower alpine belt, given its decreasing need for summer heat with increasing altitude and its frost resistance (Theurillat & Schlüssel, 2000). On the other hand, it fails competition with larch and green alder under oceanic conditions.

Gathering pollen influx thresholds for different modern vegetation types along the altitudinal gradient can be useful for more reliable reconstructions of past timberline shifts. In fact, pollen influx could help to overcome interpretation difficulties caused by percentage values (Lang, 1994). Here, tentatively calculated pollen influx for the most important species which define timberline: *Pinus cembra*, along a local altitudinal transect (La Thuile valley**, see Chapter 1**) crossing the timberline and ending ca. 200 m above the treeline. PAR values show a marked decrease with altitude: in the close forest they reach 4436 ± 1157

grains cm^{-2} yrs^{-1}, within the upper timberline ecotone are 955 ± 174 cm^{-2} yrs^{-1} and about 291 ± 121 cm^{-2} yrs^{-1} in alpine meadows above the treeline. Our data are coherent with those obtained for *Pinus cembra* PAR along a transect near Zermatt (Valais, Switzerland) (van der Knaap et al., 2001) starting in the forest and ending 500 m above treeline. Furthermore, Bortenschlager et al. (1998) obtained similar results for *Pinus cembra* in western Austria (site Vent). Similarly, Tinner & Theurillat (2003) in the central Swiss Alps used pollen percentage and influx together with stomata and charcoal data for determining whether or not a site was treeless.

The Rutor buried peat site is located ~ 60 m above the modern treeline. The high-resolution pollen record obtained between 8800 and 7400 yrs cal BP allowed us to reconstruct decadal/centennial scale timberline fluctuations during the early-middle Holocene. At the end of the Younger Dryas a temperature rise of about 3 to 4 °C within only half a century (Schwander et al., 2000; von Grafenstein et al., 2000) caused significant altitudinal displacements of alpine species (ca. 800 m within 200 years, see Tinner and Kaltenrieder, 2005). Pollen data from Crotte Basse site (**Fig. 12**) suggests the presence of *Pinus cembra* in the valley floor from at least 13000 yrs cal BP. Likewise, at Gouillé Rion (Valais, central Swiss Alps, 2343 m asl) *Pinus cembra* was present from ca. 14 000 yrs cal BP (Tinner et al. 1996) and macrofossil findings of this species in the Valais region (Simplon, 2005 m a.s.l., c. 50 km distant) confirm its Late-Glacial and early Holocene presence at lower altitudes (Lang & Tobolski 1985). Slightly before 8800 yrs cal BP, in the Rutor area, a possibly glacier oscillation interfered with the forest colonization in the glacier foreland. The latter may correspond to a cold phase recorded at Gouillé Rion pollen record (Rion-2, Tinner et al.,2005) lasted from 9300 to 8900 yrs cal BP. Afterwards, between ca. 8800 and 8400 cal yr BP, a local *Pinus cembra* steady expansion (**Fig. 21**) occurred. During this phase vegetation dynamics could have been triggered mainly by the local glacier retreat, including a primary succession within the glacier foreland (**Fig. 20**). Therefore, the reliability of temperature reconstruction for this period is uncertain (**Fig. 19** - see “no analogue” rectangles). Interestingly, a cooler rapid oscillation (1-1,5 ˚C) occurred at ca. 8370 yrs cal BP marked the beginning of the *Abies* expansion. During these 800 years (8800-8000 yrs cal BP), *Pinus cembra* PAR

values were comparable with those obtained for the modern timberline ecotone (ca. 1000 grains cm^{-2} yrs^{-1}; **Fig. 21**). Thus, the fossil site was lying in the timberline ecotone probably characterized by a mosaic of open *Pinus cembra* stands. Around 7900-7950 yrs cal BP, a temperature rise of ca. 1 ˚C (**Fig. 21**) possibly promoted an upward shift of *Pinus cembra* specimens as shown by higher fossil *Pinus cembra* PAR values, suggesting an increase in biomass. Between 7950 and 3800 yrs cal BP, high *Pinus cembra* % and PAR values (respectively 50-60% and 500-2000 grains cm^{-2} yrs^{-1}), suggest a higher than today timberline stand lasted for ca. 4000 years. During this period Rutor fossil sites: Buried peat site (2510 m asl) and Valter Mire (2594 m asl) continued to lie within the timberline ecotone.

These evidences are corroborated by the the occurrence of a *Pinus cembra* uncharred wood dated 5600 - 5700 yrs cal BP at 2594 m asl. This cm-sized macrofossil cannot have been long-distance transported, thus it indicates the presence of this species *in situ*. Indeed, transport of macroscopic particles depends on saltation (driven through strong winds) and in part on (melt) water transport. Because they are not usually transported very far from their point of origin (Birks and Birks, 1980), macrofossil results have a high (meter to decameter) spatial resolution. Additionally, from ca. 8000 to 4000 yrs cal BP, pollen-inferred TJuly reconstructions (**Fig. 22**) show higher values (~ 3°C) than today (1981-2010 period).

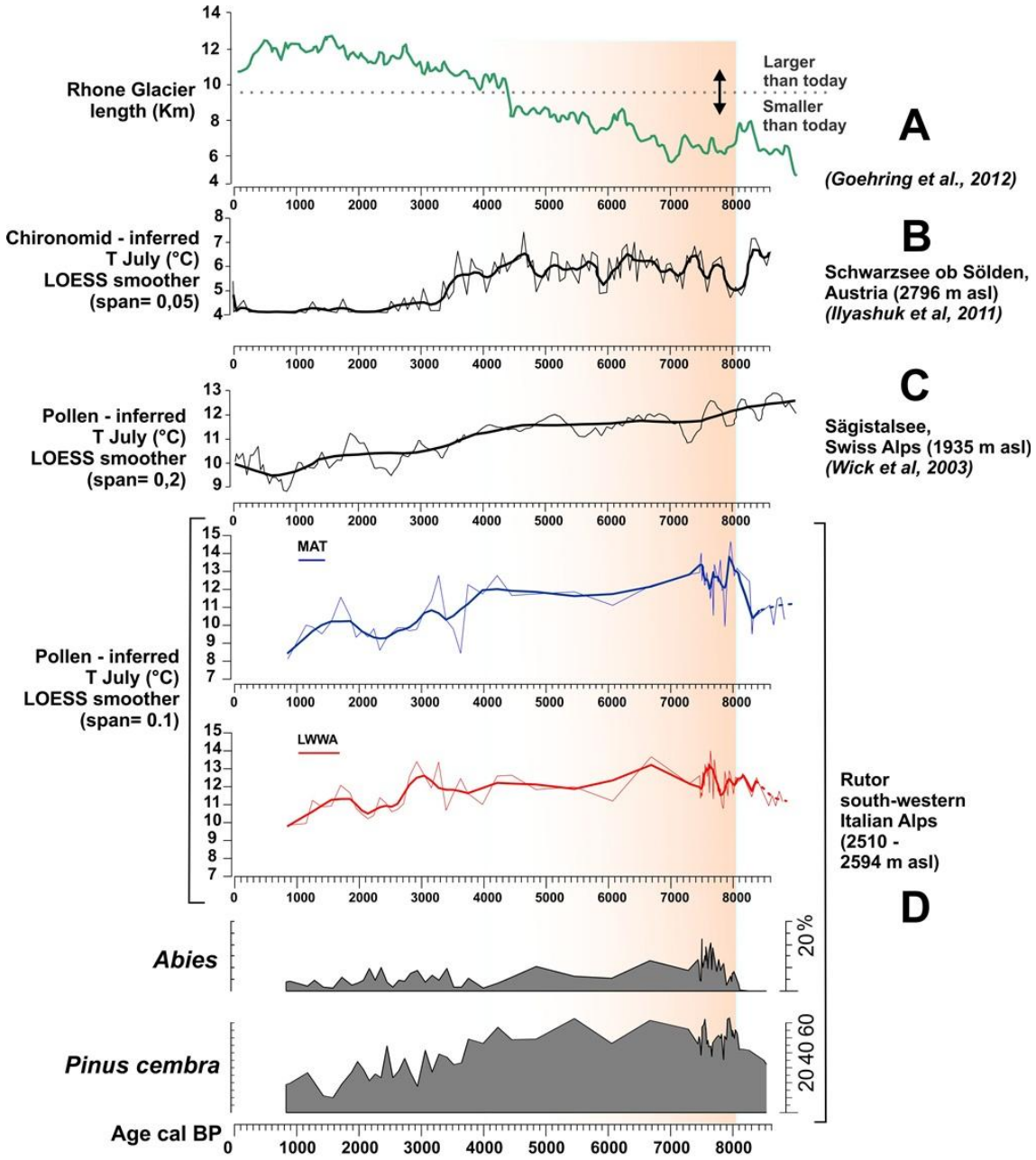

Fig. 22 - Selected published proxy records for climate variations during the last 8800 yrs from different sites in the Alps. (A) Rhone Glacier length variations (Goehring et al., 2012); (B) Chironomid-inferred temperature from Schwarzsee ob Sölden, Austria (2796 m asl); (C) Pollen-inferred temperature from Sägistalsee, Swiss Alps (1935 m asl); (D) Rutor pollen-inferred reconstructions (red line=LWWA and blue line= MAT) beside selected % pollen curves (*Pinus cembra* and *Abies*).

Most paleoecological studies indicate that during middle Holocene the upper treeline oscillated ca. 100 - 150 m from today's position (Patzelt, 1977; Burga and Perret, 1998, 2001; Haas et al., 1998, Tinner & Theurillat, 2003). Moreover, non-botanical evidence points to conditions warmer than present between ca. 10,000 – 8400 and 7600 to 4000 cal. BP in the Alps (Grosjean et al., 2007; Heiri et al., 2003, 2004; Joerin et al., 2008; von Grafenstein et al., 1998, 1999). In the Central Swiss Alps, between 10950 and 4450 yrs cal BP the uppermost limit reached by timberline and treeline was ca. 2420 and 2530 m, respectively, i.e., about 120 to 180 m asl higher than today (e.g. Gouillé Rion, Gouillé Loére (**Fig. 23**); Tinner & Theurillat, 2003). Between 5400 and 4450 yrs cal BP timberline progressively sank by about 300 m, while treeline was lowered only ca. 100 m. In this area the Bronze age began at 2200 BC (ca. 4150 yrs cal BP), indicating the onset of a new and more intensive land use system based on alpine summer farming (Tinner & Theurillat, 2003). It seems that in the Rutor area treeline experienced slightly higher positions (**Fig. 23**) while a treeline lowering occurred later, around 3800 yrs cal BP. Here, TJuly reconstructions (**Fig. 22**) clearly shown a climate deterioration of ca. 3 °C, compared with the previous period, started around 4000 – 3800 yrs cal BP. Our results are in agreement with other palaeoclimate reconstructions in the Alps, where a cooling phase occurred around 4000 yrs cal BP with a drop in temperature of ca. 2-3 ˚C, compared with the previous period, is documented: e.g. Heiri et al. 2003; Ilyashuk et al., 2011 (**Fig. 22)** and Wick et al., 2003; Ortu et al., 2008. Knowing that the first evidences of relevant human activities in the Rutor area occurred later, during the Roman time (see **Chapter 3**), this scenario suggest a local climate-driven treeline sank. Otherwise, at the Crotte Basse site (2365 m asl), just a few km from the Rutor site, local human disturbance (e.g. burning and grazing activities) started around 5600 yrs cal BP producing openings in the timbeline ecotone formerly, since the Copper age (**Fig. 23**).

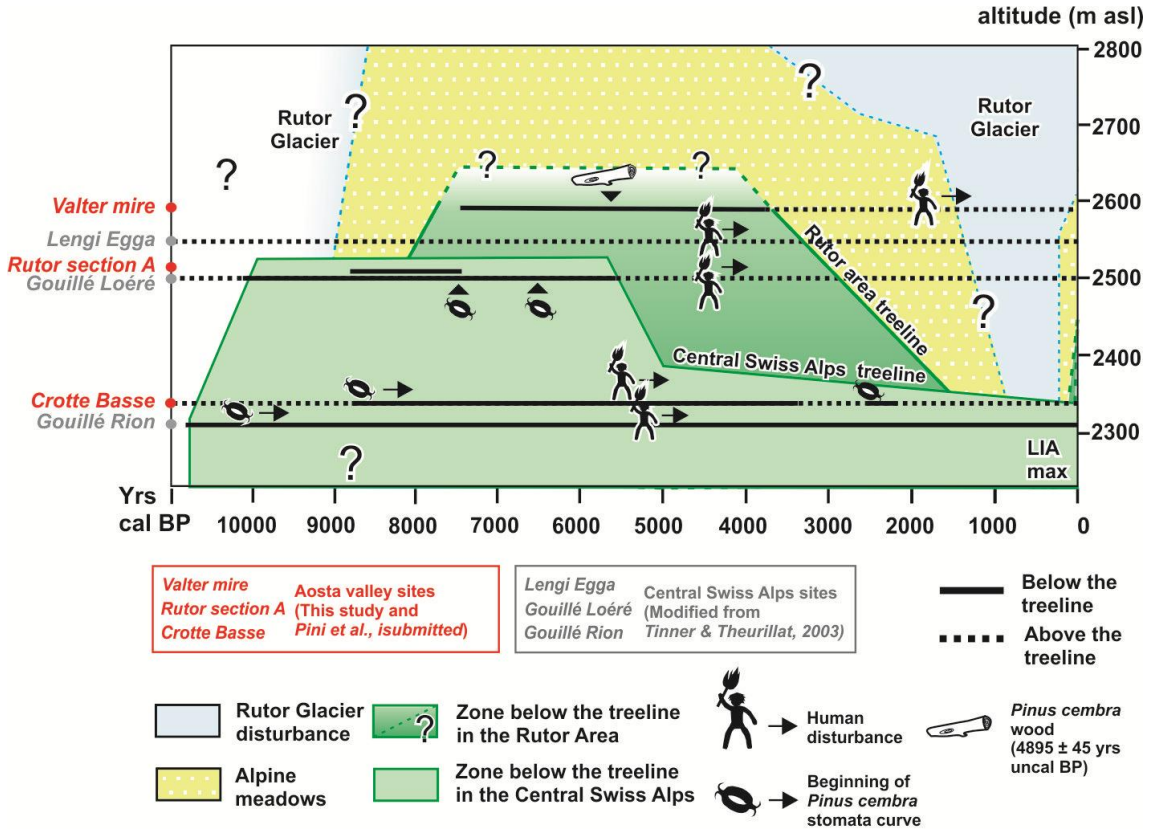

Fig. 23 - Biosketch – treeline shifts as recorded in pollen records from the Aosta Valley (Rutor area) and the Central Swiss Alps (Tinner & Theurillat, 2003) from 11000 yrs cal BP to modern time. The reconstruction is plotted against time and altitude, with relevant sites between 2300 and 2600 m asl shown on the y-axis; In red: Rutor section A, Valter mire (present study) and Crotte Basse site (Pini et al., submitted). In grey: Central Swiss Alps sites (Lengi Egga, Gouillé Loére, Gouillé Rion). Continuous/ dashed line indicates the site position below/ above the treeline during specific time intervals. Symbols (see legend) add further key elements (e.g. human disturbance, wood/stomata occurrences) useful to integrate the framework.

5.4. Evidence of Early-Middle Holocene prolonged glacier contraction and Alpine climate variability

Glacial deposits in the valley floor downhill to the Rutor Glacier highlands testify to Lateglacial advances (“La Thuile-Stage”; Charrier & Peretti, 1972; Armando et al., 1975), also recorded in the nearby Mont Blanc area (Porter and Orombelli, 1982), but not yet directly dated. In the Holocene first three millennia, the Rutor Glacier cleared the valley floor and retreated to the highlands. The evidence of

primary plant succession so far discussed at Rutor buried peat site, dated to 8800 yrs cal BP, suggests that local deglaciation occurred just a few decades earlier. The Early Holocene Venediger oscillation in Eastern Alps, currently dated to be older than 9.2. ka cal BP (Patzelt in Nicolussi and Patzelt, 2001) may be compared with the observed pattern at Rutor Glacier. Furthermore, high-frequency fluctuations of solar irradiance suggest a solar-activity minima at 9400 yrs cal BP which possibly caused a substantial cooling over the Alps and Central Europe (Muscheler et al. 2000). Similarly, a moraine of the Glacier de Tsidjore Nouve at Arolla (Valais, Switzerland; Röthlisberger, 1976) is now dated between 9.6 and 9.3 ka cal BP (Joerin et al., 2006). Interestingly, a petrographic and stable isotopic record from a cave close to the Upper Grindelvald Glacier in the Swiss Alps suggests a glacier advance U/Th dated to 9.192 ± 0.159 ka b2k (Luetscher et al., 2011). We thus suggest that the observed deglaciation high in the Rutor glacier catchement occurred at the very end of this Early Holocene cold oscillation.

According to the current Alpine framework of Holocene glacier oscillations (Joerin et al. (2006, 2008), this event took place just prior to the first Holocene warm interval (**Fig. 24**). Indeed, our data suggest persisting glacier recession during the subsequent period (8800-7400 yrs cal BP) (**Fig. 24**). Our paleobotanical data suggest a warm and dry phase with a strong seasonality during the early Holocene. At an Hemispheric scale, frequent early Holocene droughts resulted from a maximum of summer solar radiation in the Northern Hemisphere at ca 9000 cal. BP (Kutzbach and Webb, 1993). In the northern mid latitudes evaporation was at a maximum and, therefore, moisture availability at a minimum. A coeval minimum of winter solar radiation resulted in colder winters. In combination with hot summers, leading to a greater seasonal contrast than today (Kutzbach and Webb, 1993). It is likely that these climate conditions inhibited the expansion of *Abies alba* in the Alps. This forest tree is among the most drought-sensitive tree of Europe (Asthalter, 1984; Peterken and Mountford, 1996; Webster et al., 1996). *Abies alba* pollen spreads at ca. 8370 yrs cal BP (median probability of the 2 sigma calibration interval), both in the Rutor site and in the near Crotte Basse site (2365 m asl, **Fig. 12**). Temperature reconstructions show a climate cooling of about 1 - 2˚C at 8375 yrs cal BP (**Fig. 24**). Furthemore,

at this time, we observed the development of a peat mire (paludification) in the Rutor buried peat sequence indicative of precipitation increase, which is stratigraphically related to a coeval expansion of *Abies* pollen curve. *Abies* expansion is triggered by the 8.2 ka climatic oscillation (Tinner and Lotter, 2006). This event was recognized as the most extreme climatic anomaly in the Greenland ice core $\delta^{18}O$ records during the Holocene (**Fig. 24**). The duration of the entire 8.2 ka event in Greenland was ~ 160 yrs (between 8297 and 8136 yrs before A.D. 2000 [b2k]) (Alley and Ágústsdóttir, 2005; Thomas et al., 2007). In central Europe, several proxy data, e.g. isotope records from lake sediments (von Grafenstein et al., 1998, 1999) and speleothems (Boch et al., 2009) it is shown to have lasted 100 - 130 yrs, with a reconstructed temperature depression of ~1.5 – 3 °C. Other records based on plant proxies indicate that the 8.2 ka event was the onset of a longer lasting (until ca. 7.6 ka) cold and wet period in central Europe (e.g., Kofler et al., 2005) and thus advantaged the expansions of *Fagus* and *Abies* (Tinner & Lotter, 2006). However, we missed firm time constrains for this event be represented in the archive of glacier oscillations. Only Kerschner et al. (2006) proposed a 8.2 ka glacier advance based on exposure age dating. Furthermore, Nicolussi & Schlüchter (2012) presented evidence for such an advance related to the 8.2 ka event based on dendrochronological analyses for tree remains found in front of the Mont Miné Glacier (Swiss Alps). The lack of a 8,2 ka glaciological evidence in the Rutor proglacial area may be related to the effects of the preceding long recession phase (8800 - 8400 yrs cal BP), which constrained glacier fluctuations well above the current (2010 AD) glacier fronts.

The radiocarbon chronology obtained from the Buried peat sections (between 8800 and 7400 yrs cal BP) together with a further buried peat section dated between ca. 7300 and 3700 yrs cal BP (Armando et al., 1975) (**Fig. 24**), suggest an even longer phase of Rutor glacier recession, lasting ca. 4-5 ka yrs between 8800 and 3700 yrs cal BP. During this period the glacier fluctuations remained within the extent of 1975 AD, or even 2010 AD. Likewise, the Rhone Glacier remained in a position smaller than today since the early Holocene until approximately 5 ka (Goehring et al., 2012) (**Fig. 22).**

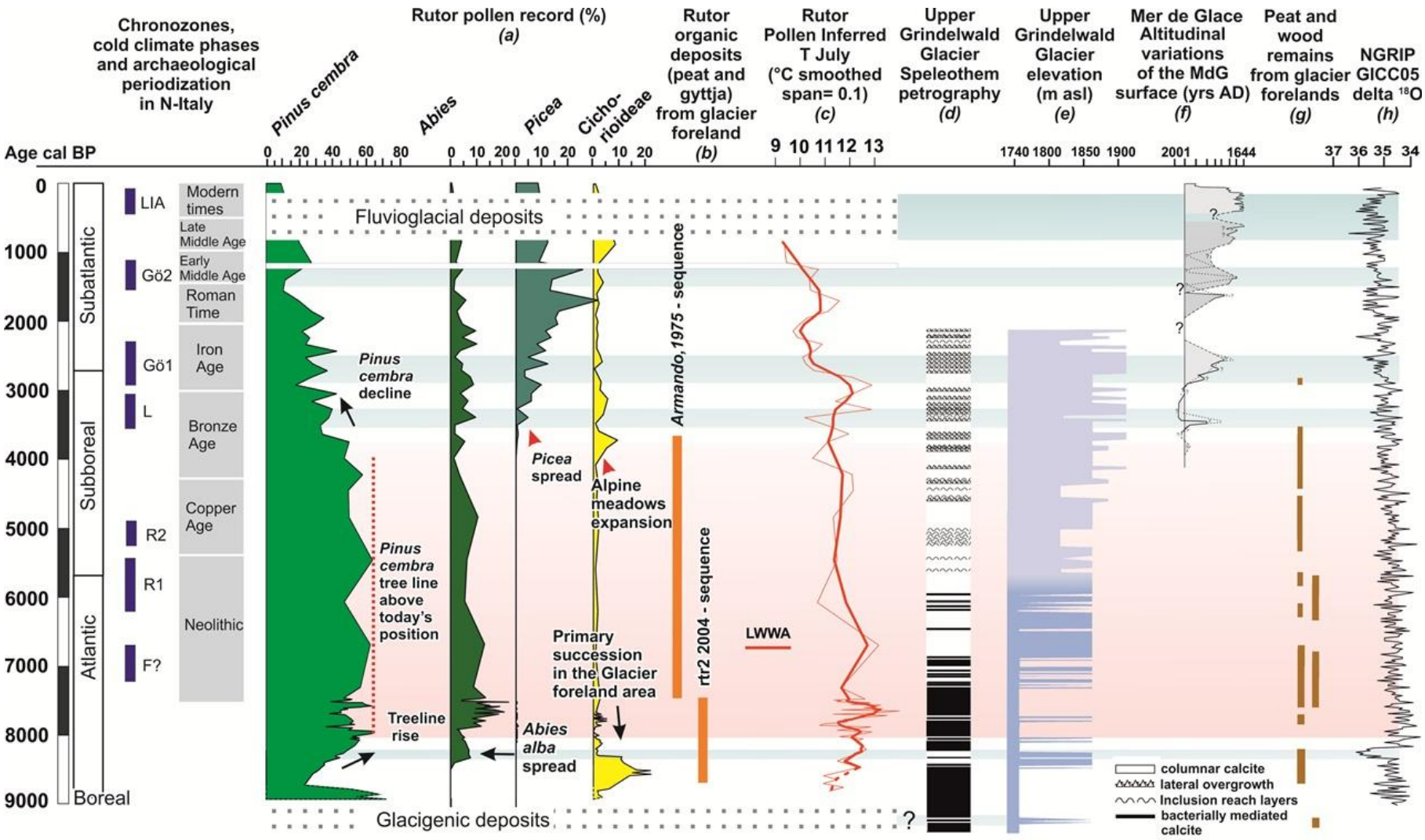
Chronozones, cold climate phases and archaeological periodization in N-Italy
Rutor pollen record (%) (a)
Pinus cembra
Abies
Picea
Cicho-rioideae
Rutor organic deposits (peat and gyttja) from glacier foreland (b)
Rutor Pollen Inferred T July (°C smoothed span= 0.1) (c)
Upper Grindelwald Glacier Speleothem petrography (d)
Upper Grindelwald Glacier elevation (m asl) (e)
Mer de Glace Altitudinal variations of the MdG surface (yrs AD) (f)
Peat and wood remains from glacier forelands (g)
NGRIP GICC05 delta 18O (h)
Age cal BP
Subatlantic
Subboreal
Atlantic
Boreal
LIA
Gö2
Gö1
L
R2
R1
F?
Modern times
Late Middle Age
Early Middle Age
Roman Time
Iron Age
Bronze Age
Copper Age
Neolithic
Fluvioglacial deposits
Glacigenic deposits
Pinus cembra decline
Pinus cembra tree line above today's position
Treeline rise
Picea spread
Alpine meadows expansion
Abies alba spread
Primary succession in the Glacier foreland area
Armando, 1975 - sequence
rtr2 2004 - sequence
LWWA
columnar calcite
lateral overgrowth
Inclusion reach layers
bacterially mediated calcite

Fig. 24

Fig. 24 - Overview of palynological and climate reconstruction from the Rutor site compared with glacier dated advance and recession phases in the Alps. a) Rutor selected % pollen curves; b) Rutor organic deposits in the glacier foreland (section A – present study and Armando et al., 1975); c) Rutor pollen-inferred Tjuly reconstruction (LWWA) d), e) Synthesis of Upper Grindelwald Glacier fluctuations interpreted from Milchbach speleothems (Luetsher et al., 2011); f) Mer de Glace altitudinal position (Le Roy et al., 2015); g) Peat and wood remains found in sediments deposited at the front of retreating Swiss glaciers (Joerin et al., 2006, 2008); h) NGRIP GICC05 delta ^{18}O (Svensson et al.,2008). F: Frosnitz; R 1-2: Rotmoos; L: Löbben oscillation; Gö 1-2: Göschener oscill.; LIA: Little Ice Age.

6. CONCLUSIONS

The study of buried peat and minerogenic deposits from the Rutor Glacier area allowed us to obtain new data, as listed below:

- The fossil records studied in the elevational foreland of the Rutor Glacier (between 2510 and 2595 m asl) document to a long phase of glacier recession between ca. 8800 and 3700 yrs cal BP.

- A continuous palynological record was obtained between 8800 and 7400 years cal BP with a mean time resolution of 28 years.

- For the first time in the Alpine literature, the palynological evidence of a deglacial plant succession developed on pre-LIA glacial deposits was documented. The comparison with similar post-LIA vegetation analogues in the Alps allowed to document similarities with modern ecological primary successions. Furthermore, the existence of this succession corroborates the stratigraphic continuity at the base of the Rutor buried peat sequence.

- A pollen-inferred temperature record has been obtained from the highest so far available site in the Alps. TJuly and TJan show a warmer Holocene between 8000 and 4000 yrs cal BP, with TJuly ca. 3 °C higher than today (1981 – 2010 period). A drop in temperature, compared with the previous period, of ca. 3 ˚C started around 4000 yrs cal BP. A first cooling step occurred between ca. 4000 and 3400 yrs cal BP, a second one between ca.

2900 and 2000 yrs cal. BP and a third from 1150 till the end of the record (853 yrs cal BP).

- According to the comparison between fossil and modern data: e.g. PAR (Pollen Accumulation Rate) values and July temperature, results are consistent with an upper timberline position of ca. 300 m above its present altitude during the middle Holocene.

- In the Rutor area a *Nardus-Leontodon* herb community expansion at high altitudes forming seasonally drained meadows is proposed as one of the primary habitats of *Nardus* in the Alps, before the onset of human impact

- The biological proxies discussed in the light of the current understanding of the climatic history in the Alps highlight the following evidences:

    - The evidence of a primary plant succession dated to 8800 yrs cal BP suggests that local deglaciation occurred just a few decades earlier

    - The lack of a 8,2 ka glaciological evidence in the Rutor proglacial area may be related to the effects of the preceding long recession phase (8800 - 8400 yrs cal BP), which constrained glacier fluctuations well above the current (2010 AD) glacier fronts

    - *Abies* expansion was triggered by the 8.2 ka event, locally marked by the development of a mire, indicative of precipitation increase

Further investigations are needed to gain new palaeoecological data from high-altitude areas, where the main driving force for vegetation dynamics is climate variability. Moreover, to contribute to our understanding of the responses to rapid climatic changes, new high-resolution pollen records and pollen-inferred temperature reconstructions in the Alps may be useful.

ACKNOWLEDGEMENTS

The results of this study could not be achieved without the help and the support of many people: Elena Champvillair for her assistance and collaboration, Giulia Furlanetto for her help with climate reconstructions, Michela Mariani and Andrea Tramelli for preparing the pollen samples as well as Sergio Pestarino for his logistic support.

Since the studied mire hadn't got a name due to its low interest in pastoral activities, and since the nearby lake has a complex name, we prefer to assign a unique denomination. Therefore we have decided to name this peat archive after its discoverer, Prof. Valter Maggi, glaciologist, an active student of the Rutor Glacier. The name "Valter mire" is being deposited at the Office of Nature Conservation of the RAVA.

REFERENCES

Aceti A. (2006). La variabilità climatica nell'Olocene: studio di torbiere e ambienti d'alta quota nelle Alpi italiane. Unpublished PhD Thesis in Geological Sciences, Univ. Milano-Bicocca, 115 pp.

Alley, R. B., & Ágústsdóttir, A. M. (2005). The 8k event: cause and consequences of a major Holocene abrupt climate change. Quaternary Science Reviews, 24(10), 1123-1149.

Ammann, B. (1994). Differential flotation of saccate pollen e a nuisance and a chance. Diss. Bot. 234, 101-110.

Armando, E., Charrier, G., Peretti, L. & Piovano, G. (1975). Ricerche sull'evoluzione del clima e dell'ambiente durante il Quaternario nel settore delle Alpi Occidentali Italiane. Bollettino del Comitato Glaciologico Italiano, 23, 7-25.

Armando, E. & Charrier, G. (1985). La torbiera del Rutor (Valle d'Aosta). Relazioni sui risultati conseguiti dallo studio palinostratigrafico di nuovi affioramenti torbosi segnalati alla fronte attuale del ghiacciaio. Geografia Fisica e Dinamica Quaternaria, 8, 144-149.

Armstrong, W. (1979), Aeration in higher plants. Adv. Bot. Res., 7, 225-332.

Asthalter, K. (1984). Dry periods and forest damage from the standpoint of forest history and site studies. Allgemeine Forstzeitschrift, (22), 549-551.

Ballesteros, E., Gacia, E., & Camarero, L. (1989). Composition, distribution and biomass of benthic macrophyte communities from lake Baciver, a Spanish alpine lake in the Central Pyrenees. In Annales de limnologie (Vol. 25, No. 2, pp. 177-184). EDP Sciences.

Baretti, M. (1880). Il Lago del Rutor (Alpi Graie Settentrionali). Annuario Club Alpino Italiano, Torino.

Berthel, N., Schwörer, C., & Tinner, W. (2012). Impact of Holocene climate changes on alpine and treeline vegetation at Sanetsch Pass, Bernese Alps, Switzerland. Review of Palaeobotany and Palynology, 174, 91-100.

Beug, H.J. (2004). Leitfaden der Pollenbestimmung für Mitteleuropa und angrenzende Gebiete. Verlag Dr. Friedrich Pfeil, München.

Birks, H. J. B., & Birks, H. H. (1980). Quaternary palaeoecology (p. 289). London: Edward Arnold.

Blaauw, M., & Christen, J. A. (2011). Flexible paleoclimate age-depth models using an autoregressive gamma process. Bayesian Analysis, 6(3), 457-474.

Brandani, A. A. (1983). Glacial processes and disturbance in vegetation richness. In: Evenson, E. B., Schlu¨chter, Ch. & Rabassa, J. (eds), Tills and related deposits. Balkema- Rotterdam, 403-410.

Boch, R., Spötl, C., & Kramers, J. (2009). High-resolution isotope records of early Holocene rapid climate change from two coeval stalagmites of Katerloch Cave, Austria. Quaternary Science Reviews, 28(23), 2527-2538.

Bortenschlager, S., Kofler, W., Nicolussi, K., Oeggl, K., & Wahlmüller, N. (1998). The FOREST project: Sensitivity of Northern, Alpine and Mediterranean Forest limits to climate—final report of the Innsbruck-group. Institut für Hochgebirgsforschung—Jahresbericht, 1997, 47-65.

Brunetti, M., Maugeri, M., Nanni, T., Simolo, C., & Spinoni, J. (2014). High-resolution temperature climatology for Italy: interpolation method intercomparison. International Journal of Climatology, 34(4), 1278-1296.

Buia, A. (1963). Les Associations á Nardus stricta L. De La R. P. R. Rev. de Biol. 8(2): 119–138.

Burga, C. A. (1991). Vegetation history and palaeoclimatology of the Middle Holocene: pollen analysis of alpine peat bog sediments, covered formerly by the Rutor Glacier, 2510 m (Aosta Valley, Italy). Global Ecology and Biogeography Letters, 143-150.

Burga, C. A. (1995). Végétation et paléoclimatologie de l'Holocène moyen d'une ancienne tourbière située au front du Glacier du Rutor, 2 510m (Vallée d'Aoste, Italie). Vegetation and paleoclimatology of the Middle Holocene of a former peat bog situated at the front of the Rutor Glacier, 2510 m (Aosta valley, Italy). Revue de géographie alpine, 83(1), 9-16.

Burga, C. A., & Perret, R. (1998). Vegetation und Klima der Schweiz seit dem jüngeren Eiszeitalter. Thun: Ott Verlag. 805 pp.

Burga, C. A., & Perret, R. (2001). Monitoring of eastern and southern Swiss alpine timberline ecotones. In Burga, C. A. and Kratochwil, A. (eds.), Biomonitoring: General and Applied Aspects on Regional and Global Scales: Tasks for Vegetation Science. Dordrecht: Kluwer. 179–194.

Caccianiga, M., Andreis, C. & Cerabolini, B. (2001). Vegetation and environmental factors during primary succession on glacier forelands: some outlines from the Italian Alps. Plant Biosystems 135 (3): 295-310.

Caccianiga, M., Luzzaro, A., Turri, D., Viapiana, G., & Andreis, C. (2002). Indagini sulla flora del Ghiacciaio del Rutor (La Thuile-AO). Revue Valdôtaine d'Histoire Naturelle, 15-35.

Caccianiga, M., & Andreis, C. (2004). Pioneer herbaceous vegetation on glacier forelands in the Italian Alps. Phytocoenologia, 34(1), 55-89.

Caccianiga, M., Luzzaro, A., Pierce, S., Ceriani, R. M., & Cerabolini, B. (2006). The functional basis of a primary succession resolved by CSR classification. Oikos, 112(1), 10-20.

Caccianiga, M., & Compostella, C. (2012). Growth forms and age estimation of treeline species. Trees, 26(2), 331-342.

Charrier, G. & Peretti, L. (1972). Ricerche sull'evoluzione del clima e dell'ambiente durante il Quatemario nel settore dell Alpi Occidentali Italiane. Allionia, 18, 167-177.

Crawford, R. M. M. (1989), Studies in plant survival: ecological case histories of plant adaptation to adversity Exp. Bot., 47 : (295), 145-159.

Christen, J. A., & Perez, S. (2009). A new robust statistical model for radiocarbon data. Radiocarbon, 51(3), 1047-1059.

D'Arrigo, R. D., & Jacoby, G. C. (1993). Tree growth-climate relationships at the northern boreal forest tree line of North America: Evaluation of potential response to increasing carbon dioxide. Global Biogeochemical Cycles, 7(3), 525-535.

Dal Piaz G.V. (ed.), (1992). Le Alpi dal M. Bianco al Lago Maggiore. Guide geologiche regionali (voll. I e II). Milano, Società Geologica Italiana, BE-MA. 311 p.

Daly C., Neilson R.P., Phillips D.L. (1994). A statistical-topographic model for mapping climatological precipitation over Mountanious Terrain. Journal of Applied Meteorology 33: 140–158.

Daly C., Gibson W.P., Taylor G.H., Johnson G.L., Pasteris P. (2002). A knowledge based approach to the statistical mapping of climate. Climate Research 22: 99–113.

Davis B. & other 80 authors (2013). The European Modern Pollen Database (EMPD) Project. Vegetation History and Archaeobotany, 22: 521-530.

Dean, W. E. Jr. (1974). Determination of carbonate and organic matter in calcareous sediments and sedimentary rocks by loss on ignition: Comparison with other methods. J. Sed. Petrol. 44, 242–248.

Ellenberg, H. (1996). Vegetation Mitteleuropas mit den Alpen, 5th edn. Ulmer, Stuttgart.

Ellenberg, H., & Leuschner, C. (1996). Vegetation mitteleuropas mit den Alpen (Vol. 1095). Ulmer, Stuttgart.

Erschbamer, B., Kneringer, E. & Niederfriniger-Schlag, R. 2001. Seed rain, soil seed bank, seedling recruitment, and survival of seedlings on a glacier foreland in the Central Alps. Flora 196, 304-312.

Gajewski, K., Payette, S., & Ritchie, J. C. (1993). Holocene vegetation history at the boreal-forest--shrub-tundra transition in North-Western Quebec. Journal of Ecology, 433-443.

van Geel, B. (1978). A palaeoecological study of Holocene peat bog sections in Germany and The Netherlands, based on the analysis of pollen, spores and macro- and microremains of fungi, algae, cormophytes and animals. Review of Palaeobotany and Palynology 25, 1-120.

van Geel, B., Bohncke, S.J.P., Dee, H. (1981). A palaeoecological study of an upper Late Glacial and Holocene sequence from 'De Borchert', The Netherlands. Review of Palaeobotany and Palinology 31, 367-449.

Goehring, B. M., Vacco, D. A., Alley, R. B., & Schaefer, J. M. (2012). Holocene dynamics of the Rhone Glacier, Switzerland, deduced from ice flow models and cosmogenic nuclides. Earth and Planetary Science Letters, 351, 27-35.

von Grafenstein, U., Erlenkeuser, H., Müller, J., Jouzel, J., & Johnsen, S. (1998). The cold event 8200 years ago documented in oxygen isotope records of precipitation in Europe and Greenland. Climate dynamics, 14(2), 73-81.

von Grafenstein, U., Erlenkeuser, H., Brauer, A., Jouzel, J., & Johnsen, S. J. (1999). A mid-European decadal isotope-climate record from 15,500 to 5000 years BP. Science, 284(5420), 1654-1657.

von Grafenstein, U., Eicher, U., Erlenkeuser, H., Ruch, P., Schwander, J., & Ammann, B. (2000). Isotope signature of the Younger Dryas and two minor oscillations at Gerzensee (Switzerland): palaeoclimatic and palaeolimnologic interpretation based on bulk and biogenic carbonates. Palaeogeography, Palaeoclimatology, Palaeoecology, 159(3), 215-229.

Grimm, J. P. (1977). Evidence for the existence of three primary strategies in plants and its relevance to ecological and evolutionary theory. Am. Nat. 111, 1169-1194. Grimm, E.C., 1987. CONISS: a FORTRAN 77 program for stratigraphically constrained cluster analysis by the method of incremental sum of squares. Comput. Geosci. 13 (1), 13-35.

Grimm, E.C. (1991-2011). Tilia 1.7.16. Illinois State Museum, Research and Collection Center, Springfield.

Grosjean, M., Suter, P. J., Trachsel, M., & Wanner, H. (2007). Rapid Communication Ice-borne prehistoric finds in the Swiss Alps reflect Holocene glacier fluctuations. Journal of Quaternary Science, 22(3), 203-207.

Guiot, J. (1990). Methodology of the last climatic cycle reconstruction in France from pollen data. Palaeogeography, Palaeoclimatology, Palaeoecology, 80(1), 49-69.

Gustafsson, Ö., Bucheli, T. D., Kukulska, Z., Andersson, M., Largeau, C., Rouzaud, J. N., ... & Eglinton, T. I. (2001). Evaluation of a protocol for the quantification of black carbon in sediments. Global Biogeochemical Cycles, 15(4), 881-890.

Haas, J. N., Richoz, I., Tinner, W., & Wick, L. (1998). Synchronous Holocene climatic oscillations recorded on the Swiss Plateau and at timberline in the Alps. The Holocene, 8, 301-309.

Heiri, O., Lotter, A. F., Hausmann, S., & Kienast, F. (2003). A chironomid-based Holocene summer air temperature reconstruction from the Swiss Alps. The Holocene, 13(4), 477-484.

Heiri, O., Tinner, W., & Lotter, A. F. (2004). Evidence for cooler European summers during periods of changing meltwater flux to the North Atlantic. Proceedings of the National Academy of Sciences of the United States of America, 101(43), 15285-15288.

Heiri, C., Bugmann, H., Tinner, W., Heiri, O., & Lischke, H. (2006). A model-based reconstruction of Holocene treeline dynamics in the Central Swiss Alps. Journal of Ecology, 94(1), 206-216.

Holtmeier, F. K. (2009). Mountain timberlines: ecology, patchiness, and dynamics (Vol. 36). Springer Science & Business Media.

Hormes, A., Müller, B. U., & Schlüchter, C. (2001). The Alps with little ice: evidence for eight Holocene phases of reduced glacier extent in the Central Swiss Alps. The Holocene, 11(3), 255-265.

Hübener T., Dreßler M., Schwarz A., Langner K., Adler S. (2008). Dynamic adjustment of training sets (‘moving-window’ reconstruction) by using transfer functions in paleolimnology - a new approach. J Paleolimnol, 40: 79–95.

Ilyashuk, E. A., Koinig, K. A., Heiri, O., Ilyashuk, B. P., & Psenner, R. (2011). Holocene temperature variations at a high-altitude site in the Eastern Alps: a chironomid record from Schwarzsee ob Sölden, Austria. Quaternary Science Reviews, 30(1), 176-191.

Ivy-Ochs, S., Kerschner, H., Maisch, M., Christl, M., Kubik, P. W., & Schlüchter, C. (2009). Latest Pleistocene and Holocene glacier variations in the European Alps. Quaternary Science Reviews, 28(21), 2137-2149.

Jackson, S. T., & J. W. Williams (2004). Modern analogs in Quaternary paleoecology: Here today, gone yesterday, Annu. Rev. Earth Planet. Sci., 32, 495–537.

Jobbágy, E. G., & Jackson, R. B. (2000). The vertical distribution of soil organic carbon and its relation to climate and vegetation. Ecological applications, 10(2), 423-436.

Joerin, U. E., Stocker, T. F., & Schlüchter, C. (2006). Multicentury glacier fluctuations in the Swiss Alps during the Holocene. The Holocene, 16(5), 697-704.

Joerin, U. E., Nicolussi, K., Fischer, A., Stocker, T. F., & Schlüchter, C. (2008). Holocene optimum events inferred from subglacial sediments at Tschierva Glacier, Eastern Swiss Alps. Quaternary Science Reviews, 27(3), 337-350.

Juggins S. and Birks H.J.B. (2012). Quantitative Environmental Reconstructions from Biological Data, Chapter 14, ess.: H.J.B. Birks et al., Tracking Environmental Change Using Lake Sediments, Developments in Palaeoenvironmental Research 5, doi. 10.1007/978-94-007-2745-8_14, Springer Science+Business Media B.V. 2012, 431- 483

Juggins, S. (2015) rioja: Analysis of Quaternary Science Data, R package version (0.9-9).

Kalliola, R. 1972. Suomen kasvimaantiede. Werner Söderström Osakeyhtiön, Helinski. 308 pp.

Kerschner, H., Hertl, A., Gross, G., Ivy-Ochs, S., & Kubik, P. W. (2006). Surface exposure dating of moraines in the Kromer valley (Silvretta Mountains, Austria)-evidence for glacial response to the 8.2 ka event in the Eastern Alps?. The Holocene, 16(1), 7-15.

Kofler, W., Krapf, V., Oberhuber, W., & Bortenschlager, S. (2005). Vegetation responses to the 8200 cal. BP cold event and to long-term climatic changes in the Eastern Alps: possible influence of solar activity and North Atlantic freshwater pulses. The Holocene, 15(6), 779-788.

Körner, C. (1998). A re-assessment of high elevation treeline positions and their explanation. Oecologia, 115(4), 445-459.

Körner, Ch. (1999a). Alpine plant life: functional plant ecology of high mountain ecosystems. Springer.

Körner, C., & Paulsen, J. (2004). A world-wide study of high altitude treeline temperatures. Journal of Biogeography, 31(5), 713-732.

Kutzbach, J. E., & Webb III, T. (1993). Conceptual basis for understanding Late-Quaternary climates. Global climates since the last glacial maximum, 5-11.

Lang, G. & Tobolski, K. (1985). Hobschensee-Late glacial and Holocene environment of a lake near the timberline. Disser- tationes Botanicae, 87, 209-228.

Lang, G. (1994). Quartäre vegetationsgeschichte Europas: methoden und ergebnisse.

Van Leeuwen, P., Punt, W., & Hoen, P. P. (1988). Polygonaceae. Review of Palaeobotany and Palynology, 57(1-2), 81-151.

Lucassen, E. C., Spierenburg, P., Fraaije, R. G. A., Smolders, A. J. P., & Roelofs, J. G. M. (2009). Alkalinity generation and sediment CO2 uptake influence establishment of Sparganium angustifolium in softwater lakes. Freshwater Biology, 54(11), 2300-2314.

Luetscher, M., Hoffmann, D. L., Frisia, S., & Spötl, C. (2011). Holocene glacier history from alpine speleothems, Milchbach cave, Switzerland. Earth and Planetary Science Letters, 302(1), 95-106.

Madsen, T. V., Olesen, B., & Bagger, J. (2002). Carbon acquisition and carbon dynamics by aquatic isoetids. Aquatic Botany, 73(4), 351-371.

Matthews, J. A. (1978). Plant colonisation patterns on a gletschervorfeld, southern Norway a meso-scale geographical approach to vegetation change and phytometric dating — Boreas 7, 155-178.

Matthews, J. A. (1992). The ecology of recently deglaciated terrain. A geoecological approach to glacier forelands and primary succession. Cambridge studies in ecology. Cambridge Univ. Press.

Milet, J., & Walton, D. W. H. (Eds.) (1993). Primary succession on land (No. 12). Blackwell Scientific Publications.

Moen, A. (1990). The plant cover of the boreal uplands of Central Norway. I. Vegetation ecology of Solender Nature Rserve. Gunneria 63, 1-451.

Moore, P.D., Webb, J.A., Collinson, M.E. (1991). Pollen Analysis. Blackwell Scientific Publications. Oxford University Press.

Muscheler, R., Beer, J., Wagner, G., & Finkel, R. C. (2000). Changes in deep-water formation during the Younger Dryas event inferred from 10Be and 14C records. Nature, 408(6812), 567-570.

Nicolussi, K., Lumassegger, G., Patzelt, G., Pindur, P., & Schiessling, P. (2001). Aufbau einer holozänen Hochlagen-Jahrring-Chronologie für die zentralen Ostalpen: Möglichkeiten und erste Ergebnisse. Innsbrucker Geographische Gesellschaft (Hrsg.): Innsbrucker Jahresbericht, 2(16), 114-136.

Nicolussi, K. & Patzelt, G. (2000). Discovery of early Holocene wood and peat on the forefield of the Pasterze Glacier, Eastern Alps, Austria. The Holocene, 10(2), 191-199.

Nicolussi, K. & Patzelt G. (2001). Untersuchungen zur holoz¨anen Gletscherentwicklung von Pasterze und Gepatschferner (Ostalpen). Zeitschrift f¨ur Gletscherkunde und Glazialgeologie 36, 1-87

Nicolussi, K. & Schlüchter, C. (2012). The 8.2 ka event—Calendar-dated glacier response in the Alps. Geology, 40(9), 819-822.

Nussbaumer, S. U., Steinhilber, F., Trachsel, M., Breitenmoser, P., Beer, J., Blass, A., ... & Zumbühl, H. J. (2011). Alpine climate during the Holocene: a comparison between records of glaciers, lake sediments and solar activity. Journal of Quaternary Science, 26(7), 703-713.

Orombelli, G., & Mason, P. (1997). Holocene glacier fluctuations in the Italian Alpine region. Glacier fluctuations during the Holocene, edited by: Harrison, SP, Frenzel, B., Boulton, GS, Glaser, B., and Huckrieder, U., Paläoklimaforschung-Paleoclim. Res, 24, 59-65.

Orombelli, G. (1998). Le torbe del Rutor: una successione significativa per la storia olocenica dei ghiacciai e del clima nelle Alpi. Studi in onore di Mario Pinna. I-Il clima e la storia del clima. Mem. Società Geografica It, 55, 153-165.

Orombelli, G. (2005). Il Ghiacciaio del Ruitor (Valle d'Aosta) nella piccola eta glaciale. Geografia Fisica e Dinamica Quaternaria, Suppl, 7, 239-251.

Ortu, E., Peyron, O., Bordon, A., de Beaulieu, J. L., Siniscalco, C., & Caramiello, R. (2008). Lateglacial and Holocene climate oscillations in the South-western Alps: an attempt at quantitative reconstruction. Quaternary International, 190(1), 71-88.

Overpeck, J. T., T. Webb III, and I. C. Prentice (1985). Quantitative interpretation of fossil pollen spectra: Dissimilarity coefficients and the method of modern analogs, Quat. Res., 23, 87–108.

Patzelt, G. (1972). Die spfitglazialen Stadien und postglazialen Schwankungen yon Ostalpengletschern. Ber Dtsch Bot Ges 85, 47-57.

Patzelt, G. & Bortenschlager, S. (1973). Postglaziale Gletscher- und Klimaschwankungen in der Venedigergruppe (Hohe Tauem, Ostalpen). Z Geomorph NF 16, 25-72.

Patzelt, G. (1977). Der zeitliche Ablauf und das Ausmass postglazialer Klimaschwankungen in den Alpen. In Frenzel, B. (ed.), Dendrochronologie und postglaziale Klimaschwankungen in Europa. Wiesbaden: F. Steiner Verlag. 248–259.

Payette, S., Delwalde, A., Morneau, C., & Lavole, C. (1996). Patterns of tree stem decline along a snow-drift gradient at treeline: a case study using stem analysis. Canadian Journal of Botany, 74(11), 1671-1683.

Peretti, L. (1935). Gruppo del Rutor e Miravidi-Lechaud. / Boll Comitato Glaciol. Italiano e della Commissione Glaciologica del C.A.I. 15, Torino, Italy.

Peretti, L. (1937). Morfologia glaciale della Valle della Dora di Verney (Alta Valle d'Aosta). Boll. Comit. Glac. It., 17.

Peretti, L. & Charrier, G. (1967). Segnalazione e analisi pollinica di torba deposta alla fronte attuale del ghiacciaio del Rutor (Valle d'Aosta). Considerazioni di paleogeografia e paleoclimatologia locale. Bollettino del Comitato Glaciologico Italiano, 14, 13-31.

Peterken, G. F., & Mountford, E. P. (1996). Effects of drought on beech in Lady Park Wood, an unmanaged mixed deciduous woodland. Forestry, 69(2), 125-136.

Pignatti, S. (1982). Flora d'Italia.

Porter S.C. (1981) – Glaciological evidence of Holocene climatic change. In: Climate and History (Wigley T.M.L. et al. eds), 148-179. Cambridge University Press, Cambridge.

Porter, S.C & Orombelli, G. (1982). Late-glacial ice advances in the western Italian Alps. Boreas, 11(2), 125-140.

Porter, S.C. & Orombelli, G. (1985). Glacier contraction during the middle Holocene in the western Italian Alps: evidence and implications. Geology, 13, 296-298.

Power, M. (1993). The predictive validation of ecological and environmental models. Ecological modelling, 68(1), 33-50.

Punt, W., Blackmore, S. (Eds.) (1976-2009). The Northwest European Pollen Flora. vol. I-IX. Elsevier Publishing Company.

R Development Core Team (2008). R: A language and environment for statistical computing. R Foundation for Statistical Computing, Vienna, Austria. ISBN 3-900051-07-0, URL http://www.R-project.org.

Raffl, C., & Erschbamer, B. (2004). Comparative vegetation analyses of two transects crossing a characteristic glacier valley in the Central Alps. Phytocoenologia, 34(2), 225-240.

Raven, J. A., Handley, L. L., MacFarlane, J. J., McInroy, S., McKenzie, L., Richards, J. H., & Samuelsson, G. (1988). The role of CO2 uptake by roots and CAM in acquisition of inorganic C by plants of the isoetid life-form: a review, with new data on Eriocaulon decangulare L. New Phytologist, 108 (2), 125-148.

Reille, M. (1992-1998). Pollen et spores d'Europe et d'Afrique du nord, vol. 1 (Suppl. IeII). Faculte S. Jerome, Universite de Marseille, Marseille.

Reimer PJ, Bard E, Bayliss A. (2013). IntCal13 and Marine13 radiocarbon age calibration curves 0-50,000 years cal BP. Radiocarbon 55, 1869-1887.

Röthlisberger, F. R. (1976). Klima-und Gletscherschwankungen der Nacheiszeit im Raum Zermatt, Ferpècle und Arolla (Doctoral dissertation).

Sacco, F. (1917). Il ghiacciaio e i laghi del Rutor. Boll. Soc. Geol. Italiana 36, 1-36.

Simpson G.L. (2007). Analogue Methods in paleoecology: using the Analogue Package – Journal of Statistical Software. 22, 2.

Schweingrüber, F. H. (1990). Anatomie europäischer Hölzer: ein Atlas zur Bestimmung europäischer Baum-, Strauch-, und Zwergstrauchhölzer. Eidgenoess. Forschungsanst. für Wald Schnee u. Landschaft, Birmensdorf: Bern, Stuttgart.

Schwander, J., Eicher, U., & Ammann, B. (2000). Oxygen isotopes of lake marl at Gerzensee and Leysin (Switzerland), covering the Younger Dryas and two minor oscillations, and their correlation to the GRIP ice core. Palaeogeography, Palaeoclimatology, Palaeoecology, 159(3), 203-214.

Smith, A. J. E. (1978). Provisional atlas of the bryophytes of the British Isles.

Smith, W. K., Germino, M. J., Hancock, T. E., & Johnson, D. M. (2003). Another perspective on altitudinal limits of alpine timberlines. Tree physiology, 23(16), 1101-1112.

Stockmarr, J. (1971). Tablets with spores used in absolute pollen analysis. Pollen Spores 13, 615-621.

Stuiver M., Reimer PJ, Reimer R. (2013). Radiocarbon calibration program Revision 7.0.2.

Svensson, A., Andersen, K. K., Bigler, M., Clausen, H. B., Dahl-Jensen, D., Davies, S. M., ... & Röthlisberger, R. (2008). A 60 000 year Greenland stratigraphic ice core chronology. Climate of the Past, 4(1), 47-57.

Theurillat, J. P., Schlüssel, A., Deil, U., & Loidi, J. (2000). Phenology and distribution strategy of key plant species within the subalpine-alpine ecocline in the Valaisan Alps (Switzerland). In Vegetation and climate. A selection of contributions presented at the 42nd Symposium of the International Association of Vegetation Science, Bilbao, Spain, 26-30 July 1999. (Vol. 30, No. 3/4, pp. 439-456). Gebrüder Borntraeger Verlagsbuchhandlung.

Thomas, E. R., Wolff, E. W., Mulvaney, R., Steffensen, J. P., Johnsen, S. J., Arrowsmith, C., ... & Popp, T. (2007). The 8.2 ka event from Greenland ice cores. Quaternary Science Reviews, 26(1), 70-81.

Tinner, W., Ammann, B., & Germann, P. (1996). Treeline fluctuations recorded for 12,500 years by soil profiles, pollen, and plant macrofossils in the Central Swiss Alps. Arctic and Alpine Research, 131-147.

Tinner, W., & Theurillat, J. P. (2003). Uppermost limit, extent, and fluctuations of the timberline and treeline ecocline in the Swiss Central Alps during the past 11,500 years. Arctic, Antarctic, and Alpine Research, 35(2), 158-169.

Tinner, W., & Kaltenrieder, P. (2005). Rapid responses of high-mountain vegetation to early Holocene environmental changes in the Swiss Alps. Journal of Ecology, 93(5), 936-947.

Tinner, W., & Lotter, A. F. (2006). Holocene expansions of Fagus silvatica and Abies alba in Central Europe: where are we after eight decades of debate?. Quaternary Science Reviews, 25(5), 526-549.

Tranquillini, W. (1979). General Features of the Upper Timberline. In Physiological ecology of the alpine timberline (pp. 1-4). Springer Berlin Heidelberg.

Trautmann, W. (1953). Zur Unterscheidung fossiler Spaltoffnungen der mitteleuropäischen Coniferen. Flora 140, 523-533.

van der Knaap, W. O., van Leeuwen, J. F., & Ammann, B. (2001). Seven years of annual pollen influx at the forest limit in the Swiss Alps studied by pollen traps: relations to vegetation and climate. Review of Palaeobotany and Palynology, 117(1), 31-52.

Villa, F., De Amicis, M., & Maggi, V. (2007). GIS analysis of Rutor Glacier (Aosta Valley, Italy) volume and terminus variations. Geografia fisica e dinamica quaternaria, 30(1), 87-95.

Villa, F., Tamburini, A., Deamicis, M., Sironi, S., Maggi, V., & Rossi, G. (2008). Volume decrease of Rutor Glacier (Western Italian Alps) since Little Ice Age: a quantitative approach combining GPR, GPS and cartography. Geografia Fisica e Dinamica Quaternaria, 31(1), 63-70.

Wallach, D., & Goffinet, B. (1989). Mean squared error of prediction as a criterion for evaluating and comparing system models. Ecological modelling, 44(3-4), 299-306.

Webster, R., Rigling, A., & Walthert, L. (1996). An analysis of crown condition of Picea, Fagus and Abies in relation to environment in Switzerland. Forestry, 69(4), 347-355.

Wick, L., van Leeuwen, J. F., van der Knaap, W. O., & Lotter, A. F. (2003). Holocene vegetation development in the catchment of Sägistalsee (1935 m asl), a small lake in the Swiss Alps. Journal of Paleolimnology, 30(3), 261-272.

Whittaker, R. J. (1993). Plant population patterns in a glacier foreland succession pioneer herbs and later-colonizing shrubs - Ecography 16 117-136.

SUPPLEMENTARY MATERIAL A

Notes on pollen identification and light microscope pictures of fossil pollen grains from section A (226 cm).

Notes on some specific pollen identification

According to Beug (2004), grains of *Trifolium badium* type (panel A) are colporate with 3 apertures, have a prolate shape with sunken inapertural area, sub-triangular contour in polar view, surface sculpturing psilate/ perforate and a mean pollen size of 27,5 – 35,3 µm. The tectum is eutectate, exine is 1,5 – 2 µm thick.

Individual species of Polygonaceae have been identified using the criteria of Leeuwen et al. (1988) and Beug (2004). *Rumex acetosa* (panel C) and *Rumex acetosella* (panel D) can be recognized by a combination of features: i.e. colpus length, small size, features of the endopori and colpi intruding in equatorial view. *Rumex acetosa* (P=19.0-(21.5)-25.8 µm) is mainly recognized by its short colpi which do not intrude. *Rumex acetosella* (P= 20.0-(25.0) 27.0 µm according to Leeuwen et al., 1988 and 22.5-27.5 µm according to Beug, 2004) is characterized by its long, intruding colpi, small size and features of the endopori. Its cytotypes may differ in minor details, but can be recognized based on the features mentioned above.

Oxyria digyna pollen (P=20.0-(23.0)-26.0 µm according to Leeuwen et al., 1988 and 20.5-29.5 µm according to Beug, 2004; panel B) closely resembles that of *Rumex acetosella*. It has distinctly intruding colpi, small size and has circular endopori. Nevertheless, there are differences and its pollen can be distinguished by the distinct, circular endopori, distinct columellae and muri of the reticulum and slightly larger size.

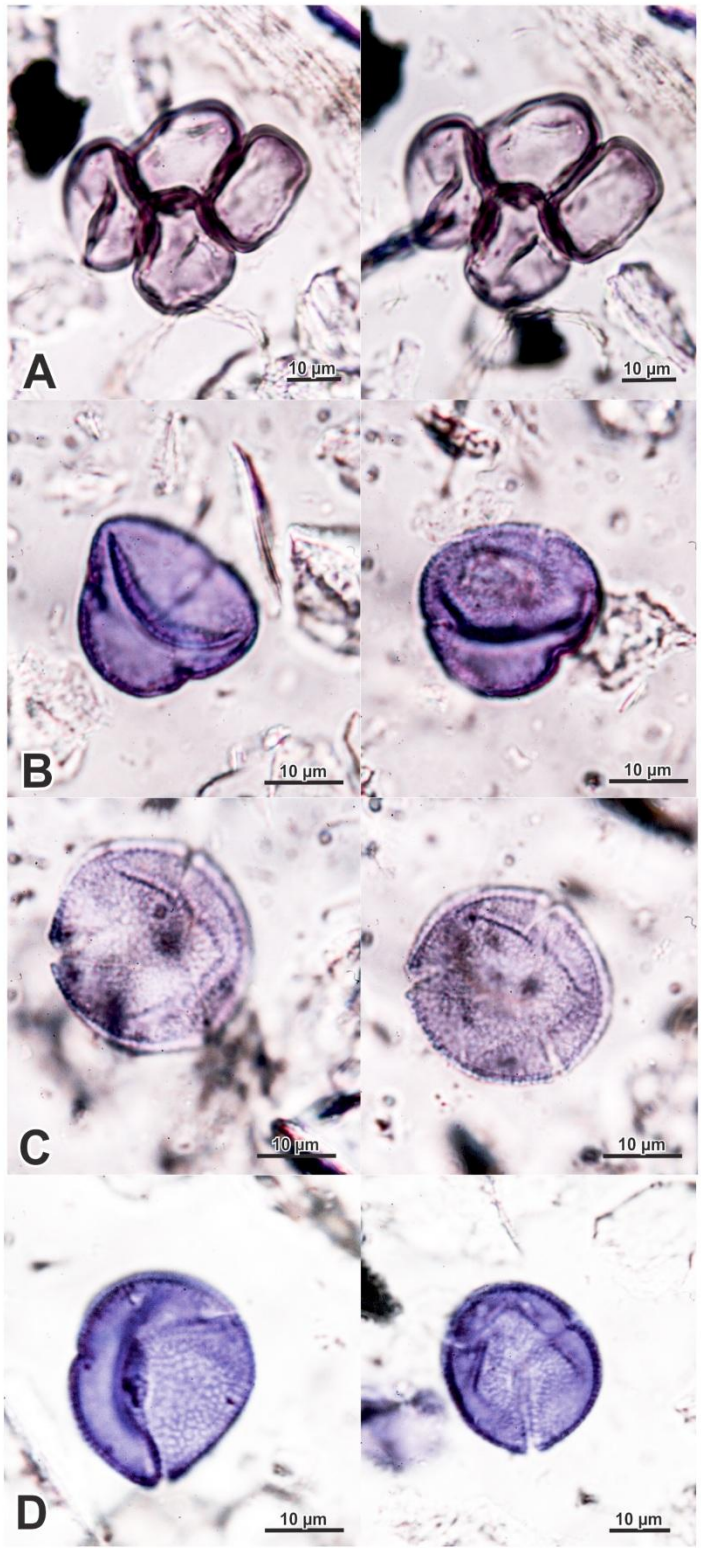

Fig. A1 – (A) Monospecific group of four pollen grains: *Trifolium badium* type (630x); (B) *Oxyria digyna* (1000x); (C) *Rumex acetosa* (1000x); (D) *Rumex acetosella* (1000x).

Manuscript 3

(In preparation)

Climate-driven vegetation dynamics during the Mid-to-Late Holocene as recorded in an elevational mire close to the Rutor Glacier

1. INTRODUCTION

High-elevation environments are particularly sensitive to rapid climate changes (Gottfried et al., 2012). Reconstructions of Holocene climate variability in the European Alps have been produced using a variety of proxies, including palaeoecological indicators of treeline variations (Haas et al., 1998; Tinner and Theurillat, 2003; Nicolussi et al., 2005; Berthel et al., 2012). Since treeline elevation is strongly controlled by climate, especially by temperature during the growing season (cf. Körner 1998), past changes in treeline location have been widely used to infer past climatic variations (Seppä & Birks 2001). Glaciers are known to be sensitive markers of climatic changes responding particularly to summer temperature variations (Oerlemans, 2005; Steiner et al., 2008). Such sensitivity has been remarkably documented in the European Alps, thanks to researches focussing on speleothems geochemistry and dating, ice flow models, glacier front reconstructions and cosmogenic nuclides geochronology (Luetscher et al., 2011; Goehring et al., 2011, 2012; Ivy-Ochs et al., 2009, Le Roy et al., 2015, Solomina et al., 2016).

Among the natural archives that can document both the history of vegetation and glaciers, mires and lakes play a major role because of the multiproxy signals (biotic and abiotic) preserved in their stratigraphic sequences. Besides natural events, several high-altitude records in the Alps document increasing fire frequency and land use changes since the Late Neolithic/Copper Age period, with an intensification of alpine summer farming at the onset of the Bronze age (Colombaroli et al., 2010; Heiri et al., 2006; Tinner and Theurillat, 2003; Tinner et al., 1996). More high-elevation sites where anthropogenic influence could have been negligible during the Holocene (e.g. remote high-alpine environments) are

needed for researches aiming at understanding of the role of climate in past vegetation changes. In this perspective, a new site (Valter mire, 2594 m asl) close to the Rutor Glacier (western Italian Alps; **Fig. 25**) but located outside its LIA maximum extent, was discovered in summer 2010. The site was chosen for paleoecological researches for several reasons:

(i) its altitude, slightly above the modern treeline (2450 m asl), possibly allow us to detect upward/downward movements of the treeline during the middle-late Holocene, a period continuously recorded at this site;

(ii) during the Little Ice Age, the Rutor Glacier was very close to the study site (ca. 200 m far) and thus we expected our site to be a valuable archive of cold events that occurred during the Mid-to-Late Holocene.

Our research aims at (1) discussing if the treeline vegetation was in dynamic equilibrium with climate during the middle-late Holocene, using also pollen-inferred TJuly reconstructions values; (2) comparing past vegetation data with reconstructed glacier oscillations in the Alps during the late Holocene; (3) disentangling the effects of climate and anthropic pressure in determining treeline position since prehistoric times.

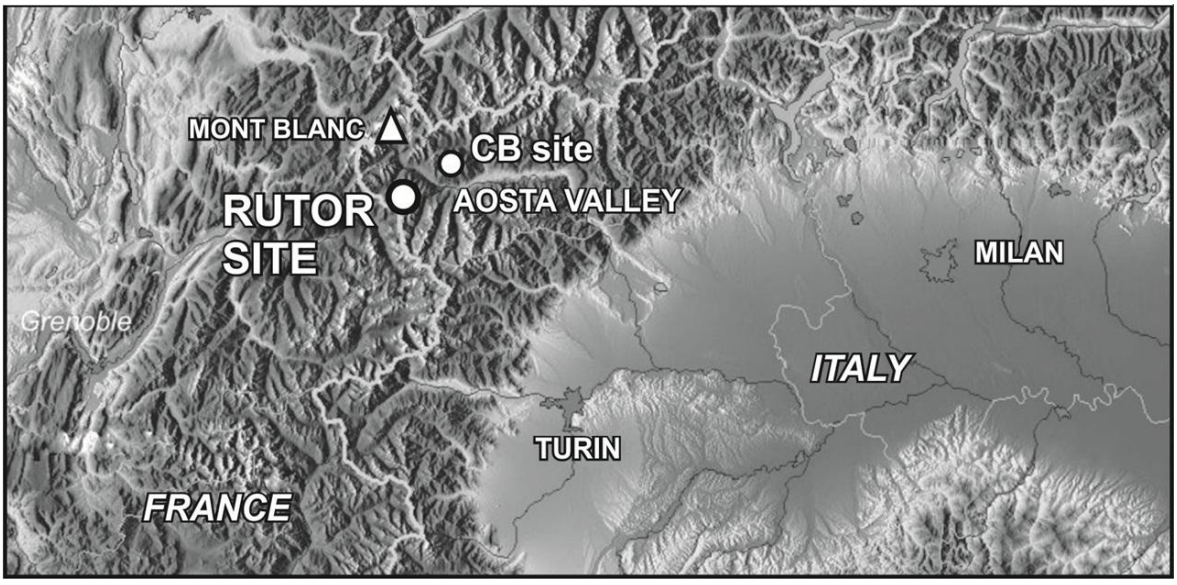

Fig. 25 - Shaded-relief map of the study area in the western Italian Alps showing the location of the Mont Blanc Massif (white triangle) and the Rutor site (Aosta Valley, big white circle). Crotte Basse (CB) site (2365 m asl) cited in the text is also indicated (small white circle).

2. GEOGRAPHICAL SETTING

The Rutor Glacier foreland (La Thuile Valley, Italy; N 45˚64' E 78˚01', 3450 - 2540 m a.s.l; **Fig. 26**), hosting several small lakes developed within depressions filled by glacial sediments and glacial meltwater (Lac des Seracs, Lac du Rutor, Lac Gris, Lac Vert, Lac Superieur and Lac dans la Roche). In September 2010, a small mire near the Lac dans la Roche, named "Valter mire" (2594 m asl), was discovered. In this context, organic sediments are valuable sources of information to reconstruct the history of high-alpine areas, vegetation and climate dynamics.

The geology of the area is relatively homogeneous; both bedrock and moraine deposits consist of metamorphic rocks such as arenaceous and conglomeratic schists, or mica and garnet schists (Dal Piaz, 1992). The Rutor Glacier covers the north-western slope of the Rutor Massif extending over an area of more than 8.5 km². Its advance and retreat phases have been recorded since the 15th century (Little Ice Age) because of the floods caused by its proglacial lake, and they have been observed directly since the second half of the 19th century. Since the mid-19th century, the Rutor Glacier has been affected by a very strong retreat (e.g. from 1820 to 2004 the glacier terminus retreated 2 km) leading to an ice volume loss of about 75% (Villa et al., 2007; Villa et al., 2008). However, some minor advances have been documented, the most important of which ended in 1926 and 1981 (Parigi et al. 1999). The Rutor moraine complex was extensively described by several authors (Baretti, 1880; Sacco, 1917, 1934; Peretti, 1935; Peretti and Charrier 1967; Porter and Orombelli 1985; Parigi et al., 1999; Orombelli 2005).

3. MATERIALS AND METHODS

3.1. The "Valter mire"

The sediment cores analysed in this study originate from the Valter mire (2594 m asl), located in the Rutor glacier foreland (**Fig. 26 a**), at ca. 500 m from the eastern glacier tongue terminus, outside the Rutor glacier LIA maximum extent. The mire lies at an altitude of 2594 m asl and extends over an area of about 350 m² (**Fig. 26 b**). A rather flat structural terrace at ca. 2590-2597 m asl delimits the

mire and the nearby “Lac dans la Roche” basin (**Fig. 26 b**), a shallow lake at the North-East side of the mire, ca. 2 m higher. Mostly during seasonal flood pulses the two basins are connected by a small outflowing stream which recharges the mire.

Treeless alpine vegetation presently grows at 2594 m asl. Around the mire, stabilized moraine ridges and slopes mostly belonging to the LIA are covered by grassland (e.g. *Poa alpina*, *Agrostis rupestris*), cushion plants (e.g. *Silene acaulis* and *Saxifraga bryoides*) and dwarf-shrubs communities (*Vaccinium myrtillus*, *Vaccinium uliginosum*, *Salix herbacea*, *Empetrum hermaphroditum*). The treeline, located at ca. 2450 m a.s.l., is indicated by *Pinus cembra* specimens.

3.2. Corings and lithostratigraphical analysis

The Valter mire was manually drilled by gouges and russian corers down to a depth of 180 cm. Lithostratigraphic logs were acquired for 3 cores (*5-bis, 5-penta and 5-lap;* **Fig. 26 b**) aligned along a W – E transect **(Fig. 28)**. The *5-bis* and *5-penta* cores are about 10 cm higher than the *5-lap* core section due to the presence of a coarser clastic level missing at the *5-lap* core top. Two additional surveys enabled a better understanding of the lateral stratigraphic development of the basin (*tbv-6 p* and *tbv-6*, **Fig. 31**). The *5-bis*, *5-penta* and *5-lap* cores were logged for thermogravimetry: 470 volumetric samples were taken every cm/ 5 mm, weighted and progressively heated at 105 ˚C, 550 ˚C and 980 ˚C to estimate water, total organic matter + sulphides (TOM+s) and the silicoclastic component + oxides contents (RES) (**Fig. 28**; Gustafsson et al., 2001). Carbonate fractions including sulphides and sulphates (CaCO3+ss) were determined stoichiometrically (Dean, 1974). The *5-lap* core was also logged for magnetic susceptibility measured with a Bartington MS2 susceptimeter equipped with a MS2E sensor operating on a 2 kHz frequency. 89 measures were taken every cm and repeated twice (**Fig. 28**).

The *5-lap* and *5-penta* cores were selected for a detailed palynostratigraphic study due to their robust radiocarbon chronology and lithostratigraphical correlation (**Fig 27**).

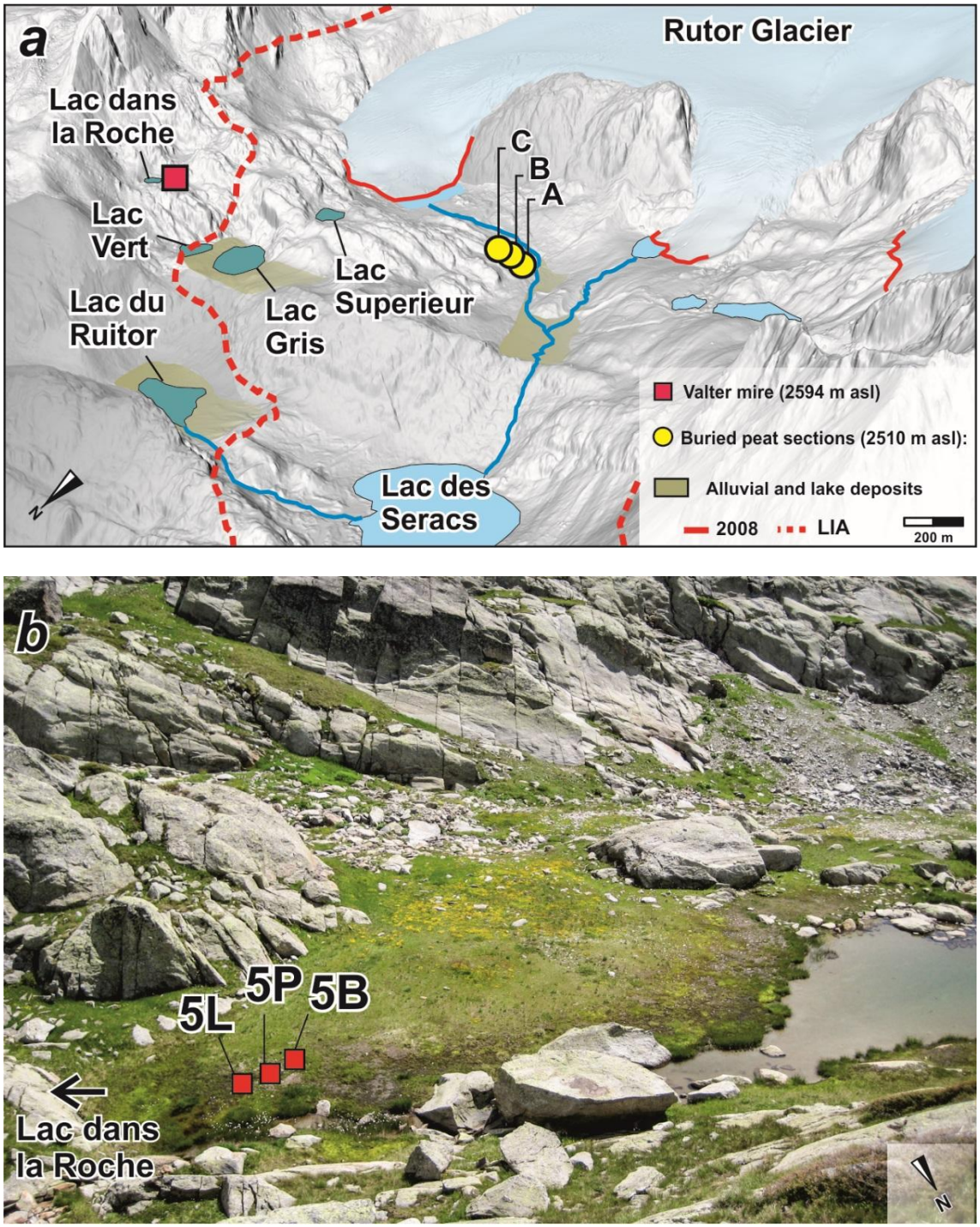

Fig. 26 - (a) Digital Terrain Model of the Rutor glacier foreland, view from NW. Continuous red line: 2008 glacier extent;, red dotted line: LIA extent. Studied sites are shown: Buried peat sections (A, B, C; 2510 m asl) and the Valter mire (2594 m asl). **(b)** Valter mire: coring sites positions are indicated (5L= 5-lap, 5P= 5-penta, 5B= 5-bis).

3.3. Radiocarbon chronology

Seven ^{14}C AMS dates were obtained from fibrous-rich bulk sediment, a wood sample and insect fragments. Radiocarbon dates are presented in **Table 7**. A wood sample identified as *Pinus cembra* (**see Chapter 2, Fig. 17**) yielded a radiocarbon age of 4895 ± 35 yrs BP (*5-bis* core section, 116,5 cm). Insect fragments (Carabid beetles) from the *5-lap* core section (97-99 cm) yielded a radiocarbon age of 4085 ± 35 yrs BP. Bryophytes bulk samples from *5-lap* and *5-penta* core sections were used to obtain further 5 dates (**Table 7**). Radiocarbon dates were calibrated using Calib 7.0.2 (Stuiver et al. 2013) based on the IntCal 13 calibration curve (Reimer et al., 2013). The chrono-stratigraphic correlation between *5-lap* and *5-penta* cores allowed the development of the Valter mire pollen record, covering the period 7300 – 850 yrs cal BP between 120 cm and 18 cm (**Fig. 29**). The chronology of the lowermost part of this record has been checked by fine biostratigraphical matching with a reference succession (Crotte Basse, 2365 m asl; Pini et al., submitted) situated at 8 km distance in the same region and then matched with the buried peat section A ("Rutor composite pollen record" in **Fig. 29**, see also **Chapter 2**).

3.4. Palynological analysis

34 samples were taken from the *5-lap* and *5-penta* core sections between 18 and 120 cm for palynological analysis (**Fig. 29**). All samples were treated according to standard methods (including HF and acetolysis) at the Lab. of Palynology and Palaeoecology of CNR-IDPA in Milano, after adding *Lycopodium* tablets for pollen and slide micro-charcoal concentration estimations (Stockmarr, 1971). Identification was carried out at x400, x630 and x1000 magnifications under a Leica DM-LB light microscope. Pollen identification followed Moore et al. (1991), Punt and Blackmore (1976-2009), Reille (1992-1998), Beug (2004) and the CNR palynological collection. Non-pollen palynomorphs were named after van Geel (1978) and van Geel et al. (1981), fossil conifer stomata after Trautmann (1953). Pollen diagrams were drawn using Tilia ver. 1.7.16 (Grimm, 1991-2011) and Corel Draw X6 for further graphic elaborations. The pollen sum used for % calculations includes trees, shrubs, chamaephytes and all upland herbs except Gramineae, with a mean pollen count of 496±80 pollen grains. Pollen zonation

was obtained by a constrained incremental sum of squares cluster analysis, using the Cavalli Sforza's chord distance as dissimilarity coefficient (CONISS, Grimm, 1987). Clustering was restricted to taxa whose pollen reached over 2%.

3.5. Statistical analysis

Principal component analysis (PCA) was used to explore the major differences in pollen composition in the Valter mire pollen record and their relationship with modern pollen data. PCA was applied on SQRT-transformed pollen percentages. Taxa with less than 2% in pollen percentages at any sample were excluded from these calculations. A predominantly linear responses of species to gradients was assumed (axis length = 1,4 standard deviation units) (ter Braak and Prentice, 1988). All ordination analysis were carried out with the program R x64 3.0.3 package Vegan version 2.2-1 (Oksanen et al, 2015).

Sample acronym	Core acronym	Sample depth (cm)	Material dated	Tecnique	^{14}C Age BP	95% calibration range (cal BP)	Median probability
Poz-52088	5_penta	32-33	peat	AMS	940 ± 30	792-924	853
Poz-56168	5_penta	35	peat	AMS	1220 ± 30	1063-1188	1146
Poz-66619	5_lap	25-25,5	peat	AMS	1565 ± 30	1391-1531	1467
Poz-66618	5_penta	48-49	peat	AMS	1905 ± 30	1776-1904	1852
Poz-66620	5_lap	59,5-60	peat	AMS	2705 ± 30	2757-2855	2804
Poz-52087	5_lap	97-99	insects	AMS	4085 ± 35	4512-4654	4588
Poz-52086	5_bis	116,5	*Pinus cembra* wood	AMS	4895 ± 35	5586-5664	5627

Table 7 - Radiocarbon dates obtained for the Valter mire stratigraphic sequence.

4. RESULTS

4.1. Age-depth model and mean sedimentation rates

The *5-lap* and *5-penta* core sections, drilled ca. 25 cm apart, were stratigraphically correlated. Six radiocarbon dates (**Fig. 27**), allowed to develop the age-depth model used for pollen diagram time plot (**Fig. 29**). Between 120 - 72 cm depth, the estimated mean sedimentation rate is about 0,1 mm/year; pollen concentration shows high values (~ 200.000 grains/cm^3). Between 72 – 22 cm depth, mean sedimentation rate reaches 0,23 mm/years; lower values of pollen concentration (~ 100.000 grains/cm^3) recorded here can be referred both to higher sedimentation rates and to a reduced pollen influx. This pattern fits with the lithostratigraphical variations along the sequence, showing that at 72 cm depth gyttja is replaced by peat, which accumulates faster than the organic mud. The continuity of the organic sequence is interrupted at 22 cm due to a fine sand layer, 2-cm thick, visible in the *5-penta* and *5-bis* core sections and missing in the *5-lap* lithostratigraphic record (**Fig. 28**). A thin bulk sample at the base of this layer yielded an age of 1220 ± 30 years BP (1063 – 1188 yrs cal BP, 1146 yrs cal BP median probability). Afterwards, peat deposition resumed until 940 ± 30 years BP (792 - 924 yrs cal BP, 853 yrs cal BP median probability), when sandy gravels deposits buried the mire.

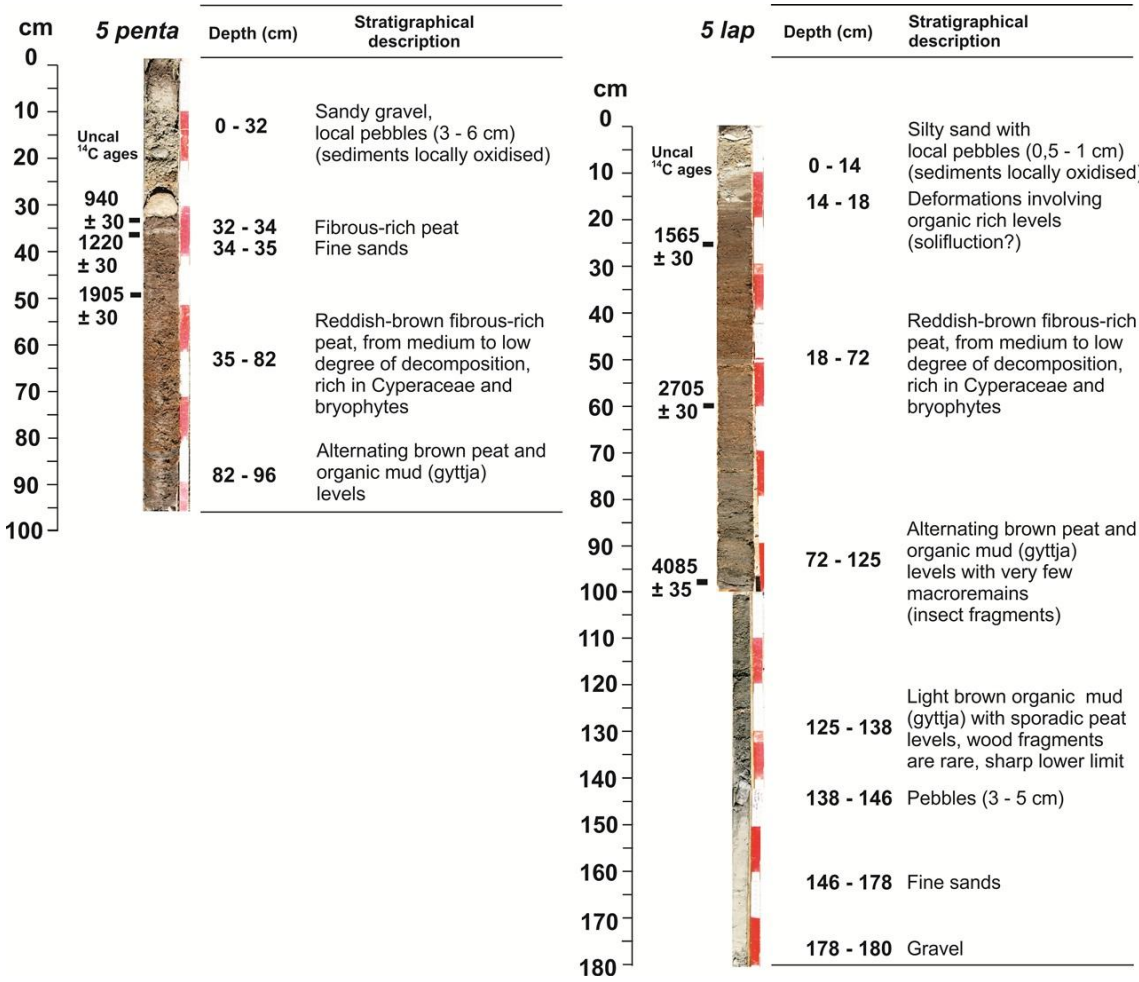

Fig. 27 - Lithostratigraphical description of the core sections 5-lap and 5-penta, chosen as 'master' cores for palynological analysis. Radiocarbon dates are shown. The two cores have been correlated on the base of chronostratigraphical and palynological data.

4.2. Lithostratigraphic assessment of the Valter mire

The *5-lap, 5-penta* and *5-bis* core sections provide evidence of different phases of sedimentation (**Fig. 28**). The deepest stratigraphical unit was reached by the *5-lap* drilling (146 – 180 cm, **Fig. 27**). Homogeneous fine sands filled the basin; the detrital component of this unit was roughly estimated by the LOI silicoclastic residue and by magnetic susceptibility. Here, micas and magnetite abraded from the crystalline rocks mark meltwater fine sands with susceptibility peaks over 10 – 15 unit SI, together with a silicoclastic residue about 90% and organic matter content at its minimum (~ 1% of dry sediment; Lithozone LdlR 1 in **Fig. 28**). Low and stable values of CaCO3+ss (ca. 4%) characterize the meltwater input in the

basin. The sharp contact (138 – 146 cm, **Fig. 28**) between this unit and the following organic mud, documented the final event of meltwater supply in the Lac dans la Roche basin. Angular pebbles mark this boundary and they might suggest an increase in slopes instability and related rock movements around the basin. Hiatuses or erosional events at this limit surface cannot be excluded. Afterwards, changing in climate conditions could have promoted the development of a shallow water lake. Between 125 and 138 cm, organic mud (gyttja) deposits occurred. The increase of total organic matter content, ranging between 35 - 70% of the dry sediment weight, point to the development of a limnic environment with expansion of local vegetation. Lower values of CaCO3+ss (ca. 3 - 4% of dry sediment weight) characterize this phase, along with a progressive decrease of magnetic susceptibility values down to 1 – 5 unit SI. Alternating brown peat and organic mud levels (72 – 125 cm) documented the ongoing paludification process in a close basin as shown in the gradual increase of the TOM+s up to 90% of dry sediment weight. During this phase, magnetic susceptibility settled around low and stable values (between 0 and 1 unit SI). Remarkably, around 50 - 55 cm (Lithozone LdlR 2 in **Fig. 28**) in the *5-lap* core section three marked peaks are recorded as for carbonates and silicoclastic residue content. Such events are missing in the *5-bis* and *5-penta* records and in the susceptibility curve too. It is reasonable to assign a local signature to those abrupt changes in geochemical composition, possibly due to the proximity of the *5-lap* core section to the Lac dans la Roche outflow stream. After a long phase of stable susceptibility values, a firs peak (~5 unit Si) occurred at 22 cm (Lithozone LdlR 3 in **Fig. 28**). This event was recorded as a geochemical variation in all core sections, especially in *5-bis* and *5-penta* core sections, where it is marked by a detrital fine level. Afterwards, peat deposition continued for about 3 cm, until a new lithological and geochemical abrupt change starting at 18 cm. Between 18 and 0 cm (Lithozone LdlR 1 in **Fig. 28**), sandy gravels with local pebbles (e.g. *5-penta* core section) buried the mire. Magnetic susceptibility reaches high values (10 -15 unit SI) along with silicoclastic residue about 90% and total organic matter content at minimum values (~ 2 - 3% of dry sediment weight). Above this detrital unit, modern vegetation established and allowed a recent minor organic matter supply, as shown at the top of the *5-penta* and *5 lap* core records.

Fig. 28 - Integrated lithostratigraphy and chronology of the core sections 5-lap, 5-bis, 5-penta (Valter mire). Lithostratigraphic proxies are shown: % TOM+s, % RES and % CaCO3+ss (see Material and methods). Those values are calculated as % of the dry sediment weight. Magnetic susceptibility profile is presented (5-lap core section- black curve), too. Light blue rectangles highlight lithozones and correlations along the W-E transect (LdlR 1-2-3-4).

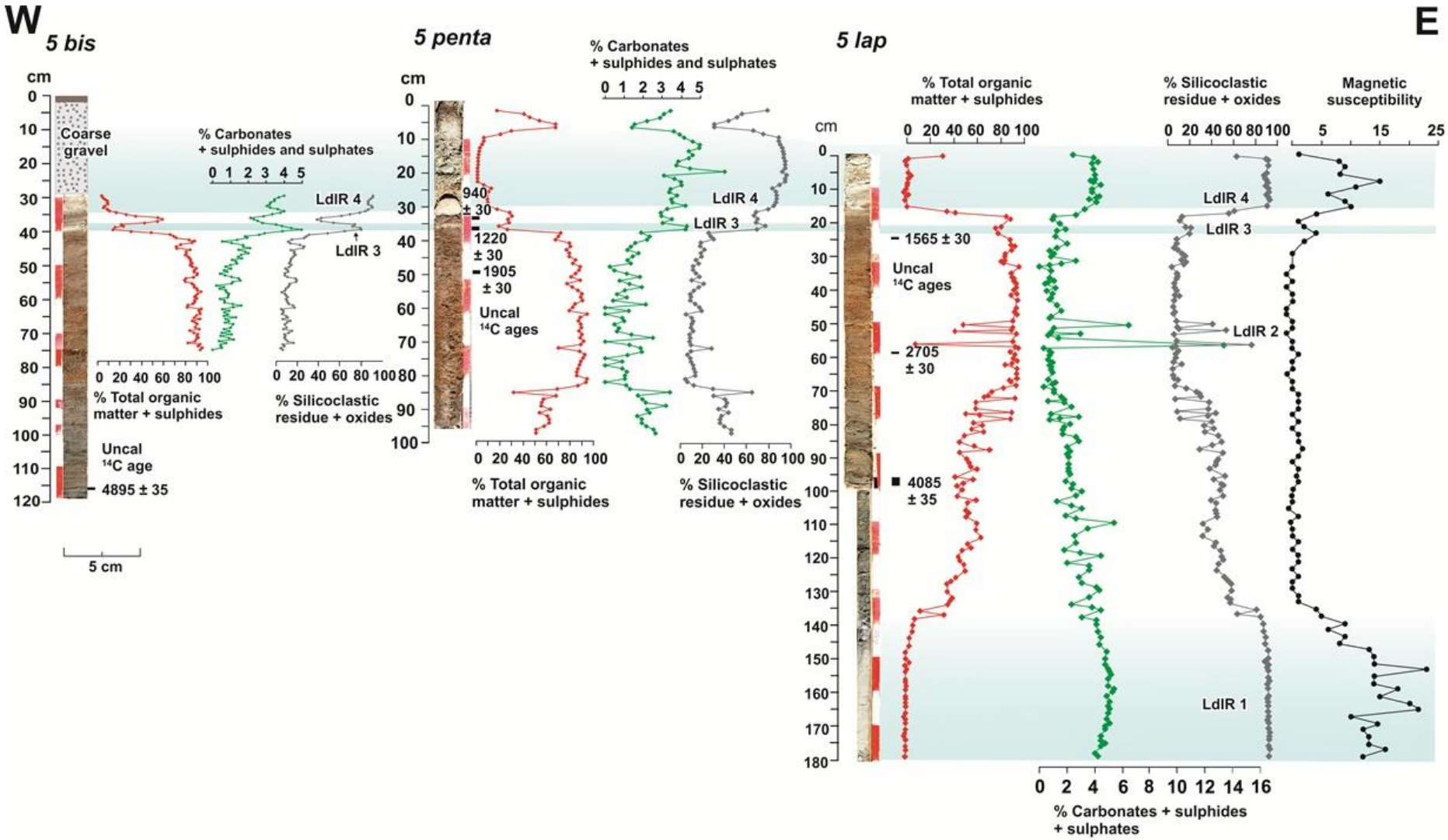
W
E
5 bis
5 penta
5 lap
cm
Coarse gravel
% Carbonates + sulphides and sulphates
0 1 2 3 4 5
LdlR 4
LdlR 3
LdlR 2
LdlR 1
0 20 40 60 80 100
% Total organic matter + sulphides
% Silicoclastic residue + oxides
Uncal ¹⁴C age
4895 ± 35
940 ± 30
1220 ± 30
1905 ± 30
Uncal ¹⁴C ages
1565 ± 30
2705 ± 30
4085 ± 35
Magnetic susceptibility
5 15 25
0 2 4 6 8 10 12 14 16
% Carbonates + sulphides + sulphates
5 cm

Fig. 28

4.3. Vegetation history and landscape reconstruction

The Valter mire pollen record was matched with the pollen record obtained from the buried peat section A, located in the outwash plain of Rutor Glacier (**Fig. 26 a**, see also **Chapter 2**). The matching between the two pollen records was checked by fine biostratigraphical correlation producing an almost complete record named “Rutor composite pollen record” for the last 8800 years. Pollen data are shown in **Fig. 29**, where a selection of taxa is presented. The lowermost part of the diagram (8800 - 7400 yrs cal BP; from *RUT 1* to *RUT 7* pollen zones) is extensively treated in **Chapter 2 (paragraph 4.4)**. Concerning the upper part, between 7300 – 850 yrs cal BP (from 120 to 18 cm), pollen data are discussed below.

The entire Valter mire organic sequence is polliniferous and can be subdivided into 3 pollen zones.

The lower pollen zone (*RUT 8*), spanning between 7300 and 3700 yrs cal BP, is characterized by the overall dominance of *Pinus cembra* pollen (~ 60%) as already recorded in the *RUT 7* pollen zone. Stable and high *Pinus cembra* % values coupled with the high PAR (ca. 1500 grains cm^{-2} yr^{-1}), suggest that the Valter mire was lying in the timberline ecotone. This hypothesis is corroborated by the finding of a *Pinus cembra* uncharred wood at 116,5 cm depth (*5-bis* core section) dated to 5600 - 5700 yrs cal BP and indicating the presence of Swiss stone pine trees at the site. Around 4800 yrs cal BP (*RUT 8-a* subzone) the record shows the first occurrence of *Plantago lanceolata*; the first *Cerealia* pollen grain occurs at ca. 4200 yrs cal BP. *Ulmus* and *Tilia* percentages decrease during this zone, possibly indicating a forest contraction at lower altitudes. Heliophilous shrubs (e.g. *Juniperus, Vaccinium* and *Rhododendron*) expanded. At 4000 yrs cal BP, the anthropogenic indicators curve, including: *Cerealia, Humulus/Cannabis* type*, Plantago lanceolata* type*, Plantago media* type*, Plantago major* type*, Trifolium repens* type*, Urtica, Ranunculus acris* type *and Rumex acetosa type*, reaches a percentages of 2%. As for the local vegetation, the occurrence of aquatic communities, including algae such as *Botryococcus* and sporadic *Pediastrum*, suggests the persistence of shallow lake conditions. The high values of the total microcharcoal concentration curve, up to 25.000

part./cm^3, are mirrored in peaks of the *Pinus cembra* curve and may reflect the abundance of biomass availability, which in turn increased regional fire frequency during this period.

Since the beginning of the *RUT 9* zone (80 cm depth) a decrease of *Pinus cembra* is mirrored by the expansion of *Picea abies* occurred around 3600-3700 yrs cal BP together with *Alnus viridis*. At that time, the dwarf shrub *Vaccinium* expanded. The occurrence of a *Juniperus* stomata (65 cm depth) suggests the presence of this species *in situ*. At 3600 yrs cal BP, Gramineae and Cichorioideae expanded. Among other herbs is noteworthy the occurrence of *Hypericum* and *Geum* type. The anthropogenic indicators curve reaches a value of ca. 3%, similar to the modern one at the studied site (~ 2,5%). These values suggest that at that time the human impact in the area surrounding the site was negligible. Furthermore, the steady microcharcoal concentration decrease seems to be correlated with a drop in *Pinus cembra* percentages. The occurrence of coprophilous fossil spores of *Sporormiella* in a single sample (77,5 cm depth) with low values (1,3% of the total pollen and spores sum), suggests a possible presence of local wild herbivores. Around ~3000 yrs cal BP the decline of *Rhododendron* curve is followed by the expansion of *Salix*. In the *RUT 9-a* subzone, a peak of algae (*Botryococcus*) around 75 cm depth, marks the last evidence of limnic conditions in the basin. Indeed, this event was followed by the expansion of telmatic plants (e.g. Cyperaceae) indicating the mire development. This process is also highlighted by the expansions of *Neorabdocoehla* oocytes and *Glomus* mycorrhizae.

The *RUT 10-a* subzone shows the increase of *Picea abies* pollen and the steady reduction of *Pinus cembra* pointing to a treeline lowering. Since ca. 2400 yrs cal BP a possibly intensification of human activities in the region is marked by the increase in the anthropogenic indicators curve (max ca. 7%), however *Plantago lanceolata* values continued to be lower than 2% and only sporadic grains of *Cerealia* occurred. Furthermore the total microcharcoal concentration curve shows the lowest values recorded in all pollen record. During this phase, a continuous % curve of fungal spores (e.g. Sordariaceae) might suggests the occurrence of rotten wood possibly linked to a woodland recession at lower altitudinal belts. Low percentages of the dung spore *Sporormiella* (between 0,1 –

1%) allow to excluded local megaherbivores grazing activities. During the subsequent *RUT 10-b* phase, a generalized fall in percentages involved all coniferous taxa, mirrored by the rise in microcharcoal concentration (especially the large size class: 50<D>250 µm) and higher values of the anthropic indicators (up to 7%). This phase, lasted for few centuries during the Roman period (between 1800 and 1400 yrs cal BP), suggesting an increase in land use and fire activities in the region. Around 1200 yrs cal BP, the first occurrence of sporadic pollen grains of *Castanea sativa* documents the introduction of this tree in the region. Around ca. 850 yrs cal BP, a huge expansion of upland herbs pollen, namely Gramineae and Cichorioideae, supports the local development of telmatic meadows dominated by *Nardus stricta* and *Leontodon* cf. *helveticus*. This process might be related to a change in the local drainage system due to the burial of the former mire by minerogenic deposits (LdlR 3 lithozone, **Fig. 28**). At this time, an expansion in cultivated areas on the valley floor is possibly marked by a rise in Cerealia pollen percentages (~4%). Afterwards, the mire was buried by fluvioglacial coarse gravel deposits. Nowadays, telmatic meadows are dominated by the above-mentioned species strongly adapted to the seasonal hydrological cyclicity. Furthermore, the presence of single pollen grains of *Castanea sativa, Juglans nigra* and *Juglans regia* in the modern pollen rain spectra, documented the introduction of these new trees on a large scale in the valley floor.

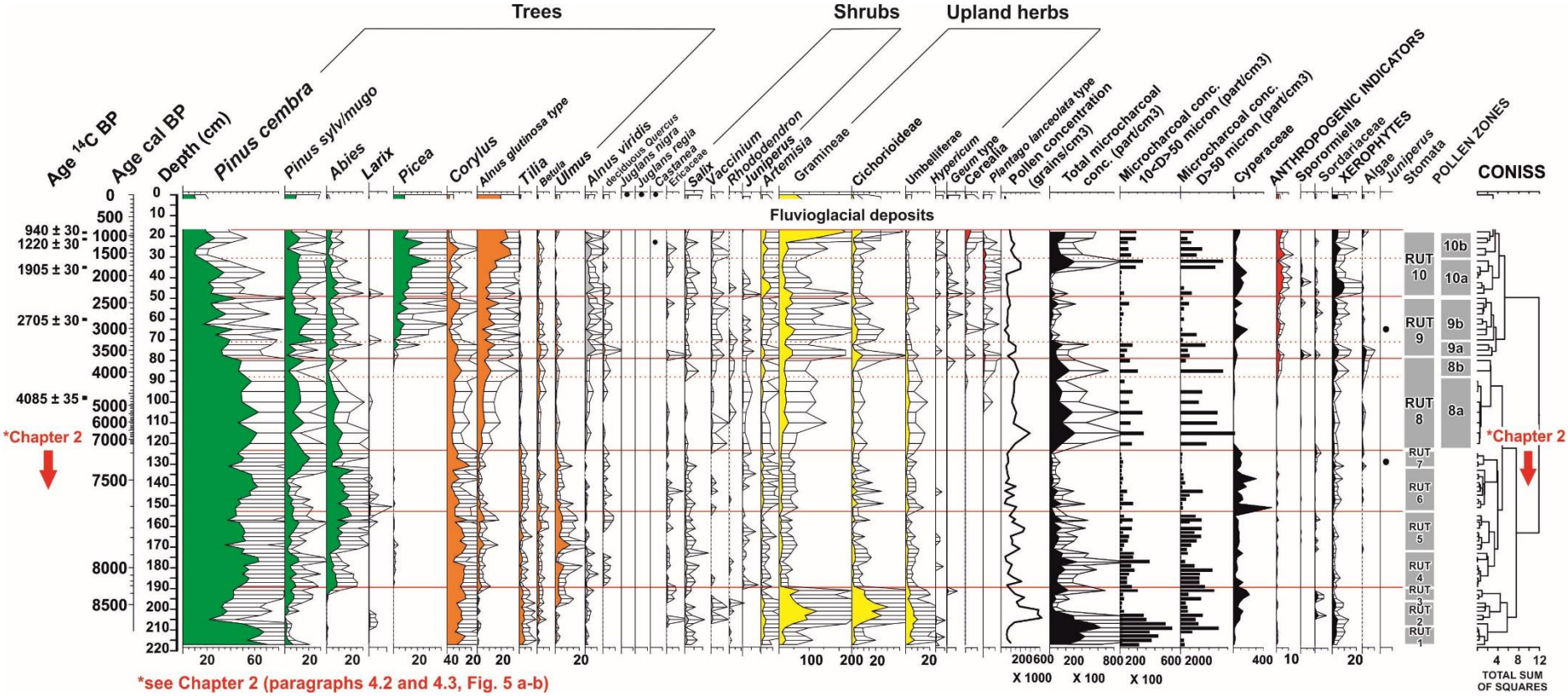

Fig. 29 - Percentage palynological record of selected taxa plotted on stratigraphic scale “Rutor composite pollen record” obtained by merging pollen data from the section A and the Valter mire records. In green: conifers; orange: deciduous trees; grey: shrubs; yellow: herbs, red: anthropogenic indicators. Also aquatic taxa and microcharcoal concentrations are shown (black curves and histograms). Magnification of percentage curves: x5. The lowermost part of the diagram indicated by a red arrow (8800 - 7400 yrs cal BP; from RUT 1 to RUT 7 pollen zones) is extensively treated in Chapter 2.

4.4. Fossil and modern pollen rain comparison

PCA scatter plot (axes 1 and 2), allows to analyze fossil pollen data of the “Rutor composite pollen record” and to compare them with the modern pollen rain at the site (**Fig. 30**). Analysis reveals long-term dynamics driven by natural processes. The first two axes explain ca. 50% of the total variance (axis 1: 34,02% and axis 2: 15.74%). A gradient from the oldest to the youngest fossil sample is shown on axis I, moving from RUT 1 - 2- 3 pollen zones (pink circles, spanning from 8800 to 8400 yrs cal BP; **Fig. 30**) to the more recent samples of RUT 10 pollen zone (blue squares, from 2300 to 853 yrs cal BP; **Fig. 30**). Major vegetation types are shown to be clearly distinguished by their fossil pollen spectra, with some overlapping between 8400 and 3800 yrs cal BP. The oldest pollen zones (RUT 1-2, pink circles; **Fig. 30**) result well separated from all other samples. Here, pollen data bear the evidence of a primary succession testifies to an ecological mechanism of colonization and establishment of early successional plants (e.g. *Oxyria*, *Rumex acetosella*, *Trifolium badium*) in the Rutor Glacier foreland around 8800 yrs cal BP. The intermediate group is defined by the pollen of conifer forests (*Pinus cembra*, *Pinus sylvestris/mugo* and *Abies alba*) as well as broad leaved forest pollen deriving from lower altitudinal belts (*Ulmus*, *Tilia* and *Corylus*). Finally, the younger group corresponds to pollen spectra with high amounts of *Picea* and *Alnus viridis.* PCA 2 might reflect a humidity gradient from dry to moister conditions. One extreme of PCA axis 2 this is marked by drought-tolerant herbs such as *Artemisia*, Cichorioideae and *Anthemis* type, while the species at the opposite extreme is the drought-sensitive *Abies alba*. Composition of modern pollen rain recorded at the Valter mire (**Fig. 30**; surface sample) differs significantly from the older samples of fossil record and seem to be consistently similar to spectra from the uppermost and youngest pollen zone (RUT 10), slightly differing in that it indicates somehow drier and more open forest conditions. The modern pollen rain spectra (see the surface sample at 0 cm depth in **Fig. 29**), shows lower percentages of *Pinus cembra* compared with those recorded in the uppermost pollen zone (RUT 10). Furthermore, only sporadic grains of *Abies* are found in the modern pollen rain at the Valter mire. In the fossil record *Abies* pollen decrease occurred at the onset of the Middle Age, after a climatic deterioration set in the Late Iron Age and a subsequent period of

increasing fire disturbance (Roman time). Differently, comparable pollen percentages characterize modern *Picea* % values with those predating the Little Ice Age.

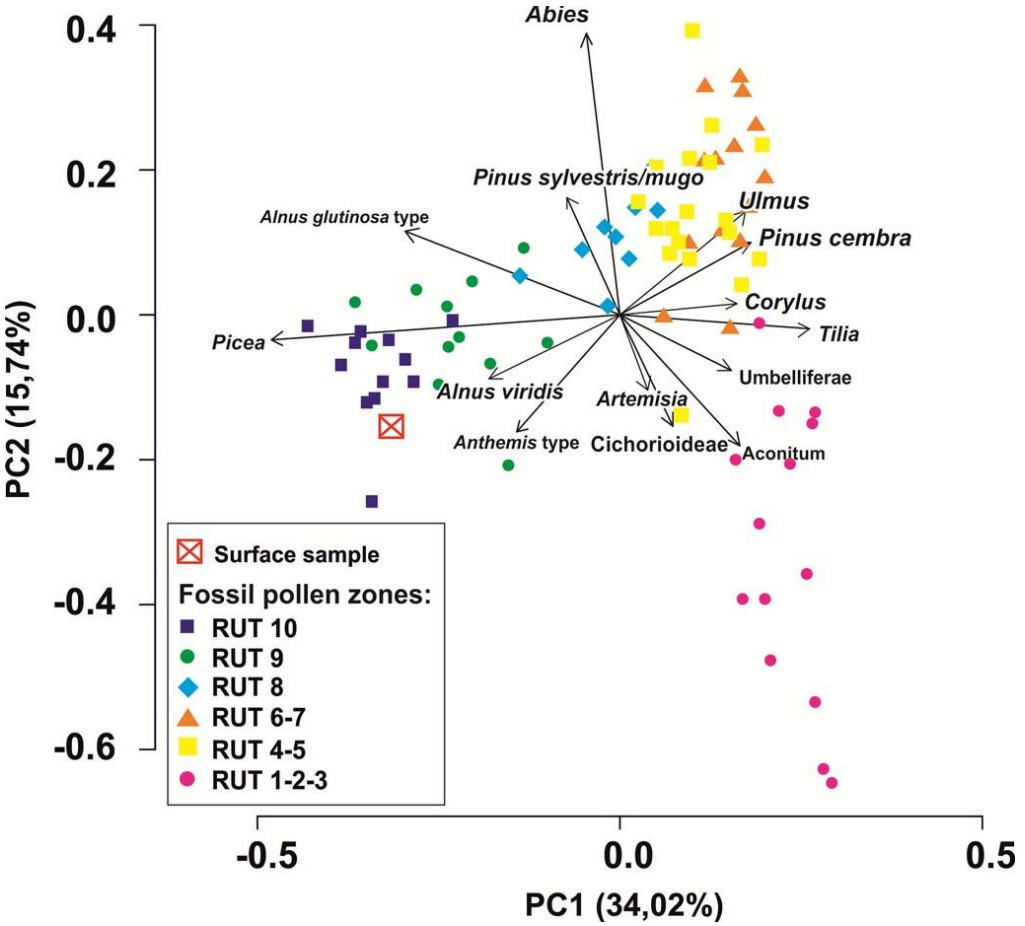

Fig. 30 - PCA scatter-plot based on pollen composition (%) of fossil samples from the "Rutor composite pollen record" (see Fig. 29) and comparison with modern pollen rain spectra (Surface sample) from Valter mire.

5. DISCUSSION

5.1. Holocene Rutor Glacier oscillations before the Little Ice Age

The studied mire lies ca. 500 m far from the present-day Rutor Glacier eastern lobe. A sharp ridge, culminating at 2670 m asl, edges ~ 50 m over the modern glacier tongue terminus. Its steep slopes obstructed the E-SE to W-NW-oriented glacial flow during the advance phases. Then, N-facing slopes connected the

peak (2670 m asl) with a flat terrace at ca. 2590-2597 m, where the Valter mire is hosted (**Fig. 31**). Its favorable position allowed for a continuous and undisturbed organic deposition during the middle and late Holocene.

During this period and up to 1140 yrs cal BP, the Rutor Glacier experienced a period of small ice extent (**Fig. 31-A**), fluctuating on a scale comparable or even smaller than today, as documented by studies on other alpine glacier systems. This period of generally glacier-hostile climatic conditions is documented at several of the larger glaciers in the Alps (Porter and Orombelli, 1985; Burga, 1991, 1993; Baroni and Orombelli, 1996; Orombelli and Mason, 1997; Hormes et al., 2001, 2006; Joerin et al., 2006, 2008). After ca. 5-6 Ka years of undisturbed organic deposition, the Valter mire was buried by detrital deposits containing mostly fine sand at ca. 1220±30 yrs BP, median probability: 1146 yrs cal BP (762 - 887 yrs cal. AD). This event is lithostratigraphically documented in all core sections (ca. 1 cm thick minerogenic layer in *5 bis* and *5 pent* core sections) and also bears a clear geochemical signal (**Fig. 28**; LdlR 3 lithozone). As shown in **Fig. 31-B**, it could possibly be interpreted as a distal fluvioglacial supply due to a glacier highstand in the immediate vicinity of the edge culminating at 2670 m asl. Other glaciers in the Western Alps have also provided evidence of an early 9^{th} century AD advance, for example at the Lower Grindelvald Glacier (dendro-dates spanning from 823 to 836 AD are reported by Holzhauser and Zumbühl, 1996, 2003) and at the Rhône Glacier, where an advance up to a position ~300 m exceeding the 1856 AD moraine occurred just after 1260±65 BP (650 - 940 yrs cal AD), likewise to be ascribed to this period (Zumbühl and Holzhauser, 1988). Furthermore, in the Mont Blanc Massif there is sparse evidence of a prominent 9^{th}-century AD advance, including ^{14}C and dendro-dating of logs at Brenva and Argentière Glaciers (Orombelli and Porter, 1982; Le Roy, 2012).

At the study site, this event is followed by resuming peat deposition for ca. 300 yrs (between ca. 800 AD and 1100). At this time, a phase of moderate Rutor Glacier retreat possibly occurred. Consistently, a general retreat of glacier termini for the late 9^{th} to 11^{th} centuries is also suggested by the sediment record of Lake Blanc Huez in the Western French Alps (Simonneau et al., 2014), and the youngest artefacts from the alpine Schnidejoch Pass indicating that it was possible to cross it at that time (Hafner, 2012). Afterwards, increased Rutor

Glacier extent possibly reached/overtook the edge at 2670 m asl and a meltwater stream draining out of the Rutor Glacier reached the Valter mire. Here, fluvioglacial deposits buried the site (coarse gravel sediments visible in *5 bis* and *5 penta* core sections) (**Fig. 31-C**). A radiocarbon age of 940±30 yrs BP, median probability: 853 yrs cal BP (1026 - 1158 yrs cal. AD), made on a 1 cm thick bulk sample underlied fluvioglacial deposits, is possibly close to, or slightly earlier than the onset of the burial event. These fluvioglacial deposits covered most of the mire surface, damming a small flood basin system in the eastern zone of the mire (**Fig. 31-C**). The latter possibly received lateral flow from Lac dans la Roche, documented by a fine-grained deposit at the top of *5 lap core section* (**Fig. 27**). The onset of this glacier-friendly phase falls during the beginning of the Late Medieval Age. Other studies documented to a cooling phase interrupting the Medieval Climate Anomaly (MCA) during the 12th century AD. For example, in the Mer de Glace record a large advance is constrained around 1178 AD (Le Roy et al., 2015) (**Fig. 32**). Similarly, in the Lys Glacier foreland (Aosta Valley, Pennine Alps) a complex sequence of alternating organic/detrital layers documented a pronounced glacier position at least from ca. 1095 AD (960±30 yrs BP; median probability: 856 yrs cal BP) (Ravazzi, 2011). In the Alps, other sites where Late Medieval advance has been dendro-dated (dendrodates for Swiss glaciers are taken from Holzhauser, 2010) include Ferpècle Glacier (1125 AD; Röthlisberger et al., 1980), Lower Grindelvald (1137 AD; Holzhauser and Zumbühl, 2003), Gepatsch (1172 AD; Nicolussi and Patzelt, 2001) and Gorner (1186 AD; Holzhauser, 2010). At Great Aletsch, a maximum age of 1100 AD constrained this advance (Holzhauser, 1984: 237-243; Holzhauser et al., 2005).

After this first burial event, the upper part of the record shows alternating detrital levels interrupted by thin organic, locally oxidized, deposits until the top of the core (see **Fig. 28**, *5 penta* core section). The lack of radiocarbon dates within this interval do not allow a clear chronostratigraphical interpretation for the more recent events. Nevertheless, it is evident that the debris flow activity continued, even if unevenly, during the Little Ice Age. Orombelli (2005) documented the existence of a LIA – meltwater stream coming out from the eastern lobe of the Rutor Glacier (at ca. 2670 m asl) and reaching Lac dans la Roche and Lac du Ruitor (**Fig. 26 a**). Historical documents testify to max LIA advance occurring

between 1751 and 1864 AD, possibly in phase with the 1820 advance shown by other Aosta Valley glaciers (Sacco, 1917). Furthermore, Rutor Glacier is sadly famous for the catastrophic floods of the S. Margherita marginal lake which have occurred repeatedly since 16th century, when the glacier barring the west side of the lake was no longer able to hold the water pressure (Le Roy Ladurie, 1967; Baretti, 1880). More recently, the maximum extent reached by the Rutor Glacier during the LIA was reconstructed on the basis of a geomorphologic survey of marginal morains, drift limits and erosional trimlines. At LIA maximum the glacier was 27% larger than the 1991 extent and its terminus was 370 m lower than in 1991 (Orombelli, 2005). Moreover, the Equilibrium Line Altitude changed from 2775 m in the Little Ice Age maximum to 2850 m in 1991 (Villa et al., 2007).

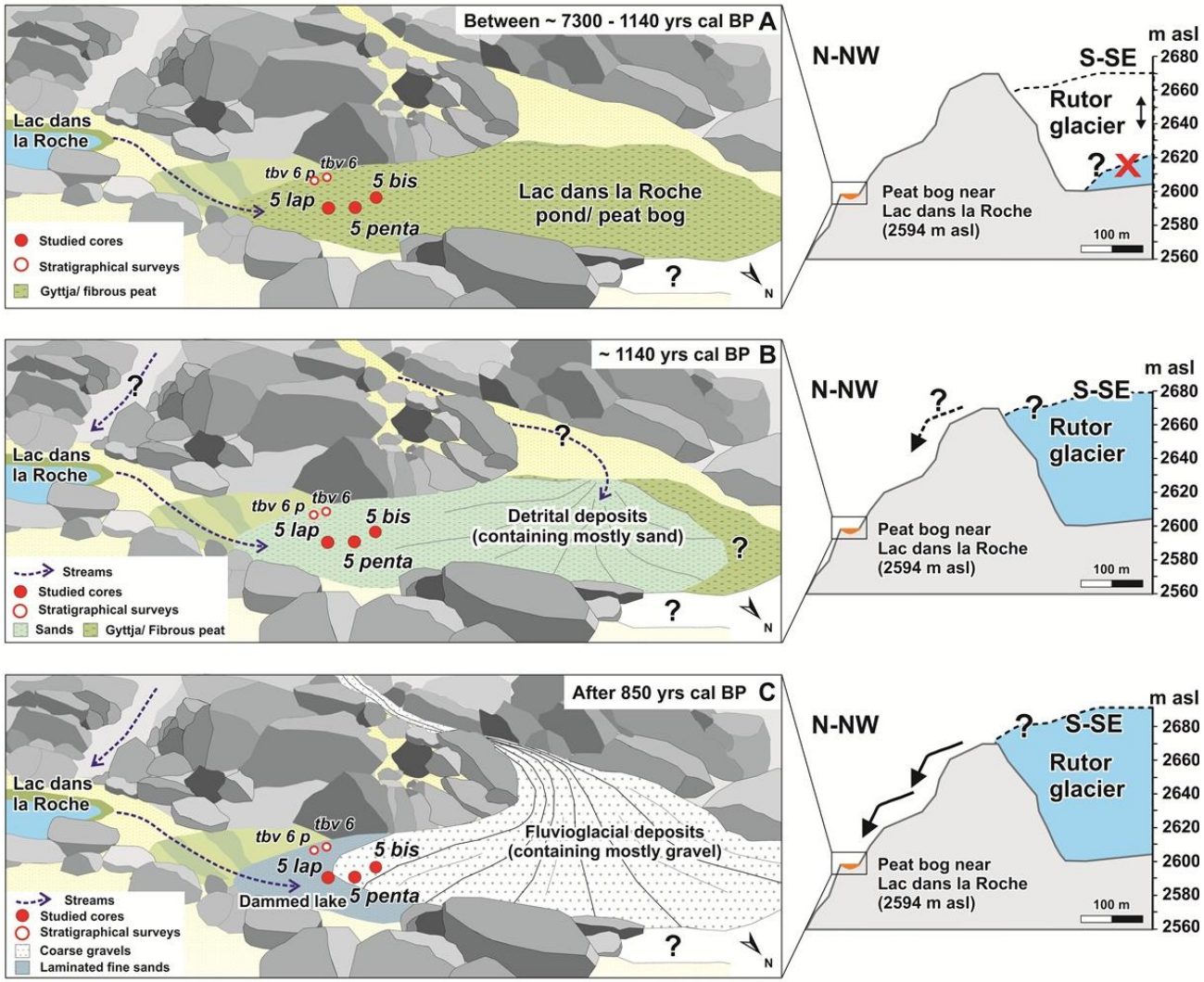

Fig. 31 - The evolution of the Valter mire between 7300 and 850 yrs cal BP is summarized in three cartoons (left) along with the Rutor Glacier reconstructed positions (right). (A) Rutor Glacier low stand period, continuous and undisturbed organic deposition characterized the Valter mire. (B) Rutor Glacier possibly reached an high-stand position in the immediate vicinity of the edge culminating at 2670 m asl, the Valter mire was buried by a mud flow containing mostly fine sand at ca. 1146 yrs cal BP (median probability); (C) Rutor Glacier reached an higher-stand position at least at the edge culminating at 2670 m asl, a glacier – related debris flow buried the site around 853 yrs cal BP (median probability).

5.2. The end of the Climatic Optimum: Pinus cembra decline and Picea expansion under unstable climatic conditions

In the Rutor area at least from 8800 until ca. 4000 yrs cal BP, high treeline altitudes, high summer temperatures and small glacier extent were documented (see also **Chapter 2**). After 4000 yrs cal BP, regional vegetation composition changed significantly. *Pinus cembra* and *Abies alba* gradually reduced their extent while *Picea abies* and *Alnus viridis* became dominant. Spruce forests expanded after 3600 cal. BP, in agreement with the Crotte Basse pollen record, just a few km from the Rutor area (Pini et al., submitted).

During this phase, treeline steadily decreased, as can be inferred from lower *Pinus cembra* percentages and PAR values <500 grains cm^{-2} yrs^{-1}. Starting from ~3800 yrs cal BP, the increase of Gramineae and Cichorioideae suggest the expansion of alpine meadows. Furthermore, at ca. 3000 yrs cal BP the decline of *Rhododendron* pollen curve is followed by the expansion of *Salix*. These taxa may be considered excellent indicators of subalpine/alpine belts. Indeed, modern data document that *Rhododendron ferrugineum* has a consistent pollen–vegetation altitudinal pattern restricted to the timberline ecotone, while the dwarf shrubs *Salix herbacea* and *Salix foetida* are present and locally more abundant above the treeline. These evidences (see Chapter 1), document the transition from treeline ecotone to treeless conditions at the study site.

Starting from ca. 4000 yrs cal BP, TJuly show a decrease of ca. 3 °C compared to the previous warmer period (8000 – 4000 yrs cal BP) (**Fig. 32**). Our data are in agreement with other palaeoclimate reconstructions in the Alps. Indeed, a cooling phase started around 5000 – 4000 yrs cal BP and leading to a temperature drop of ca. 2-3 ˚C is elsewhere documented (Heiri et al. 2003; Wick et al., 2003; Ortu et al., 2008; Ilyashuk et al., 2011). Different studies suggest that *Picea abies* and *Alnus viridis* may have been favoured by cooler and moister climatic conditions (Heiri et al., 2006; Lotter et al., 2006; Valsecchi and Tinner, 2010). The global climate system experienced a drastic reorganization during this time period. Other proxy data from the Alps reveal glacier advances and timberline depressions after ca 4500 yrs cal BP related to the development of cooler, wetter and more oceanic climate conditions (Leeman and Niessen, 1994; Haas et al.,

1998; Tinner and Theurillat, 2003). Our data has a good correspondence with the Mer de Glace (Mont Blanc Massif, French Alps) altitudinal variation curve during the late Holocene (Le Roy et al., 2015). Indeed, the most prominent glacier advances fit with lowering in pollen percentages of coniferous taxa (e.g. *Pinus cembra*, *Picea*) as well as the minima in Tjuly reconstruction for the Rutor area (see light blue rectangles in **Fig. 32**). Furthermore, the modeled Rhone Glacier (Switzerland) oscillations point to reduced ice extent in a position smaller than today until approximately 5 ka. After 5 ka, the Rhone Glacier was larger than today, but smaller than its LIA maximum extent (Goehring et al., 2012) (**Fig. 32**). Similarly, reconstructed surface elevations of the Ober Grindelwald Glacier (Luetscher et al., 2011) highlights a change in extent towards larger glacier just before 4 ka. These data are in agreement with observations of prolonged glacier advances throughout the Alps after 3 - 4 ka (Holzhauser et al., 2005; Ivy-Ochs et al., 2009).

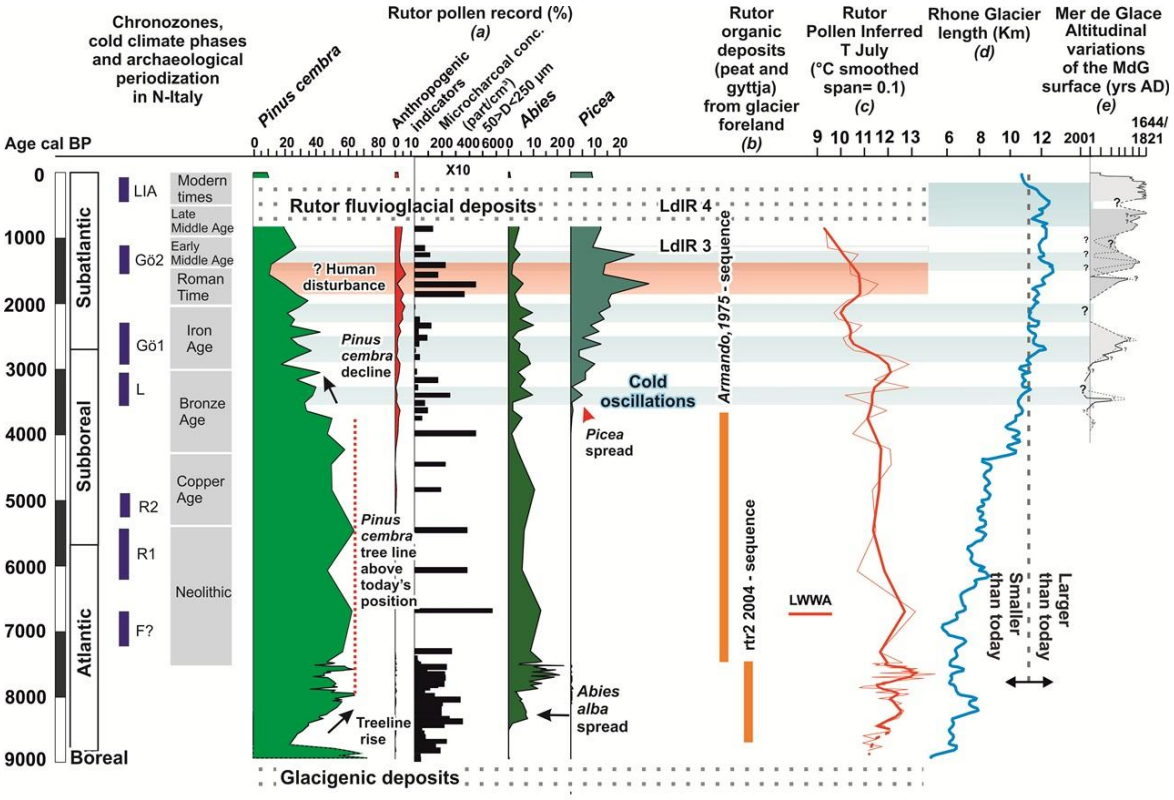

Fig. 32 - Overview of palaeoecological and climate reconstruction from the Rutor site compared with glacier dated advance and recession phases in the Alps. a) Rutor selected % pollen curves and microcharcoal concentration (particles size: 50<D>250 µm); b) age of the organic deposits in the Rutor Glacier foreland (section A – present study and Armando et al., 1975); c) Rutor pollen-inferred Tjuly reconstruction (LWWA); d) Rhone Glacier length variations (Goehring et al., 2012); e) Mer de Glace altitudinal position (Le Roy et al, 2015); Abbreviations: F: Frosnitz; R 1-2: Rotmoos; L: Löbben oscillation; Gö 1-2: Göschener oscill.; LIA: Little Ice Age. LdlR 3-4: Lac dans la Roche 3-4 lithozones corresponding to the Rutor Glacier colder oscillations.

5.3. Human activities in the Rutor area: the Roman period

First sporadic occurrences of *Plantago lanceolata* pollen grains (<1%) are dated ca. 4800 yrs cal BP while first single pollen grain of *Cerealia* was documented at 4200 yrs cal BP. These values are consistent with a long-distance transport from the valley floor. The anthropogenic indicators curve (including e.g. *Cerealia*, *Plantago lanceolata*, *Urtica*, *Rumex acetosa* type) became almost continuous at ca. 4000 yrs cal BP showing values comparable to the modern ones at the

studied site (ca. 2,5%). Considering the modern negligible human activities at high altitude in the Rutor area, a similar scenario can be supposed during the Bronze age. A steady decrease in microcharcoal concentration occurred since ca. 4000 yrs cal BP, possibly is related to the burnable biomass decrease due to the treeline drop. Our record bears no evidences supporting a forest clearing induced by anthropic fire activity during the Bronze age or earlier. Since the onset of the Late Iron age (ca. 2400 yrs cal BP) anthropogenic indicators curve up to 5% (e.g. *Plantago lanceolata* <2%) couples with a minimum in microcharcoal concentration, suggest a long distance transport, possibly from lower altitudes. Low percentages of the dung spore *Sporormiella* (between 0,1 – 1%) allow to excluded local megaherbivores grazing activities. Moreover, during the Late Iron age (ca. 2400 – 2000 yrs cal BP) a cooler centennial oscillation of about 1 -1,5 ˚C (T_{july}) has been reconstructed (**Fig. 32**). Afterwards, during the Roman time and the Early Middle Ages an increase in microcharcoal concentration (**Fig. 32**) indicating enhanced fire activity possibly linked to a remarkable drop in coniferous pollen curves (e.g. *Picea abies* and *Pinus cembra*). Archaeological data suggest that the I^{th} century was an important period for the establishment of mining and metallurgy-related activities (e.g. in the Savoie department), with expansion continuing through the III^{th} and IV^{th} centuries (Rémy et al., 1996; Maréchal J-R., 1960). Changes in plant cover documented in our pollen record during this period might be correlated with a pattern of increased land use in the region.

6. CONCLUSIONS

The Rutor area, at least from 8800 until ca. 4000 yrs cal BP, experienced high treeline altitudes, high summer temperatures and small glacier extent. After 4000 yrs cal BP, regional vegetation composition changed significantly, since *Pinus cembra* and *Abies alba* gradually declined and *Picea abies* and *Alnus viridis* became dominant. According to the reconstructed pollen-based July temperature the most significant climatological signal during the middle and late Holocene has been represented by a decrease of ca. 2-3 °C from ca. 4000 yrs cal BP. This cooling trend is in agreement with observations of prolonged glacier advances throughout the Alps during the late Holocene (Goehring et al., 2012; Luetscher et

al., 2011). After 3800 yrs cal BP, the treeline (*Pinus cembra*) steadily decreased while spruce forests expanded in the lower altitudinal belts after 3600 cal. BP. A good correspondence is observed between Rutor July temperature cooling oscillations centered at ca. 3400, 2700, 2150 and 1100 yrs cal BP, with most prominent glacier advance at the Mer de Glace (Mont Blanc Massif, French Alps; Le Roy et al., 2015). These events correspond to declines in pollen percentages of conifer taxa (e.g. *Pinus cembra*, *Picea abies*). Locally, evidences of a Rutor Glacier advanced position occurred around ca. 1140 and 850 yrs cal BP (median probability).

The human activity in this area was negligible for most of the Holocene, changes in timberline ecotone appear to be related to climate changes. It is likely that only during more recent times human activities amplified the effect of climatic changes.

REFERENCES

Baretti, M. (1880). Il Lago del Rutor (Alpi Graie Settentrionali). Annuario Club Alpino Italiano, Torino.

Baroni, C., & Orombelli, G. (1996). The alpine “Iceman” and Holocene climatic change. Quaternary Research, 46(1), 78-83.

Berthel, N., Schwörer, C., & Tinner, W. (2012). Impact of Holocene climate changes on alpine and treeline vegetation at Sanetsch Pass, Bernese Alps, Switzerland. Review of Palaeobotany and Palynology, 174, 91-100.

Beug, H.J. (2004). Leitfaden der Pollenbestimmung für Mitteleuropa und angrenzende Gebiete. Verlag Dr. Friedrich Pfeil, München.

Burga, C. A. (1991). Vegetation history and palaeoclimatology of the Middle Holocene: pollen analysis of alpine peat bog sediments, covered formerly by the Rutor Glacier, 2510 m (Aosta Valley, Italy). Global Ecology and Biogeography Letters, 143-150.

Burga, C. A. (1993). Swiss alpine palaeoclimate during the Holocene: pollen analytical evidence and general features. Solifluction and Climatic Variation in the Holocene. European Science Foundation, Verlag, Stuttgart, 11-22.

Ter Braak, C. J., & Prentice, I. C. (1988). A theory of gradient analysis. Advances in ecological research, 18, 271-317.

Colombaroli, D., Henne, P. D., Kaltenrieder, P., Gobet, E., & Tinner, W. (2010). Species responses to fire, climate and human impact at tree line in the Alps as evidenced by palaeo-environmental records and a dynamic simulation model. Journal of Ecology, 98(6), 1346-1357.

Dal Piaz G.V. (ed.), (1992). Le Alpi dal M. Bianco al Lago Maggiore. Guide geologiche regionali (voll. I e II). Milano, Società Geologica Italiana, BE-MA. 311 p.

Dean, W. E. Jr. (1974). Determination of carbonate and organic matter in calcareous sediments and sedimentary rocks by loss on ignition: Comparison with other methods. J. Sed. Petrol. 44, 242–248.

van Geel, B. (1978). A palaeoecological study of Holocene peat bog sections in Germany and The Netherlands, based on the analysis of pollen, spores and macro- and microremains of fungi, algae, cormophytes and animals. Review of Palaeobotany and Palynology 25, 1-120.

van Geel, B., Bohncke, S.J.P., Dee, H. (1981). A palaeoecological study of an upper Late Glacial and Holocene sequence from 'De Borchert', The Netherlands. Review of Palaeobotany and Palinology 31, 367-449.

Goehring, B. M., Schaefer, J. M., Schluechter, C., Lifton, N. A., Finkel, R. C., Jull, A. T., ... & Alley, R. B. (2011). The Rhone Glacier was smaller than today for most of the Holocene. Geology, 39 (7), 679-682.

Goehring, B. M., Vacco, D. A., Alley, R. B., & Schaefer, J. M. (2012). Holocene dynamics of the Rhone Glacier, Switzerland, deduced from ice flow models and cosmogenic nuclides. Earth and Planetary Science Letters, 351, 27-35.

Gottfried, M., Pauli, H., Futschik, A., Akhalkatsi, M., Barančok, P., Alonso, J. L. B., ... & Krajči, J. (2012). Continent-wide response of mountain vegetation to climate change. *Nature Climate Change*, *2* (2), 111-115.

Grimm, J. P. (1977). Evidence for the existence of three primary strategies in plants and its relevance to ecological and evolutionary theory. Am. Nat. 111, 1169-1194. Grimm, E.C., 1987. CONISS: a FORTRAN 77 program for stratigraphically constrained cluster analysis by the method of incremental sum of squares. Comput. Geosci. 13 (1), 13-35.

Grimm, E.C. (1991-2011). Tilia 1.7.16. Illinois State Museum, Research and Collection Center, Springfield.

Gustafsson, Ö., Bucheli, T. D., Kukulska, Z., Andersson, M., Largeau, C., Rouzaud, J. N., ... & Eglinton, T. I. (2001). Evaluation of a protocol for the quantification of black carbon in sediments. Global Biogeochemical Cycles, 15(4), 881-890.

Haas, J. N., Richoz, I., Tinner, W., & Wick, L. (1998). Synchronous Holocene climatic oscillations recorded on the Swiss Plateau and at timberline in the Alps. The Holocene, 8, 301-309.

Hafner, A. (2012). Archaeological discoveries on Schnidejoch and at other Ice Sites in the European Alps. Arctic 65 (Suppl. 1), 189e202. Hall, B.L., Baroni, C., Denton, G.H., 2008.

Heiri, O., Lotter, A. F., Hausmann, S., & Kienast, F. (2003). A chironomid-based Holocene summer air temperature reconstruction from the Swiss Alps. The Holocene, 13(4), 477-484.

Heiri, C., Bugmann, H., Tinner, W., Heiri, O., & Lischke, H. (2006). A model-based reconstruction of Holocene treeline dynamics in the Central Swiss Alps. Journal of Ecology, 94 (1), 206-216.

Holzhauser, H. (1984). Zur Geschichte der Aletsch- und des Fieschergletschers. In: Physische Geographie, vol. 13. Zürich. 448 p.

Holzhauser, H., & Zumbühl, H. J. (1996). To the history of the Lower Grindelwald Glacier during the last 2800 years-paleosols, fossil wood and historical pictorial records-new results. Zeitschrift fur Geomorphologie Supplementband, 95-127.

Holzhauser, H., & Zumbühl, H. J. (2003). Nacheiszeitliche Gletscherschwankungen. Hydrologischer Atlas der Schweiz (Tafel 3.8). Bundesamt für Landestopographie, Bern–Wabern.

Holzhauser, H., Magny, M., Zumbühl, H.J., (2005). Glacier and lake-level variations in west-central Europe over the last 3500 years. Holocene 15 (6), 789-801.

Holzhauser, H. (2010). Zur geschichte des Gornergletschers e Ein puzzle aus historischen dokumenten und fossilen hölzern aus dem gletschervorfeld. In: Geographica Bernensia, vol. G 84. Institute of Geography, University of Bern, 253 p.

Hormes, A., Müller, B. U., & Schlüchter, C. (2001). The Alps with little ice: evidence for eight Holocene phases of reduced glacier extent in the Central Swiss Alps. The Holocene, 11(3), 255-265.

Hormes, A., Beer, J., & Schlüchter, C. (2006). A geochronological approach to understanding the role of solar activity on Holocene glacier length variability in the Swiss Alps. Geografiska Annaler: Series A, Physical Geography, 88(4), 281-294.

Ilyashuk, E. A., Koinig, K. A., Heiri, O., Ilyashuk, B. P., & Psenner, R. (2011). Holocene temperature variations at a high-altitude site in the Eastern Alps: a chironomid record from Schwarzsee ob Sölden, Austria. Quaternary Science Reviews, 30(1), 176-191.

Ivy-Ochs, S., Kerschner, H., Maisch, M., Christl, M., Kubik, P. W., & Schlüchter, C. (2009). Latest Pleistocene and Holocene glacier variations in the European Alps. Quaternary Science Reviews, 28 (21), 2137-2149.

Joerin, U. E., Stocker, T. F., & Schlüchter, C. (2006). Multicentury glacier fluctuations in the Swiss Alps during the Holocene. The Holocene, 16(5), 697-704.

Joerin, U. E., Nicolussi, K., Fischer, A., Stocker, T. F., & Schlüchter, C. (2008). Holocene optimum events inferred from subglacial sediments at Tschierva Glacier, Eastern Swiss Alps. Quaternary Science Reviews, 27(3), 337-350.

Körner, C. (1998). A re-assessment of high elevation treeline positions and their explanation. Oecologia, 115(4), 445-459.

Le Roy, M. (2012). Reconstitution des fluctuations glaciaires holocènes dans les Alpes occidentales: apports de la dendrochronologie et de la datation par isotopes cosmogéniques produits in situ (Doctoral dissertation, Université Grenoble Alpes).

Le Roy, M., Nicolussi, K., Deline, P., Astrade, L., Edouard, J. L., Miramont, C., & Arnaud, F. (2015). Calendar-dated glacier variations in the western European Alps during the Neoglacial: the Mer de Glace record, Mont Blanc massif. Quaternary Science Reviews, 108, 1-22.

Le Roy Laduríe, E., Rousseau, D., & Vasak, A. (1967). Les fluctuations du climat de l'an mila nos jours. Flammarion, Paris.

Leemann, A., & Niessen, F. (1994). Holocene glacial activity and climatic variations in the Swiss Alps: reconstructing a continuous record from proglacial lake sediments. The Holocene, 4 (3), 259-268.

Lotter, A. F., Heiri, O., Hofmann, W., Van der Knaap, W. O., Van Leeuwen, J. F., Walker, I. R., & Wick, L. (2006). Holocene timber-line dynamics at Bachalpsee, a lake at 2265 m asl in the northern Swiss Alps. Vegetation history and archaeobotany, 15(4), 295-307.

Luetscher, M., Hoffmann, D. L., Frisia, S., & Spötl, C. (2011). Holocene glacier history from alpine speleothems, Milchbach cave, Switzerland. Earth and Planetary Science Letters, 302 (1), 95-106.

Maréchal J.-R., Armand, H. (1960). Recherches scientifiques sur la sidérurgie aux époques de la Tène et the l'occupation romaine en Savoie. Dans Actes du 85e Congrès National des Sociétés Savantes, Chambéry-Annecy, Paris, 1962, 61-82.

McCormick, M., Büntgen, U., Cane, M. A., Cook, E. R., Harper, K., Huybers, P., ... & Nicolussi, K. (2012). Climate change during and after the Roman Empire: reconstructing the past from scientific and historical evidence. Journal of Interdisciplinary History, 43(2), 169-220.

Moore, P.D., Webb, J.A., Collinson, M.E. (1991). Pollen Analysis. Blackwell Scientific Publications. Oxford University Press.

Nicolussi, K. & Patzelt G. (2001). Untersuchungen zur holoz¨anen Gletscherentwicklung von Pasterze und Gepatschferner (Ostalpen). Zeitschrift f¨ur Gletscherkunde und Glazialgeologie 36, 1-87

Nicolussi, K., Kaufmann, M., Patzelt, G., & Thurner, A. (2005). Holocene tree-line variability in the Kauner Valley, Central Eastern Alps, indicated by dendrochronological analysis of living trees and subfossil logs. Vegetation History and Archaeobotany, 14 (3), 221-234.

Oerlemans, J. (2005). Extracting a climate signal from 169 glacier records. Science, 308(5722), 675-677.

Oksanen, J., Blanchet, F. G., Kindt, R., Legendre, P., Minchin, P. R., O'Hara, R. B., ... & Wagner, H. (2015). Package vegan version 2.2-1: community ecology package.

Orombelli, G., & Porter, S. C. (1982). Late Holocene Fluctuations of Breva Glacier. Comitato Glaciologico Italiano.

Orombelli, G., & Mason, P. (1997). Holocene glacier fluctuations in the Italian Alpine region. Glacier fluctuations during the Holocene, edited by: Harrison, SP, Frenzel, B., Boulton, GS, Glaser, B., and Huckrieder, U., Paläoklimaforschung-Paleoclim. Res, 24, 59-65.

Orombelli, G. (2005). Il Ghiacciaio del Ruitor (Valle d'Aosta) nella piccola eta glaciale. Geografia Fisica e Dinamica Quaternaria, Suppl, 7, 239-251.

Ortu, E., Peyron, O., Bordon, A., de Beaulieu, J. L., Siniscalco, C., & Caramiello, R. (2008). Lateglacial and Holocene climate oscillations in the South-western Alps: an attempt at quantitative reconstruction. Quaternary International, 190(1), 71-88.

Parigi, A., Maggi, W. and Orombelli, G. (1999). Variazioni frontali del Ghiacciaio del Rutor dal 1820 al 1998. 8th Italian Glaciol. Congr., Bormio, Settembre 1999.

Peretti, L. (1935). Gruppo del Rutor e Miravidi-Lechaud. / Boll Comitato Glaciol. Italiano e della Commissione Glaciologica del C.A.I. 15, Torino, Italy.

Peretti, L. & Charrier, G. (1967). Segnalazione e analisi pollinica di torba deposta alla fronte attuale del ghiacciaio del Rutor (Valle d'Aosta). Considerazioni di paleogeografia e paleoclimatologia locale. Bollettino del Comitato Glaciologico Italiano, 14, 13-31.

Porter, S.C. & Orombelli, G. (1985). Glacier contraction during the middle Holocene in the western Italian Alps: evidence and implications. Geology, 13, 296-298.ÉPunt, W., Blackmore, S. (Eds.) (1976-2009). The Northwest European Pollen Flora. vol. I-IX. Elsevier Publishing Company.

Punt, W., Blackmore, S. (Eds.) (1976-2009). The Northwest European Pollen Flora. vol. I-IX. Elsevier Publishing Company.

Ravazzi, C. (2011) - Tremila anni di storia del cima in valle d'Aosta. La registrazione dell'anfiteatro del ghiacciaio del Lys. Augusta,16-19.

Reille, M. (1992-1998). Pollen et spores d'Europe et d'Afrique du nord, vol. 1 (Suppl. IeII). Faculte S. Jerome, Universite de Marseille, Marseille.

Reimer PJ, Bard E, Bayliss A. (2013). IntCal13 and Marine13 radiocarbon age calibration curves 0-50,000 years cal BP. Radiocarbon 55, 1869-1887.

Rémy B., Ballet Fr., Ferber É. (1996). Carte Archéologique de la Gaule. La Savoie. CAG 73, n°076, p. 140, Paris.

Röthlisberger, H., Haas, P., Holzhauser, H., Keller, W., Bircher, W., Renner, F. (1980). Holocene climatic fluctuations - radiocarbon dating of fossil soils (fAh) and woods from moraines and glaciers in the Alps. Geogr. Helv. 35 (5), 21-52.

Sacco, F. (1917). Il ghiacciaio e i laghi del Rutor. Boll. Soc. Geol. Italiana 36, 1-36.

Sacco, F. (1934). L'anfiteatro morenico recente del Rutor. L'Universo, Anno15 11, 1-16.

Seppä, H., & Birks, H. J. B. (2001). July mean temperature and annual precipitation trends during the Holocene in the Fennoscandian tree-line area: pollen-based climate reconstructions. The Holocene, 11(5), 527-539.

Simonneau, A., Chapron, E., Garçon, M., Winiarski, T., Graz, Y., Chauvel, C., Debret, M., Motelica- Heino, M., Desmet, M., Di Giovanni, C. (2014). Tracking Holocene glacial and high-altitude alpine environments fluctuations from minerogenic and organic markers in proglacial lake sediments (Lake Blanc Huez, Western French Alps). Quat. Sci. Rev. 89, 27-43.

Solomina, O. N., Bradley, R. S., Jomelli, V., Geirsdottir, A., Kaufman, D. S., Koch, J., ... & Nicolussi, K. (2016). Glacier fluctuations during the past 2000 years. Quaternary Science Reviews, 149, 61-90.

Steiner, D., Pauling, A., Nussbaumer, S. U., Nesje, A., Luterbacher, J., Wanner, H., & Zumbühl, H. J. (2008). Sensitivity of European glaciers to precipitation and temperature–two case studies. Climatic Change, 90 (4), 413-441.

Stockmarr, J. (1971). Tablets with spores used in absolute pollen analysis. Pollen Spores 13, 615-621.

Stuiver M., Reimer PJ, Reimer R. (2013). Radiocarbon calibration program Revision 7.0.2.

Tinner, W., Ammann, B., & Germann, P. (1996). Treeline fluctuations recorded for 12,500 years by soil profiles, pollen, and plant macrofossils in the Central Swiss Alps. Arctic and Alpine Research, 131-147.

Tinner, W., & Theurillat, J. P. (2003). Uppermost limit, extent, and fluctuations of the timberline and treeline ecocline in the Swiss Central Alps during the past 11,500 years. Arctic, Antarctic, and Alpine Research, 35 (2), 158-169.

Trautmann, W. (1953). Zur Unterscheidung fossiler Spaltoffnungen der mitteleuropäischen Coniferen. Flora 140, 523-533.

Villa, F., De Amicis, M., & Maggi, V. (2007). GIS analysis of Rutor Glacier (Aosta Valley, Italy) volume and terminus variations. Geografia fisica e dinamica quaternaria, 30 (1), 87-95.

Valsecchi, V., & Tinner, W. (2010). Vegetation responses to climatic variability in the Swiss Southern Alps during the Misox event at the early–mid Holocene transition. Journal of Quaternary Science, 25 (8), 1248-1258.

Villa, F., Tamburini, A., Deamicis, M., Sironi, S., Maggi, V., & Rossi, G. (2008). Volume decrease of Rutor Glacier (Western Italian Alps) since Little Ice Age: a quantitative approach combining GPR, GPS and cartography. Geografia Fisica e Dinamica Quaternaria, 31 (1), 63-70.

Wick, L., van Leeuwen, J. F., van der Knaap, W. O., & Lotter, A. F. (2003). Holocene vegetation development in the catchment of Sägistalsee (1935 m asl), a small lake in the Swiss Alps. Journal of Paleolimnology, 30(3), 261-272.

Zumbühl, H. J., & Holzhauser, H. (1988). Glaciers des Alpes du Petit âge glaciaire. Editions du Club Alpin Suisse.

LIST OF FIGURES

LIST OF TABLES